

Coastal and Oceanographic  
Engineering Laboratory

Technical Report No. 14

EVALUATION AND DEVELOPMENT OF WATER WAVE THEORIES FOR  
ENGINEERING APPLICATION

VOLUME I - PRESENTATION OF RESEARCH RESULTS

By

R. G. Dean  
College of Engineering  
University of Florida  
Gainesville, Florida

Prepared Under

Contract No. DACW 72-67-0009  
Coastal Engineering Research Center  
U. S. Army Corps of Engineers  
Washington, D. C.

December, 1972

## ABSTRACT

Volume I of this report presents the results of a research program to evaluate and develop water wave theories for engineering application. A second volume of this report presents wave tables developed for preliminary design in offshore problems.

Volume I describes: (1) an evaluation of the degree to which various available wave theories satisfy the nonlinear water wave mathematical formulation and (2) a comparison of water particle velocities measured in the laboratory with those predicted by a number of available wave theories. The results of these studies indicated that the Stream function wave theory provided generally better agreement with both the mathematical formulation and the laboratory data. Volume I also includes a number of examples illustrating the application of the wave tables (described below) to offshore design problems.

Based on the evaluation phase described above, a set of wave tables was developed and is presented as Volume II. The tables consist of dimensionless quantities which describe the kinematic and dynamic fields of a two dimensional progressive water wave. In addition, quantities are included

which are directly applicable to frequently required design calculations and also parameters which should be of interest to the researcher and scientist.

## TABLE OF CONTENTS

|  | Page |
|--|------|
| ABSTRACT .....   | ii   |
| LIST OF TABLES .....   | viii |
| LIST OF FIGURES .....  | x    |
| LIST OF SYMBOLS .....  | xiv  |
| ACKNOWLEDGEMENTS .....   | xix  |
| <br>   |      |
| I. INTRODUCTION .....  | 1    |
| II. STREAM FUNCTION WAVE THEORY .....  | 6    |
| <i>Introduction</i> .....  | 6    |
| <i>Formulation</i> .....   | 7    |
| <i>Differential Equation</i> .....   | 7    |
| <i>Boundary Conditions</i> .....   | 9    |
| <i>Bottom boundary condition (BBC)</i> .....   | 9    |
| <i>Kinematic free surface boundary condition (KFSBC)</i> .....                         | 9    |
| <i>Dynamic free surface boundary condition (DFSBC)</i> .....                           | 9    |
| <i>The Stream Function Solution</i> .....  | 12   |
| III. EVALUATION OF VALIDITIES OF WAVE THEORIES ....                                    | 14   |
| <i>Introduction</i> .....  | 14   |
| <i>Discussion of Differences Between Stream Function and Other Wave Theories</i> ..... | 14   |
| <i>Analytical Validity</i> .....   | 17   |
| <i>Definition of Boundary Condition</i> .....  |      |
| <i>Errors</i> .....  | 18   |
| <i>Results of Analytical Validity</i> .....  |      |
| <i>Comparison</i> .....  | 20   |
| <i>Comparison with Stream function theory developed by Von Schwind and Reid</i> .....  | 30   |
| <i>Conclusions Resulting from the Analytical Validity Study</i> .....                  | 31   |
| <i>Experimental Validity</i> .....   | 36   |
| <i>Conclusions Resulting from the Experimental Validity Study</i> .....                | 54   |

TABLE OF CONTENTS—Continued

|  | Page |
|--|------|
| IV. DESCRIPTION OF TABLES .....                  | 56   |
| Introduction .....                               | 56   |
| Variables Presented in Tabular Form .....        | 57   |
| Internal Field Variables Depending               |      |
| on $\theta$ and $S$ .....                        | 65   |
| Horizontal water particle velocity               |      |
| component, $u(\theta, S)$ .....                  | 67   |
| Vertical water particle velocity                 |      |
| component, $w(\theta, S)$ .....                  | 68   |
| Horizontal water particle                        |      |
| acceleration, $Du/Dt$ .....                      | 68   |
| Vertical water particle                          |      |
| acceleration, $Dw/Dt$ .....                      | 68   |
| Drag force component, $F_D(\theta, S)$ .....     | 69   |
| Inertia force component, $F_I(\theta, S)$ .....  | 69   |
| Drag moment component, $M_D(\theta, S)$ .....    | 69   |
| Inertia moment component, $M_I(\theta, S)$ ..... | 69   |
| Dynamic pressure component,                      |      |
| $p_D(\theta, S)$ .....                           | 70   |
| Variables Depending on $\theta$ Only .....       | 70   |
| Water surface displacement, $\eta(\theta)$ ..... | 70   |
| Total drag force component, $F_D(\theta)$ .....  | 70   |
| Total inertia force component,                   |      |
| $F_I(\theta)$ .....                              | 71   |
| Total drag moment component, $M_D(\theta)$ ..... | 71   |
| Total inertia moment component,                  |      |
| $M_I(\theta)$ .....                              | 71   |
| Kinematic free surface boundary                  |      |
| condition error, $\epsilon_1(\theta)$ .....      | 72   |
| Dynamic free surface boundary                    |      |
| condition error, $\epsilon_2(\theta)$ .....      | 72   |
| Overall Variables (do not depend                 |      |
| on $\theta$ or $S$ ) .....                       | 72   |
| Wave length, $L$ .....                           | 72   |
| Average potential energy, $PE$ .....             | 73   |
| Average kinetic energy, $KE$ .....               | 73   |
| Average total energy, $TE$ .....                 | 74   |
| Average total energy flux, $F_{TE}$ .....        | 74   |
| Group velocity, $CG$ .....                       | 74   |
| Average momentum, $M$ .....                      | 75   |
| Average momentum flux in wave                    |      |
| direction, $F_{m_x}$ .....                       | 75   |
| Average momentum flux transverse                 |      |
| to wave direction, $F_{m_y}$ .....               | 76   |

TABLE OF CONTENTS—Continued

|   | Page      |
|---|-----------|
| <i>Kinematic free surface boundary condition errors, <math>\epsilon_1</math></i> .....        | 76        |
| <i>Dynamic free surface boundary condition errors, <math>\epsilon_2</math></i> .....          | 76        |
| <i>Kinematic free surface breaking parameter, <math>\beta_1</math></i> .....                  | 77        |
| <i>Dynamic free surface breaking parameter, <math>\beta_2</math></i> .....                    | 77        |
| <i>Variables Presented in Graphical Form—Combined Effect of Shoaling and Refraction</i> ..... | 77        |
| <b>V. EXAMPLES ILLUSTRATING USE OF WAVE TABLES</b> .....                                      | <b>84</b> |
| <i>Introduction</i> .....   | 84        |
| <i>Example 1 - Deck Elevation and Wave Forces and Moments on an Offshore Platform</i> .....   | 85        |
| <i>Deck Elevation</i> .....   | 87        |
| <i>Forces on Member "a"</i> .....   | 88        |
| <i>Forces on Member "b"</i> .....   | 89        |
| <i>Forces on Member "c"</i> .....   | 91        |
| <i>Moments on Member "a"</i> .....  | 97        |
| <i>Moments on Member "b"</i> .....  | 100       |
| <i>Moments on Member "c"</i> .....  | 102       |
| <i>Example 2 - Wave Characteristics, Kinematics and Pressure Fields</i> .....                 | 104       |
| <i>Wave Length</i> .....  | 104       |
| <i>Wave Profile</i> .....   | 105       |
| <i>Water Particle Kinematics</i> .....  | 105       |
| <i>Dynamic Pressure</i> .....   | 108       |
| <i>Example 3 - Free Surface Boundary Condition Errors</i> .....                               | 109       |
| <i>Distributed Boundary Condition Errors</i> .....  | 109       |
| <i>Overall Kinematic Free Surface Boundary Condition Errors</i> .....                         | 112       |
| <i>Overall Dynamic Free Surface Boundary Condition Errors</i> .....                           | 112       |
| <i>Example 4 - Calculation of Energy, Momentum, and Energy and Momentum Fluxes</i> .....      | 113       |
| <i>Average Potential Energy</i> .....   | 114       |
| <i>Average Kinetic Energy</i> .....   | 114       |
| <i>Total Energy</i> .....   | 114       |
| <i>Energy Flux</i> .....  | 114       |

TABLE OF CONTENTS—Continued

|  | Page |
|--|------|
| <i>Group Velocity</i> .....  | 114  |
| <i>Average Momentum</i> .....  | 115  |
| <i>Average Momentum Flux in</i><br><i>Wave Direction</i> .....                         | 115  |
| <i>Average Momentum Flux Transverse</i><br><i>to Wave Direction</i> .....              | 115  |
| <i>Example 5 - Free Surface Breaking</i><br><i>Parameters</i> .....                    | 115  |
| <i>Example 6 - Combined Shoaling/</i><br><i>Refraction</i> .....                       | 117  |
| <i>Example 6-a</i> .....   | 117  |
| <i>Example 6-b</i> .....   | 119  |
| <i>Example 7 - Use of Tables for</i><br><i>Nontabulated Wave Conditions</i> .....      | 122  |
| <i>Method</i> .....  | 123  |
| <i>Example 7-a - Numerical Illustration</i><br><i>of Interpolation Procedure</i> ..... | 125  |
| <i>Example 7-b - Assessment of the</i><br><i>Interpolation Method</i> .....            | 129  |
| VI. SUMMARY .....  | 134  |
| VII. REFERENCES .....  | 136  |
| APPENDIX   |      |
| I. NUMERICAL SOLUTION OF STREAM FUNCTION<br>PARAMETERS .....                           | 139  |
| <i>Introduction</i> .....  | 140  |
| <i>Review of Problem Formulation</i> .....   | 140  |
| <i>Stream Function Solution</i> .....  | 141  |
| II. DEVELOPMENT OF COMBINED SHOALING/<br>REFRACTION COEFFICIENTS .....                 | 147  |
| <i>Introduction</i> .....  | 148  |
| <i>Background</i> .....  | 148  |
| <i>Method</i> .....  | 150  |
| <i>Solution</i> .....  | 151  |
| III. SAMPLE SET OF WAVE TABLES FOR<br>CASE 4-D .....                                   | 155  |

## LIST OF TABLES

| Table  | Page |
|--|------|
| A. Water Wave Theories Included in Evaluation Presented in Reference 1.....                      | 19   |
| B. Experimental Waves; Characteristics and Variables Measured .....                              | 41   |
| C. Standard Deviation of Differences Between Horizontal Velocities: Measured vs. Predicted ..... | 53   |
| D. Internal Field Variables (Functions of $\theta$ and S) .....                                  | 59   |
| E. Variables Depending on $\theta$ Only .....  | 61   |
| F. Overall Variables (Do Not Depend on $\theta$ or S) .....                                      | 63   |
| G. Horizontal Wave Forces on Member "a" .....  | 91   |
| H. Horizontal Wave Forces on Member "b" .....  | 93   |
| I. Horizontal Wave Forces on Member "c" .....  | 95   |
| J. Summary of Maximum Wave Forces on Several Platform Components .....                           | 97   |
| K. Wave Moments (About Mudline) on Member "a" .....  | 98   |
| L. Wave Moments (About Mudline) on Member "b" .....  | 100  |
| M. Wave Moments (About Mudline) on Member "c" .....  | 102  |
| N. Summary of Maximum Wave Forces and Moments .....  | 104  |

LIST OF TABLES—*Continued*

| Table | Page   |
|-------|--|
| O.    | Calculated Wave Profile, Kinematics,<br>and Dynamic Pressure ..... 106   |
| P.    | Free Surface Boundary Condition<br>Errors ..... 110  |
| Q.    | Summary of $F_D'(0^\circ, \text{Surf.})$ Required<br>for Example 7-a ..... 128   |
| R.    | Wave Characteristics Selected for<br>Accuracy Evaluation of<br>Interpolation Method ..... 129                                    |
| S.    | Summary of Percentage Differences<br>Between Values Determined by<br>Stream Function Solutions and<br>by Interpolation ..... 131 |

## LIST OF FIGURES

| Figure |   | Page |
|--------|---|------|
| 1.     | Definition Sketch, Progressive<br>Wave System .....   | 8    |
| 2.     | Wave Characteristics Selected for<br>Evaluation .....   | 21   |
| 3.     | Dimensionless Error, $\sqrt{\epsilon_1^2}$ , in Kinematic<br>Free Surface Boundary Condition,<br>$H/H_B = 0.25$ ; All Wave Theories .....       | 23   |
| 4.     | Dimensionless Error, $\sqrt{\epsilon_1^2}$ , in Kinematic<br>Free Surface Boundary Condition,<br>$H/H_B = 1.0$ ; All Wave Theories .....        | 24   |
| 5.     | Dimensionless Error, $\sqrt{\epsilon_2^2}/H$ , in Dynamic<br>Free Surface Boundary Condition,<br>$H/H_B = 0.25$ ; All Wave Theories .....       | 25   |
| 6.     | Dimensionless Error, $\sqrt{\epsilon_2^2}/H$ , in Dynamic<br>Free Surface Boundary Condition,<br>$H/H_B = 1.0$ ; All Wave Theories .....        | 26   |
| 7.     | Periodic Wave Theories Providing Best<br>Fit to Dynamic Free Surface<br>Boundary Condition (Analytical<br>Theories Only) .....                  | 28   |
| 8.     | Periodic Wave Theories Providing Best<br>Fit to Dynamic Free Surface<br>Boundary Condition (Analytical<br>and Stream Function V Theories) ..... | 29   |
| 9.     | Comparison of Errors in Dynamic Free<br>Surface Boundary Condition for<br>Three Numerical Wave Theories,<br>Wave No. 1 .....                    | 32   |

LIST OF FIGURES—*Continued*

| Figure |   | Page |
|--------|---|------|
| 10.    | Comparison of Errors in Dynamic Free Surface Boundary Condition for Three Numerical Wave Theories, Wave No. 2 ..... | 33   |
| 11.    | Comparison of Errors in Dynamic Free Surface Boundary Condition for Three Numerical Wave Theories, Wave No. 3 ..... | 34   |
| 12.    | Experimental Wave Characteristics .....   | 40   |
| 13.    | Horizontal Water Particle Velocity Under the Crest, Case 1 .....  | 42   |
| 14.    | Horizontal Water Particle Velocity Under the Crest, Case 2 .....  | 43   |
| 15.    | Horizontal Water Particle Velocity Under the Crest, Case 3 .....  | 44   |
| 16.    | Horizontal Water Particle Velocity Under the Crest, Case 4 .....  | 45   |
| 17.    | Horizontal Water Particle Velocity Under the Crest, Case 5 .....  | 46   |
| 18.    | Horizontal Water Particle Velocity Under the Crest, Case 6 .....  | 47   |
| 19.    | Horizontal Water Particle Velocity Under the Crest, Case 7 .....  | 48   |
| 20.    | Horizontal Water Particle Velocity Under the Crest, Case 8 .....  | 49   |
| 21.    | Vertical Water Particle Velocity, Case 9 .....  | 50   |
| 22.    | Free Surface Elevation, Case 10 .....   | 51   |
| 23.    | Wave Characteristics Selected for Tabulation .....  | 58   |

LIST OF FIGURES—*Continued*

| Figure |   | Page |
|--------|---|------|
| 24.    | Example Output for Dimensionless<br>Horizontal Velocity Component<br>Field .....                | 66   |
| 25.    | Combined Shoaling/Refraction for a<br>Deep Water Wave Direction,<br>$\alpha_0 = 0^\circ$ .....  | 79   |
| 26.    | Combined Shoaling/Refraction for a<br>Deep Water Wave Direction,<br>$\alpha_0 = 10^\circ$ ..... | 80   |
| 27.    | Combined Shoaling/Refraction for a<br>Deep Water Wave Direction,<br>$\alpha_0 = 20^\circ$ ..... | 81   |
| 28.    | Combined Shoaling/Refraction for a<br>Deep Water Wave Direction,<br>$\alpha_0 = 40^\circ$ ..... | 82   |
| 29.    | Combined Shoaling/Refraction for a<br>Deep Water Wave Direction,<br>$\alpha_0 = 60^\circ$ ..... | 83   |
| 30.    | Definition Sketch, Wave Approaching<br>Platform .....   | 86   |
| 31.    | Horizontal Wave Forces on<br>Member "a" .....   | 90   |
| 32.    | Horizontal Wave Forces on<br>Member "b" .....   | 92   |
| 33.    | Horizontal Wave Forces on<br>Member "c" .....   | 96   |
| 34.    | Wave Moments on Member "a" .....  | 99   |
| 35.    | Wave Moments on Member "b" .....  | 101  |
| 36.    | Wave Moments on Member "c" .....  | 103  |
| 37.    | Example Calculations of Wave Profile,<br>Kinematics and Dynamic Pressure .....                  | 107  |

LIST OF FIGURES—Continued

| Figure | Page  |
|--------|---|
| 38.    | Free Surface Boundary Condition<br>Errors ..... 111   |
| 39.    | Example 6-b, Shoaling/Refraction<br>for $\alpha_0 = 10^\circ$ . Interpolation<br>from $h/L_0 = 0.0814$ and<br>$H/L_0 = 0.0271$ to<br>$h/L_0 = 0.0542$ ..... 121 |
| 40.    | Interpolation Aid ..... 124   |
| 41.    | Auxiliary Plot of $F'_D$ for<br>Example 7a ..... 127  |
| II-1   | Definition Sketch for Shoaling/<br>Refraction Considerations ..... 149  |
| II-2   | Variation of $F'_{TE}$ and $L'$ for<br>$h/L_0 = 0.02$ ..... 153   |

## LIST OF SYMBOLS

| <u>Symbol</u> | <u>Description</u>   |
|---------------|--|
| BBC           | Bottom boundary condition, defined by Equation (10)  |
| C             | Wave celerity  |
| $C_D$         | Drag coefficient   |
| $C_G$         | Group velocity   |
| $C'_G$        | Dimensionless group velocity, defined by Equation (42)   |
| $C_M$         | Inertia coefficient  |
| D             | Pile diameter  |
| DFSBC         | Dynamic free surface boundary condition, defined in Equation (12)  |
| DFSBP         | Dynamic free surface breaking parameter defined in Equation (49)   |
| $\bar{D}$     | Subscript "D" denoting "design" value, also drag component of force and moment   |
| $e_2$         | Dynamic free surface boundary condition error, utilized by Chappelear and Von Schwind and Reid defined in Equation (17a) |
| $E_1$         | Root mean square error in kinematic free surface boundary condition  |
| $E_2$         | Root mean square error in dynamic free surface boundary condition  |
| $E$           | Mean square error in dynamic free surface boundary condition   |
| $F_D$         | Drag force component   |

LIST OF SYMBOLS—*Continued*

| <u>Symbol</u> | <u>Description</u>   |
|---------------|--|
| $F'_D$        | Dimensionless drag force component, defined by Equation (25)       |
| $F_I$         | Inertia force component  |
| $F'_I$        | Dimensionless inertia force component, defined by Equation (26)    |
| $F_{TE}$      | Total energy flux in direction of wave propagation, per unit width |
| $F'_{TE}$     | Dimensionless form of $F_{TE}$ , defined by Equation (41)          |
| $F_{m_x}$     | Momentum flux in direction of wave propagation                     |
| $F'_{m_x}$    | Dimensionless form of $F_{m_x}$ , defined by Equation (44)         |
| $F_{m_y}$     | Momentum flux transverse to direction of wave propagation          |
| $F'_{m_y}$    | Dimensionless form of $F_{m_y}$ , defined by Equation (45)         |
| $g$           | Gravitational constant   |
| $h$           | Water depth  |
| $h'$          | Freeboard used in establishing deck elevation                      |
| $h_B$         | Breaking water depth   |
| $H$           | Wave height  |
| $H_B$         | Breaking wave height   |
| $H_0$         | Deep water wave height   |
| $j$           | Index used in summation  |
| $J$           | Maximum value of $j$ in summation                                  |

LIST OF SYMBOLS—*Continued*

| <u>Symbol</u>   | <u>Description</u>  |
|-----------------|---|
| KE              | Kinetic energy of waves   |
| KE'             | Dimensionless form of KE, defined by Equation (39)                  |
| KFSBC           | Kinematic free surface boundary condition, defined in Equation (11) |
| KFSBP           | Kinematic free surface breaking parameter, defined by Equation (48) |
| L               | Wave length   |
| L'              | Dimensionless form of L, defined by Equation (37)                   |
| L <sub>0</sub>  | Small amplitude deep water wave length = $gT^2/(2\pi)$              |
| $\bar{L}$       | Subscript "L" denoting "lower"                                      |
| M <sub>D</sub>  | Drag moment component   |
| M' <sub>D</sub> | Dimensionless form of M <sub>D</sub> , defined in Equation (27)     |
| M <sub>I</sub>  | Inertia moment component  |
| M' <sub>I</sub> | Dimensionless form of M <sub>I</sub> , defined in Equation (28)     |
| n               | Index used in summation   |
| NN              | Order of wave theory  |
| p               | Pressure  |
| p <sub>a</sub>  | Atmospheric pressure  |
| p <sub>D</sub>  | Dynamic component of wave pressure                                  |
| p' <sub>D</sub> | Dimensionless form of p <sub>D</sub> , defined in Equation (29)     |
| Q               | Bernoulli term, defined in Equation (8)                             |

LIST OF SYMBOLS—*Continued*

| <u>Symbol</u> | <u>Description</u>   |
|---------------|--|
| $\bar{Q}$     | Average value of $Q$   |
| $S$           | Vertical coordinate, referenced to bottom, positive upwards            |
| $t$           | Time coordinate  |
| $T$           | Wave period  |
| $u$           | Horizontal component of water particle velocity                        |
| $u'$          | Dimensionless form of $u$ , defined in Equation (21)                   |
| $u_M$         | Measured horizontal component of water particle velocity               |
| $u_T$         | Theoretical horizontal component of water particle velocity            |
| $\bar{U}$     | Subscript "U" denoting upper value                                     |
| $w$           | Vertical component of water particle velocity                          |
| $w'$          | Dimensionless form of $w$ , defined in Equation (22)                   |
| $W_{L,U}$     | Weighting coefficients, defined by Equation (50)                       |
| $x$           | Horizontal coordinate  |
| $X$           | Stream function coefficients   |
| $z$           | Vertical coordinate, referenced to still water level, positive upwards |
| $\alpha$      | Wave crest alignment relative to bottom contours                       |
| $\alpha_0$    | Deep water value of $\alpha$   |
| $\alpha_B$    | Wave crest alignment at breaking conditions                            |

LIST OF SYMBOLS—*Continued*

| <u>Symbol</u> | <u>Description</u>  |
|---------------|---|
| $\beta_1$     | Kinematic free surface breaking parameter, defined by Equation (48)   |
| $\beta_2$     | Dynamic free surface breaking parameter, defined by Equation (49)     |
| $\gamma$      | Specific weight of water  |
| $\epsilon_1$  | Distributed error in kinematic free surface boundary condition        |
| $\epsilon_2$  | Distributed error in dynamic free surface boundary condition          |
| $\epsilon_2'$ | Dimensionless form of $\epsilon_2$ , defined by Equation (36)         |
| $\eta$        | Water surface displacement  |
| $\eta'$       | Dimensionless form of $\eta$ , defined by Equation (30)               |
| $\theta$      | Phase angle   |
| $\pi$         | Numerical constant, 3.14159....                                       |
| $\rho$        | Mass density of water   |
| $\sigma$      | Standard deviation  |
| $\phi$        | Velocity potential  |
| $\psi$        | Stream function   |
| $\psi_\eta$   | Stream function value evaluated on free surface of an "arrested" wave |

## ACKNOWLEDGEMENTS

This report has received the benefit of constructive criticism and contributions from a number of individuals. In the initial phases of the study, Messrs. Eric Olsen and Bruce Beechley carried out some of the computer calculations and organization of results. Throughout the study, M. P. O'Brien offered constructive suggestions and discussions concerning the Stream function wave tables. D. Lee Harris served as liaison between the writer and the sponsor and provided encouragement and useful comments regarding the format of the tables. J. R. Weggel attended a short course which centered on the application of the tables and he has made several very useful suggestions which simplified the application of the tables to design problems. R. A. Dalrymple assisted in the later phases of the study by applying some of the Stream function computer techniques which he has developed. Finally, the Coastal Engineering Research Center requested review of an early draft of this report by a number of individuals actively involved in offshore design and/or wave theory studies; the constructive comments and suggestions resulting from these reviews are greatly appreciated.

## I. INTRODUCTION

The following were the primary goals of the research reported herein: (1) for given wave conditions, to establish a rational basis for selection of one of the numerous available progressive water wave theories and (2) to tabulate the most appropriate wave theory or theories in a form convenient for preliminary design use. The main emphasis of this investigation has been an attempt to assist the engineer in his selection and application of wave theories to marine design problems. The research has proceeded in several distinct phases which are described briefly below.

An early phase of the research was related to evaluating the *analytical* validity of water wave theories; that is, the degree to which the various available water wave theories satisfy the equations constituting the mathematical formulation. The results of this phase, first published in September, 1968,<sup>1</sup> established, that of the eight theories included in the study, the Stream function fifth order provided the best fit over a wide range of wave conditions. For very shallow water waves, the Airy and first order Cnoidal theories provided the best fit. However, because the Stream function wave theory can be extended to quite high orders, it was expected that it

would provide the best fit, even for most shallow water wave conditions. Based on the results of this study, the following phases of the study concentrated on further exploration and development of the Stream function wave theory for engineering application.

The second phase represented an examination of near-breaking wave conditions using the Stream function theory.<sup>2</sup> This problem is complicated because breaking conditions represent a mathematical as well as a hydrodynamic instability and therefore the computational aspects are not straightforward. The results of this study indicated that of the two stability criteria, the kinematic criterion rather than the dynamic criterion governs at breaking. It was also found that near breaking, the pressure distribution was hydrostatic rather than characterized by a zero pressure gradient as predicted by some other studies. The complexities of the numerical computations led to an attempt to establish the breaking index for only three relative water depths (shallow, intermediate and deep). It was found that for shallow and deep water waves, the breaking heights established from the Stream function wave theory were up to 28% higher than those established earlier by other investigations. For intermediate depth conditions, however, the breaking heights determined in the study agreed well with those of earlier investigations.

The third phase of the investigation<sup>3</sup> was related to the "experimental validity of water wave theories" as compared to "analytical validity." The motivation of this phase was the recent (1968) publication<sup>4</sup> of a fairly comprehensive set of measurements of water particle velocities for shallow water waves and comparison with a number of wave theories by Le Méhauté, et al.; a comparison with the Stream function theory was therefore conducted as a part of the present study. On an overall basis, the Stream function wave theory provided a significantly better fit to the measured water particle velocities than the other theories. The standard deviation between the measured and Stream function representations was 0.17 ft/sec as compared to 0.24 ft/sec for the theory providing the next best fit. The primary significance of this phase of the study is that the wave conditions are in the shallow-water region where theories other than the Stream function would be expected to provide better comparisons with measurements. Although this favorable comparison is not taken as demonstration of the superiority of the Stream function for all wave conditions, the results were very encouraging and to some extent, surprising.

The final phase of the investigation has been the development of a computer program to tabulate wave quantities that would be of value to engineers in design and that

would also be valuable to individuals concerned with the further development and improvement of water wave theories. During the development of the tables, it has been found that more meaningful information than originally anticipated could be presented.

In the early phases of this study, dimensional variables (i.e., water depth/(wave period)<sup>2</sup> and wave height/(wave period)<sup>2</sup>) were used to characterize the wave conditions; this feature will be evident in the description of some of the results. In the latter phases of the study, a decision was made to characterize the wave conditions by the following dimensionless quantities:  $h/L_0$  and  $H/L_0$ , where  $h$ ,  $H$  and  $L_0$  represent the water depth, wave height and small amplitude deep water wave length, respectively. The tables are developed for forty cases of ( $h/L_0$ ,  $H/L_0$ ).

The results of the research are presented in two volumes. The present report (Volume I) documents the research results and describes the wave tables and their application. Volume II presents the wave tables which have been developed for 40 cases encompassing most conditions encountered in engineering design.

In concluding the Introduction, it should be noted that all of the available wave theories have not been included in the comparisons described earlier. Some of the theories omitted were developed during the period of

this research and some have been available, but were not compared, usually because they are not employed extensively for engineering purposes.

## II. STREAM FUNCTION WAVE THEORY

### *Introduction*

As discussed previously, at an early stage of the research, the study indicated that the Stream function wave theory generally provided a better fit to the boundary conditions and also to available laboratory measurements; the study therefore developed into an effort to explore and develop the Stream function wave theory for engineering application. Prior to presenting this work, the basis for the Stream function wave theory will be described in some detail in an attempt to define the similarities with and differences from other theories. It should be noted that there are two representations of the Stream function theory: (1) for a given wave height,  $H$ , water depth,  $h$ , and wave period,  $T$ , a (symmetrical) representation can be developed to describe the kinematics and dynamics of the motion and (2) for a given *measured* water surface displacement,  $\eta(t)$  representing a single oscillation (e.g., trough-to-trough), a representation can be determined which completely defines the kinematics and dynamics of the wave motion. The first case is, of course, of more interest to designers, whereas in another application, the second case

has been employed for the analysis of hurricane-generated wave and wave force data. Only the first mode has been explored under the present study.

### *Formulation*

The water wave phenomenon of interest here can be idealized as a two-dimensional boundary value problem of ideal flow. The assumption of ideal flow is essential to a mathematical formulation which can be readily solved by known techniques. See Fig. 1 for a definition of terms employed in the formulation.

### *Differential Equation*

Ideal flow incorporates the assumptions of an incompressible fluid and irrotational motion. For pressures normally experienced in progressive water wave motions, the incompressibility assumption can be shown to be quite valid; shock pressures due to a wave breaking against a seawall may be an important exception; however, that case is not encompassed by the results of this research. There may be some question regarding the assumption of irrotational flow. Probably the best reason for this consideration at this stage is that it does allow formulation of a boundary value problem which can be solved in an approximate manner. The solutions can then be compared with measurements to determine the apparent need for the refinement to include a non-zero rotation.

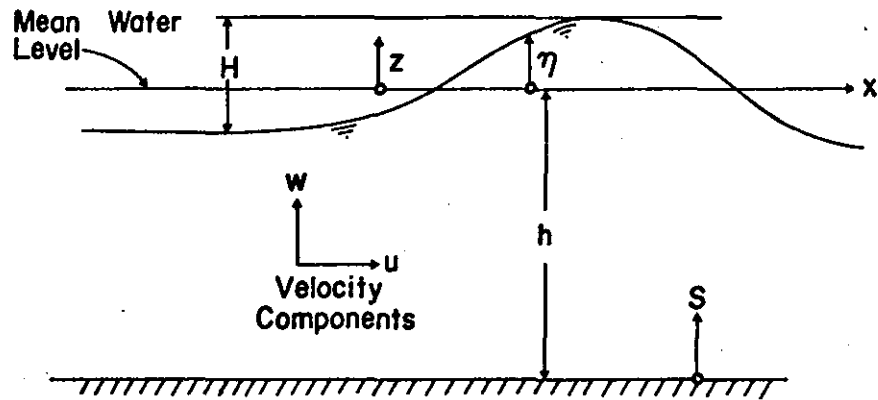


FIGURE 1 DEFINITION SKETCH, PROGRESSIVE WAVE SYSTEM

The differential equation (DE) for two-dimensional ideal flow is the Laplace equation and can be presented in terms of either the velocity potential,  $\phi$  or stream function,  $\psi$ ,

$$\nabla^2 \phi = 0 \quad (1)$$

$$\nabla^2 \psi = 0 \quad (2)$$

where, in two dimensions

$$\nabla^2 \equiv \frac{\partial^2}{\partial x^2} + \frac{\partial^2}{\partial z^2} \quad (3)$$

and  $\phi$  and  $\psi$  are defined in terms of the velocity components  $u$  and  $w$  (see Fig. 1) as

$$\begin{aligned} u &= -\frac{\partial\phi}{\partial x} = -\frac{\partial\psi}{\partial z} \\ w &= -\frac{\partial\phi}{\partial z} = +\frac{\partial\psi}{\partial x} \end{aligned} \quad (4)$$

### *Boundary Conditions*

Two types of boundary conditions are required on the upper and lower surfaces; for the present study, it will be assumed that the depth is uniform. The kinematic boundary condition applies to both boundaries and simply requires that the components of flow at these boundaries be in accordance with the geometry and motion (if any) of the boundaries. This condition can be stated as follows

*Bottom boundary condition (BBC)*

$$w = 0, \quad z = -h \quad (5)$$

*Kinematic free surface boundary condition (KFSBC)*

$$\frac{\partial\eta}{\partial t} + u\frac{\partial\eta}{\partial x} = w, \quad z = \eta(x,t) \quad (6)$$

*Dynamic free surface boundary condition (DFSBC)*

The remaining free surface boundary condition is the so-called dynamic free surface boundary condition (DFSBC) and requires that the pressure immediately below the free surface be uniform and equal to the atmospheric pressure,  $p_a$ .

$$\eta + \frac{P_a}{\rho g} + \frac{1}{2g} (u^2 + w^2) - \frac{1}{g} \frac{\partial \phi}{\partial t} = \text{constant} \equiv Q',$$

$$z = \eta(x, t) \tag{7}$$

In the above formulation, it is tacitly assumed that surface tension effects are negligible. It is customary to incorporate the atmospheric pressure term into the constant,  $Q'$ , to yield a new constant,  $Q$

$$\eta + \frac{1}{2g} (u^2 + w^2) - \frac{1}{g} \frac{\partial \phi}{\partial t} = Q \tag{8}$$

In the formulation presented, no requirements have been placed on the *permanence of wave form*, that is, the wave could change form as it propagates due to the relative motion and interference of components propagating with various phase speeds. The treatment of this general problem including the nonlinearities is quite complex and was not the subject of this research. Rather, in the present investigation, it is assumed that the wave propagates with constant speed,  $C$ , and without change of form. It is then possible to choose a coordinate system propagating with the speed of and in the same direction as the wave, and relative to this coordinate system, the motion does not change and is therefore steady. The time dependency in the formulation vanishes, the horizontal velocity component with respect to the moving coordinate system is  $u-C$ ; and the formulation may be summarized as:

$$\text{DE: } \nabla^2 \phi = \nabla^2 \psi = 0 \quad (9)$$

|                        |   |   |
|------------------------|---|---|
| Boundary<br>Conditions | { | BBC: $w = 0, z = -h$ <span style="float: right;">(10)</span>  |
|                        |   | KFSBC: $\frac{\partial \eta}{\partial x} = \frac{w}{u - C}, z = \eta(x)$ <span style="float: right;">(11)</span>              |
|                        |   | DFSBC: $\eta + \frac{1}{2g} ((u - C)^2 + w^2)$<br>$- \frac{C^2}{2g} = Q, z = \eta(x)$ <span style="float: right;">(12)</span> |
|                        |   | Motion is periodic in $x$ with<br>spatial periodicity of the<br>wave length, $L$ . <span style="float: right;">(13)</span>    |

In order to avoid any misimpressions regarding the assumptions and formulation presented here and those employed in other investigations of nonlinear waves, it is noted that the formulation incorporating the assumption of propagation without change of form is common to the development of all the following nonlinear water wave theories:

Stokes 2nd, and higher order wave theories

Cnoidal 1st and 2nd order theories by Keulegan & Patterson, Laitone, etc.

Solitary wave theory, 1st order by Boussinesq

Solitary wave theory, 2nd order by McCowan

Stream function wave theory by von Schwind and Reid

To reiterate, *analytical validity* will be based on the degree to which a theory satisfies the boundary value problem formulation, Equations (9) - (13). If a theory could be found which provided exact agreement to the

formulations, then the analytical validity would be perfect. There is no guarantee that good analytical validity ensures that a theory will provide a good representation of the natural phenomenon because implicit in the formulation are the assumptions that capillary and rotation forces and other effects are negligible. *Experimental validity* will be based on the agreement between wave theories and measured data.

### *The Stream Function Solution*

For the formulation expressed in Equations (9) - (13), a Stream function solution may be expressed as:

$$\psi(x, z) = \frac{L}{T} z + \sum_{n=1}^{NN} X(n) \sinh \left( \frac{2\pi n}{L} (h + z) \right) \cos \left( \frac{2\pi n}{L} x \right) \quad (14)$$

Evaluating this expression on the free surface, i.e., setting  $z = \eta$ , we find

$$\eta = \frac{T}{L} \psi_{\eta} - \frac{T}{L} \sum_{n=1}^{NN} X(n) \sinh \left( \frac{2\pi n}{L} (h + \eta) \right) \cos \left( \frac{2\pi n}{L} x \right) \quad (15)$$

where NN represents the "order" of the representation, i.e., the number of terms contributing to the series expression,  $\psi_{\eta}$  represents the (constant) value of the Stream function

on the free surface,  $L$  is the (undetermined) wave length, and the  $X(n)$  represent, at this stage, undetermined coefficients.

For particular wave conditions, it is regarded that the wave height, period and water depth are specified. Equation (14) exactly satisfies the governing differential equation and the bottom and free surface kinematic boundary conditions for arbitrary values of  $L$ ,  $\psi_\eta$  and the  $X(n)$  coefficients. The Stream function expression is also periodic in  $x$  with wave length,  $L$ . The only remaining boundary condition is the dynamic free-surface boundary condition; the parameters  $L$  and the  $X(n)$ 's are to be chosen such that this boundary condition is best satisfied for a specified wave height.

The procedure for determining the unknown parameters, which can be considered as a nonlinear numerical perturbation procedure, is presented in Appendix I.

### III. EVALUATION OF VALIDITIES OF WAVE THEORIES

#### *Introduction*

As discussed earlier, there are two types of validity that were examined. "Analytical validity" is based on the degree to which a theory satisfies the governing equations (of the boundary value problem formulation). Good analytical validity, however, does not *necessarily* imply good representation of the natural phenomenon. "Experimental validity" is based on the agreement between a theory and measurements. To date, some reasonably good laboratory data are available, and at least two field measurements of water particle velocities are reportedly underway (as of 1972) in the petroleum industry, and hopefully, will be available within the next few years.

#### *Discussion of Differences Between Stream Function and Other Wave Theories*

In later paragraphs of this section, it will be shown that the Stream function wave theory provides a better fit than other theories to the boundary conditions and also provides a better fit to laboratory measurements of water particle velocities; it is therefore worthwhile

to compare some of the inherent features of the Stream function and other theories. Although it is difficult to discuss *all* other theories in general statements, an attempt will be made to present the more significant representative differences.

Consider, as an example, the Stokes higher order wave theories. The general *form* of the solution exactly satisfies the differential equation, the bottom boundary condition and, of course, is properly periodic in the *x*-direction. The solution does not provide exact fits to either the kinematic or dynamic free surface boundary conditions. Suppose that the  $(n-1)$ *th* order solution is known and that the *n**th* order theory is to be developed. The *n**th* coefficients are determined such that they minimize the errors in the two free surface boundary conditions at the  $(n-1)$ *th* order. A significant problem is that the configuration of the *n**th* order water surface is not known, *a priori*; it is therefore necessary to best satisfy the boundary conditions on an approximate expansion of the *n**th* order water surface. The *apparent* effect of minimizing the errors present on the approximate *n**th* order water surface is that the resulting theory of a given order, if convergent, may not provide the best fit possible for the number of terms (order) included.

As a comparison with the preceding discussion of the Stokes' theory, consider the corresponding features of

a Stream function theory solution. The general form of the solution exactly satisfies all of the boundary value problem requirements except the DFSBC; at this stage, one inherent advantage of the Stream function theory is evident which is that all of the "free" parameters can be chosen to provide a best fit to the DFSBC. A second and important inherent advantage is that for a given  $n$ th order wave theory, *all* of the coefficients are chosen such that they best satisfy the boundary condition on the  $n$ th order water surface. The distinction is that because a numerical iteration approach is used, the  $n$ th order wave form is known (through iteration) at that order of solution. Other advantages of the Stream function wave theory are that a solution can readily be obtained to any reasonable order, and that a measure of the fit to the one remaining boundary condition is more or less automatically obtained in the course of the solution. Also, the form of the terms in the solution is inherently better for representing nonlinear waves due to the  $\eta$  term appearing in the argument of the hyperbolic sine term (cf. Equation (15)). The disadvantage of the Stream function wave theory is that, unless tabulated parameters are available, it does require the use of a digital computer with a reasonably large memory. The complexity of other nonlinear theories, however, generally also requires the use of a high speed computer. It is noted that a similar but different Stream

function wave theory has been developed and reported by Von Schwind and Reid <sup>5</sup> subsequent to the analytical validity study reported herein and employs a definition of the DFSBC error which is different than that in the present study. The paper by Von Schwind and Reid presents boundary condition errors for three wave cases; a comparison between their errors and those resulting from the Stream function theory described herein will be presented.

#### *Analytical Validity*

The analytical validity of a particular wave theory has been previously defined as the degree to which the theory satisfies the defining equations, i.e., Equations (9) - (13). Again, for the sake of emphasis, it is noted that a theory providing an exact fit to the boundary conditions would have a perfect analytical validity, however, due to assumptions of ideal flow, etc., in the formulation of the problem, a perfect analytical validity does not ensure that the theory would provide a good representation of the laboratory or field phenomenon. The reason for viewing the problem in two steps, i.e., analytical and experimental validity, is that the results of the analytical validity test would at least tend to indicate the relative applicability of the available wave theories for particular wave conditions and also the results would provide guidance

whether the most fruitful approach would be directed toward a more representative formulation of water wave theories or toward the improvement of the solutions of existing formulations.

*Definition of Boundary Condition Errors*

Most wave theories exactly satisfy the governing differential equation and bottom boundary condition, although some the solutions only approximately satisfy the differential equation. Table A lists a number of the theories available for design use and also indicates the conditions of the formulation which are satisfied exactly by each of the theories. Inspection of Table A shows that the two nonlinear (free surface) boundary conditions provide the best basis for assessing the analytical validity because no theory exactly satisfies both of these conditions.

Errors based on the dynamic and kinematic free surface boundary conditions, are defined as functions of phase angle ( $\theta$ ) as follows:

$$\epsilon_1(\theta) \equiv \frac{\partial \eta}{\partial x} - \frac{w}{u - c} \quad (16)$$

$$\epsilon_2(\theta) \equiv \eta + \frac{1}{2g} [(u - c)^2 + w^2] - \frac{c^2}{2g} - \bar{Q} \quad (17)$$

TABLE A

Water Wave Theories Included in Evaluation  
Presented in Reference 1

| Theory  | Exactly Satisfies |     |       |       | Reference |
|---|-------------------|-----|-------|-------|-----------|
|   | DE                | BBC | KFSBC | DFSBC |           |
| Linear Wave Theory<br>(Airy)  | X                 | X   |       |       | 6         |
| Third Order Stokes<br>(Skjelbreia and<br>Hendrickson, as<br>summarized by Le<br>Méhauté and Webb) | X                 | X   |       |       | 7         |
| Fifth Order Stokes<br>(Skjelbreia and<br>Hendrickson)   | X                 | X   |       |       | 8         |
| First Order Cnoidal<br>(Laitone)  |                   | X   |       |       | 9         |
| Second Order<br>Cnoidal (Laitone)   |                   | X   |       |       | 9         |
| First Order Solitary<br>(Boussinesq, as<br>Summarized by<br>Munk)                                 | X                 | X   |       |       | 10        |
| Second Order Solitary<br>(McCowan as<br>Summarized by<br>Munk)                                    | X                 | X   | X     |       | 10        |
| Stream Function<br>Numerical Wave<br>Theory (Dean)<br>Fifth Order                                 | X                 | X   | X     |       | 11        |

where  $\bar{Q}$  represents the mean value of the quantity  $Q$  (Bernoulli "constant") defined in Equation (12). "Overall" errors are defined as the root mean squares of the distributed errors,

$$E_1 \equiv \sqrt{\frac{1}{J} \sum_{j=1}^J \epsilon_{1j}^2} \equiv \sqrt{\epsilon_1^2} \quad (18)$$

$$E_2 \equiv \sqrt{\frac{1}{J} \sum_{j=1}^J \epsilon_{2j}^2} \equiv \sqrt{\epsilon_2^2} \quad (19)$$

where  $j$  represents sampling at various (evenly spaced) phase angles.

#### *Results of Analytical Validity Comparison*

Most of the results of the study of analytical validity carried out under this project has been published elsewhere<sup>1</sup> and therefore will only be reviewed briefly here.

The study included forty wave cases as shown in Figure 2. For each of these cases, the overall errors,  $E_1$  and  $E_2$  were calculated for the wave theories shown in Table A. The overall dynamic free surface boundary condition errors were made dimensionless by dividing by the wave height,  $H$ , i.e.

$$E_2' = E_2/H \quad (20)$$

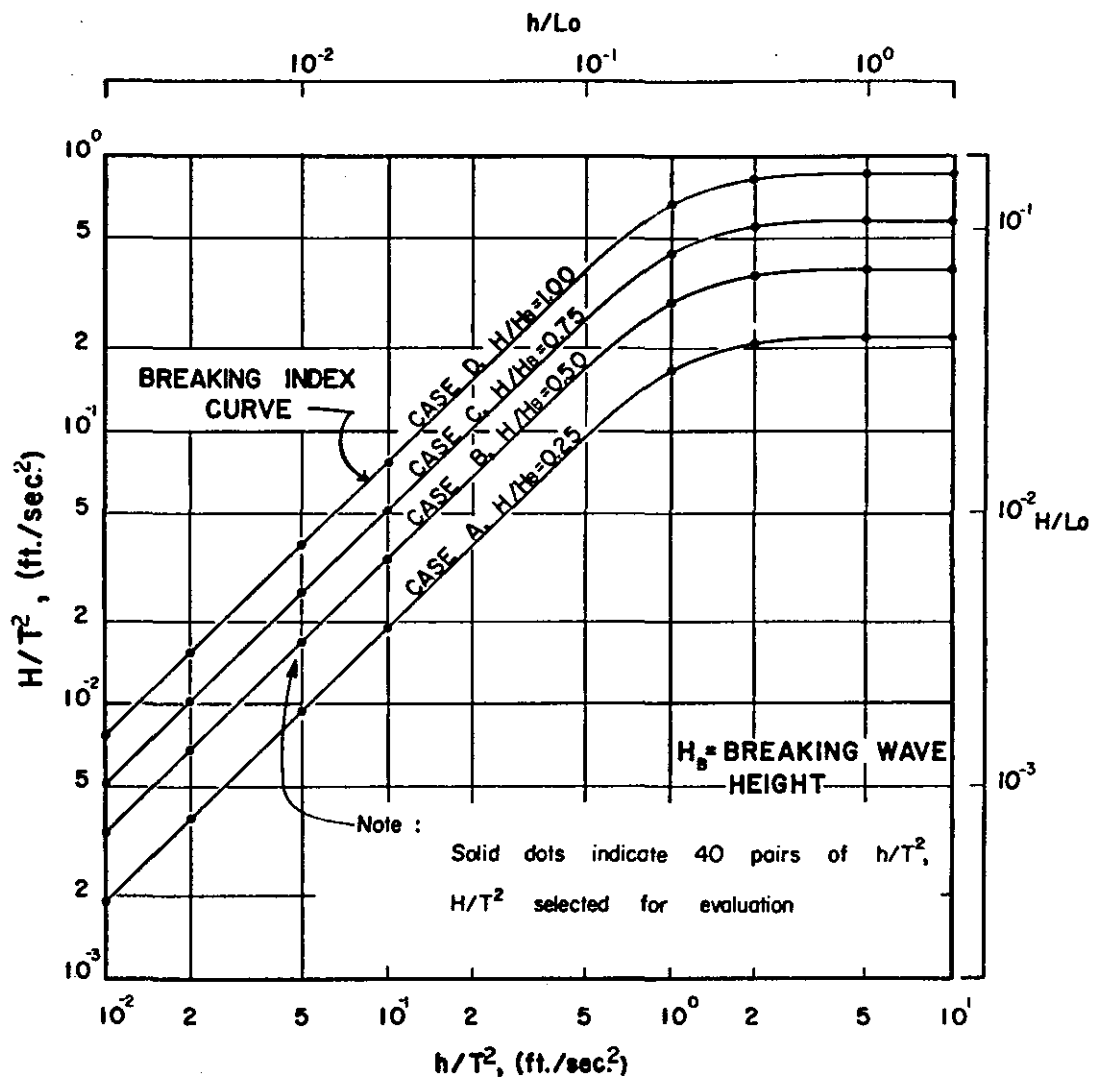


FIGURE 2. WAVE CHARACTERISTICS SELECTED FOR EVALUATION.

The overall kinematic free surface boundary condition error is dimensionless as defined in Equation (18).

Plots of the dimensionless kinematic and dynamic free surface boundary condition errors are presented in Figures 3, 4, 5, and 6 for Cases of  $H/H_B = 0.25$  and  $1.0$  ( $H_B =$  breaking wave height). It is noted that the KFSBC error is identically zero for the Stream function and McCowan theories.

As stated previously, it is difficult to select a single index that would clearly be representative of the overall validity of all wave theories. However, an index was chosen which provided an especially severe test for the Stream function wave theory, and yet this theory emerged as providing the best general analytical validity.

The following evaluation plan was adopted, the results of which would be somewhat biased against the Stream function wave theory. Most of the wave theories do not satisfy exactly either the DFSBC or KFSBC, however, the Stream function theory does satisfy exactly the KFSBC. It therefore seems reasonable that if the Stream function wave theory can be shown to compare favorably against other theories on the basis of *only* the DFSBC, then it should provide an even better analytical validity than the comparison shows.

In the analytical validity investigation, the eight wave theories shown in Table A were examined. Because the

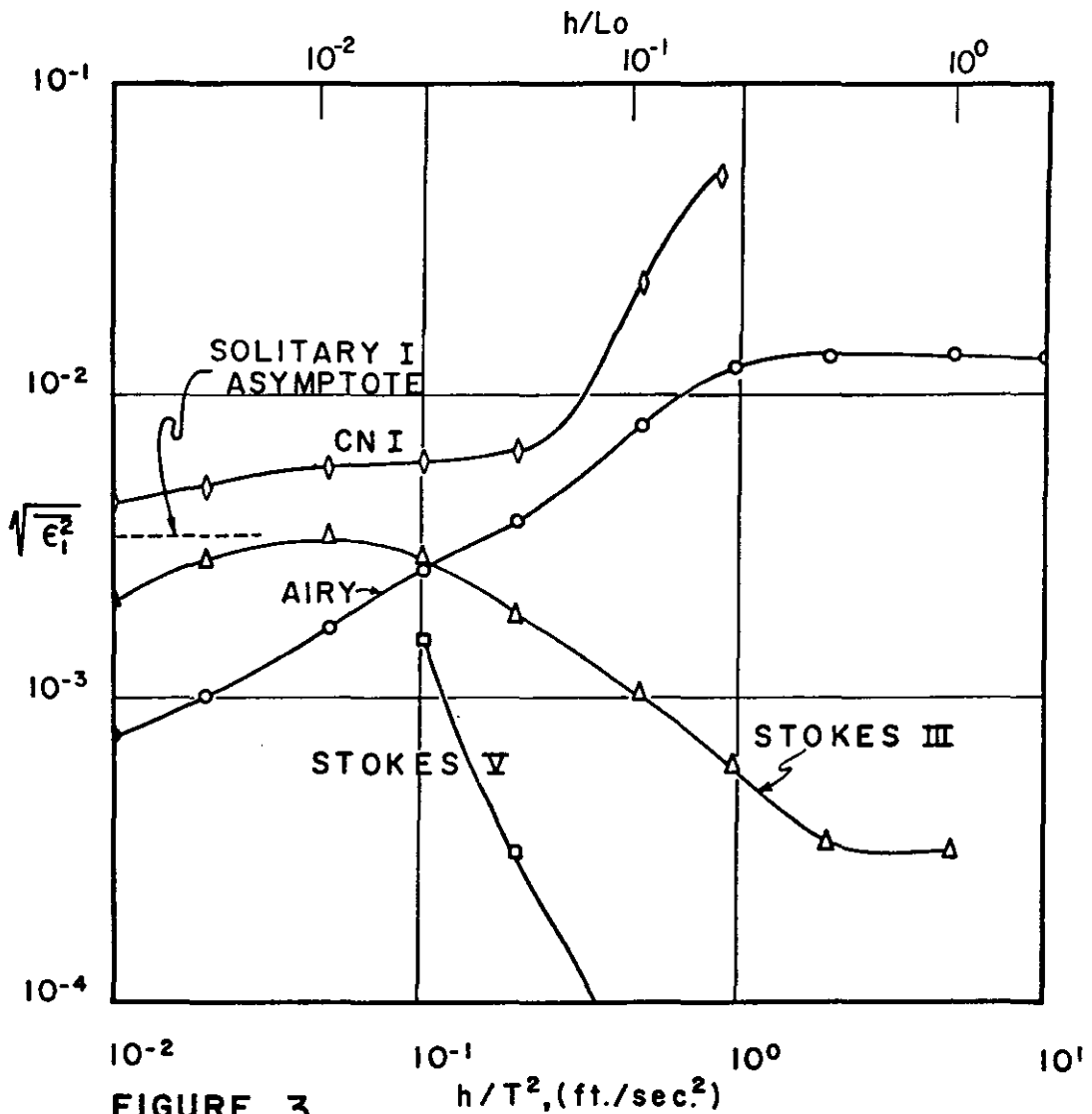
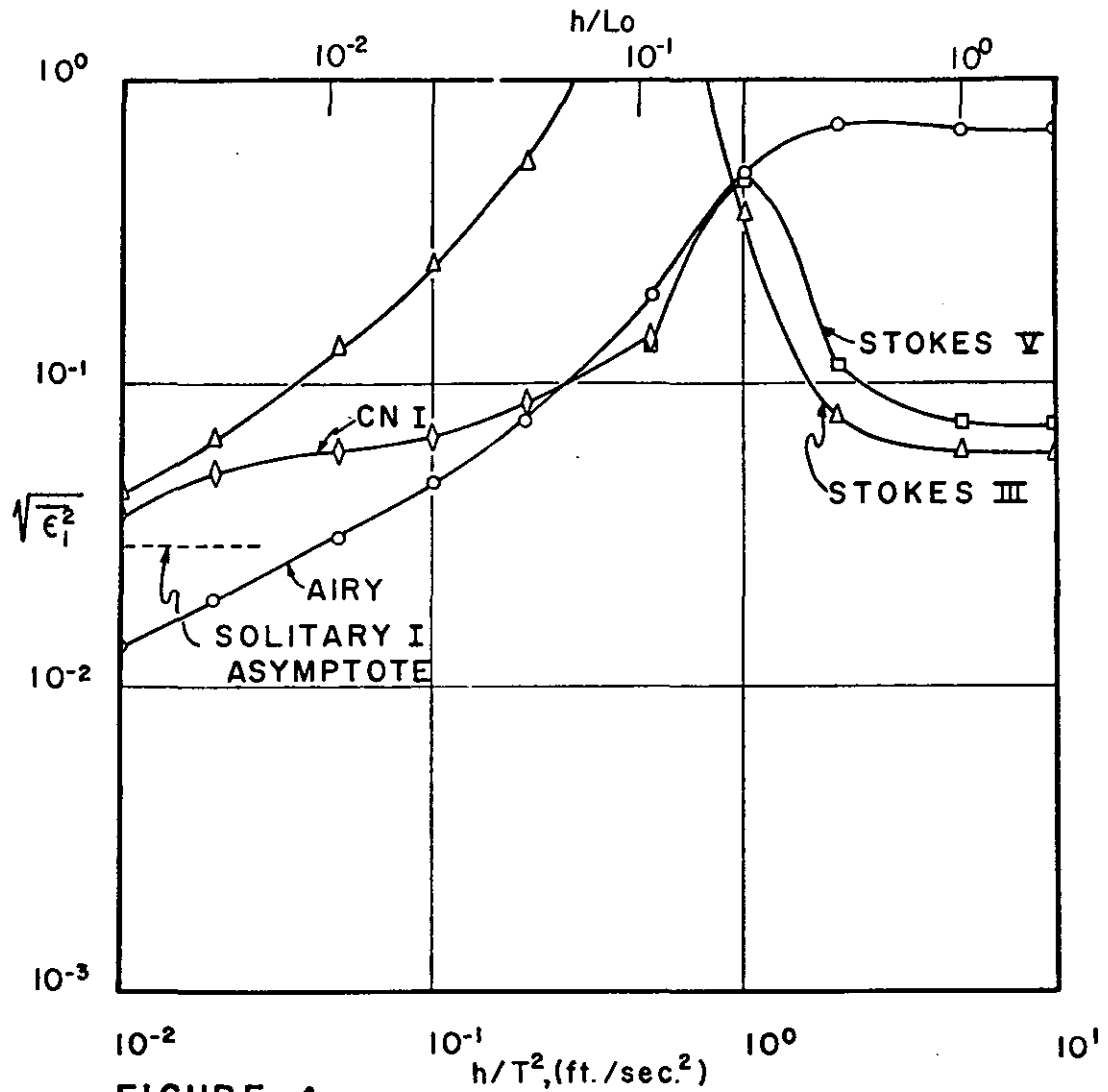


FIGURE 3.  
 DIMENSIONLESS ERROR,  $\sqrt{\epsilon_i^2}$ , IN KINEMATIC  
 FREE SURFACE BOUNDARY CONDITION,  
 $H/H_b = 0.25$ ; ALL WAVE THEORIES



**FIGURE 4.**  
 DIMENSIONLESS ERROR,  $\sqrt{\epsilon_1^2}$ , IN KINEMATIC  
 FREE SURFACE BOUNDARY CONDITION,  
 $H/H_0=1.0$ ; ALL WAVE THEORIES

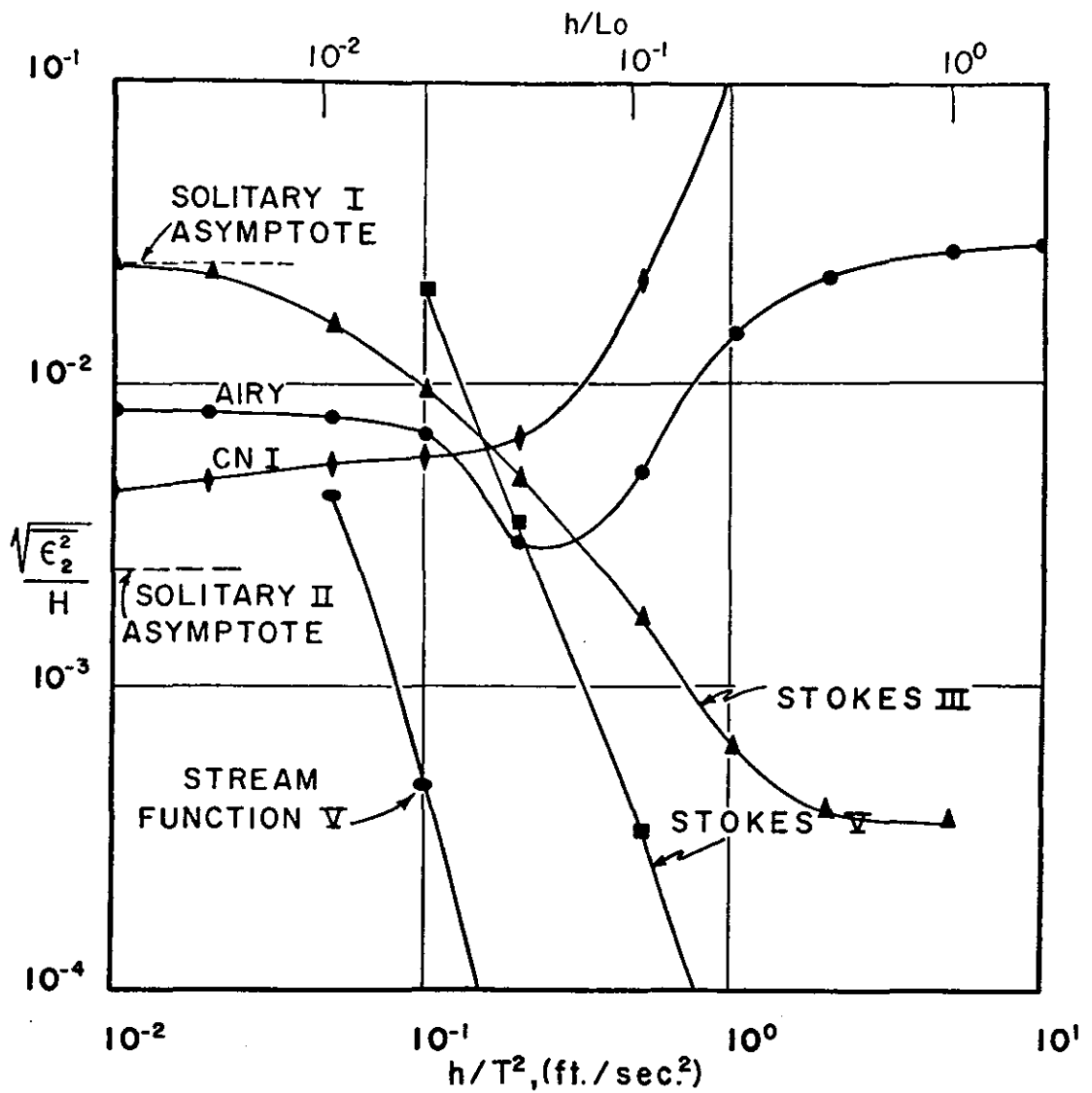


FIGURE 5.  
 DIMENSIONLESS ERROR,  $\sqrt{\epsilon_2^2}/H$ , IN DYNAMIC  
 FREE SURFACE BOUNDARY CONDITION,  
 $H/H_0 = 0.25$ , ALL WAVE THEORIES

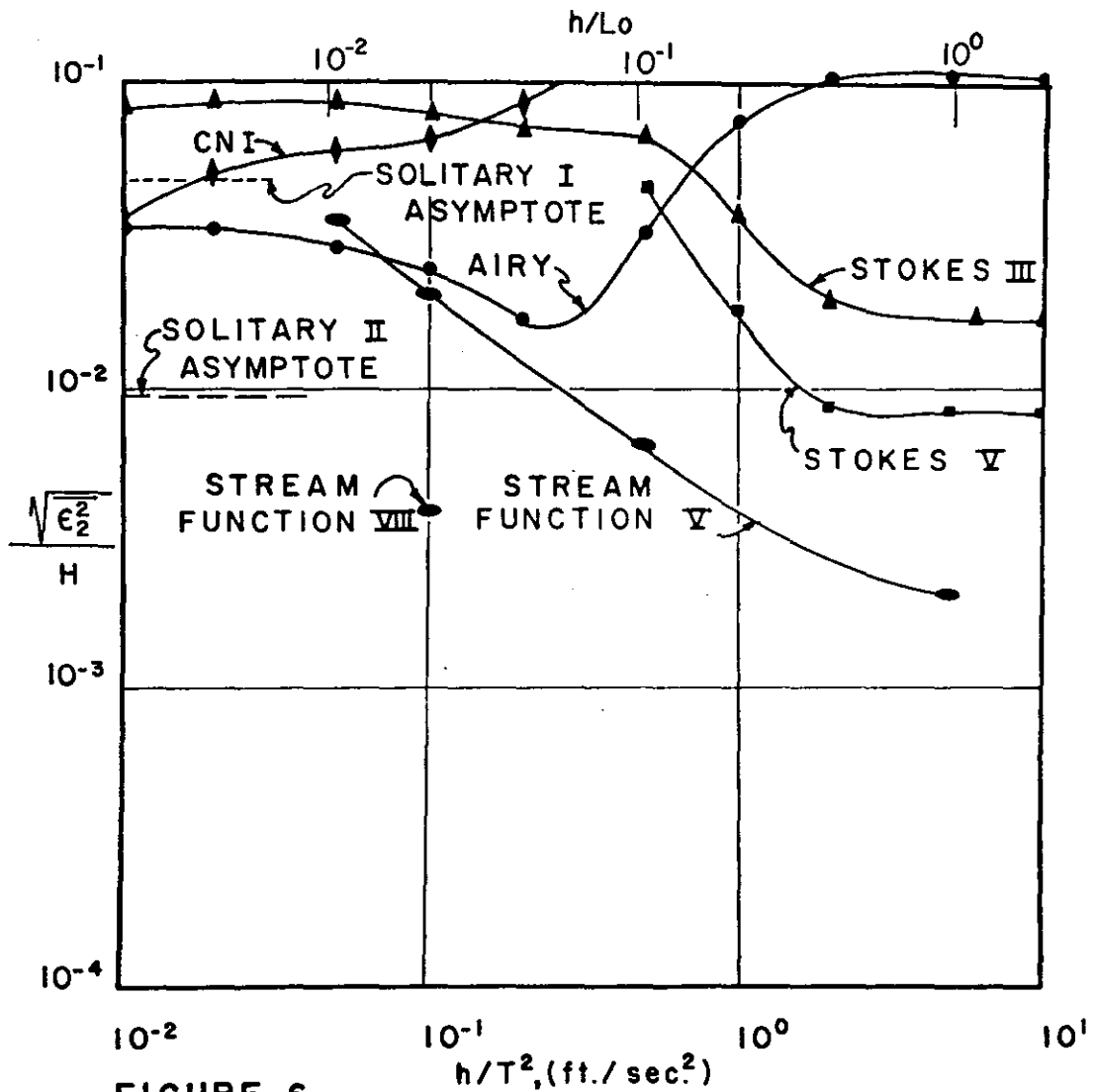


FIGURE 6.  
 DIMENSIONLESS ERROR,  $\sqrt{\epsilon_2^2}/H$  IN DYNAMIC  
 FREE SURFACE BOUNDARY CONDITION,  
 $H/H_0=1.0$ ; ALL WAVE THEORIES

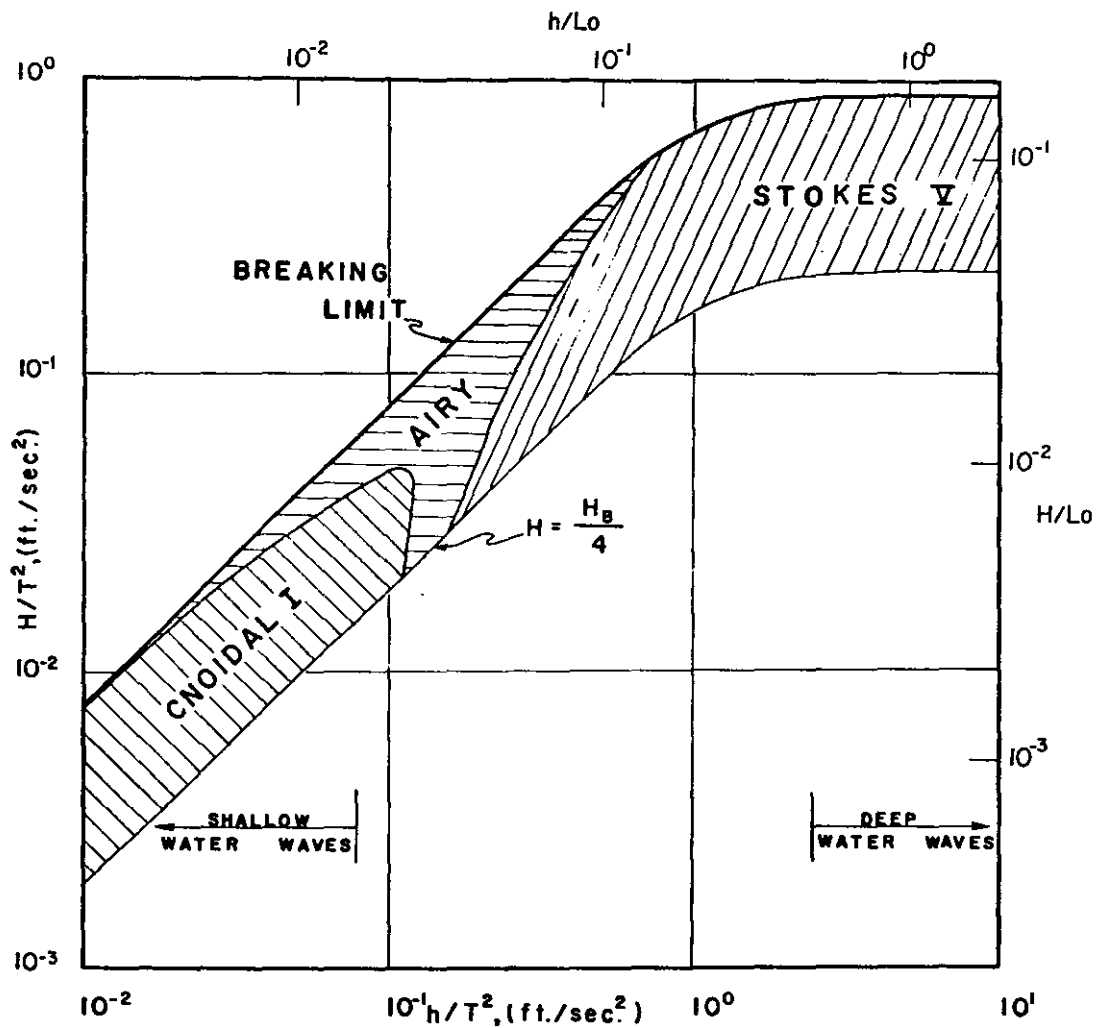
fifth order was the highest of the Stokes theories available, it was somewhat arbitrarily decided to include the Stream function wave theory only to the fifth order.

The evaluation was then based on comparisons presented in Figures 3, 4, 5, and 6 and also on the corresponding figures for  $H/H_B = 0.50$  and  $0.75$ , which are not presented here. The results of this study are shown in Figures 7 and 8.

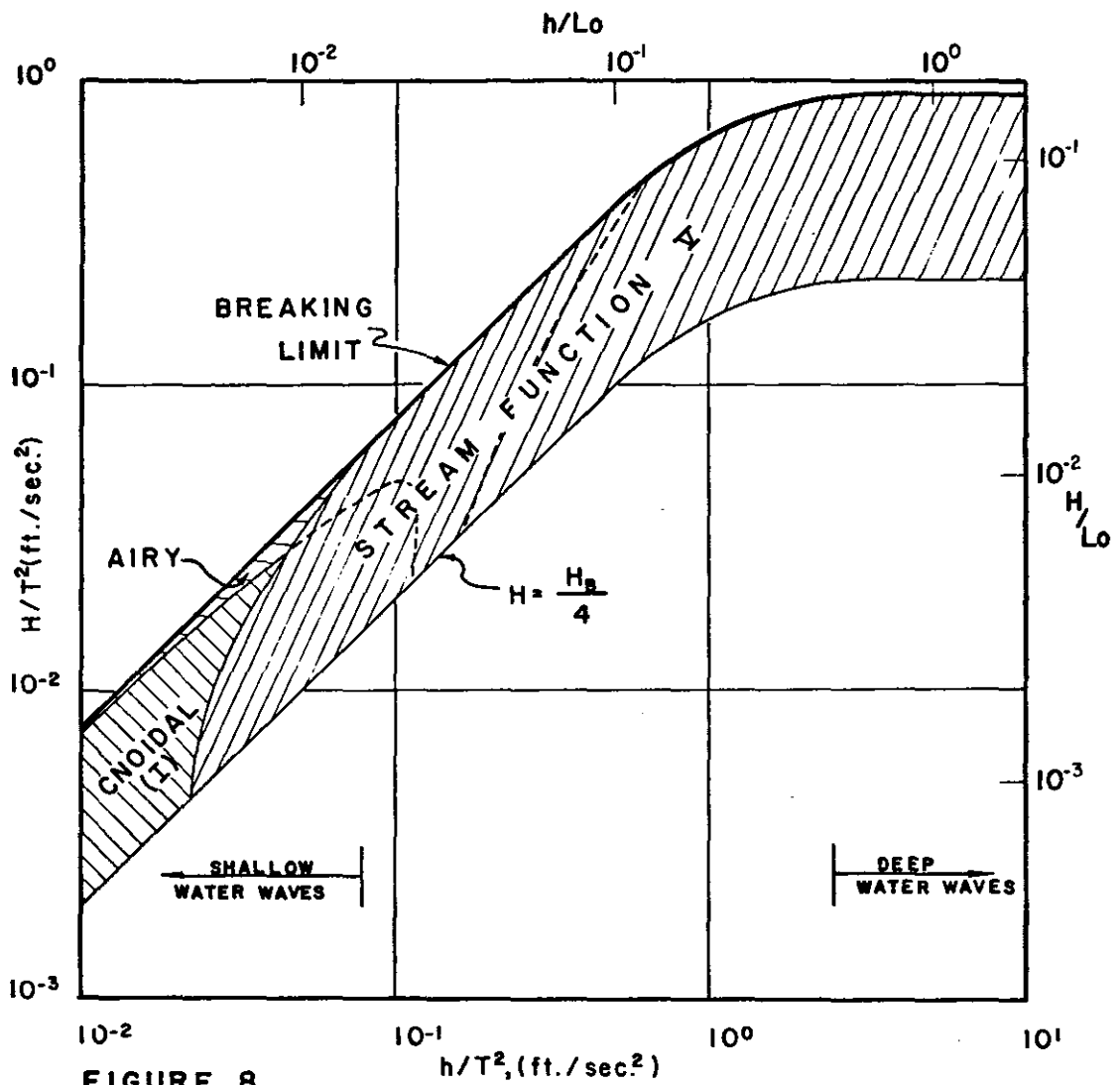
Figure 7 presents the results for all theories excluding the Stream function wave theory. It is seen that the Stokes V theory provides the best fit for deep water, the Airy theory provides the best fit in a portion of the intermediate and shallow water ranges and the first order Cnoidal wave theory generally provides the best fit in the shallow water range.

Figure 8 presents the same type of information, only the fifth order Stream function theory is included and provides the best fit over a wide range including *all* of the intermediate and deep water wave regions and also a significant portion of the shallow water range included in the comparison. The Airy wave theory provides the best fit for a small portion of the shallow water near-breaking waves and the first order Cnoidal wave theory provides the best fit for the remainder of the shallow-water region.

In evaluating the results obtained in the shallow water region, it is noted that one eighth order Stream



**FIGURE 7.**  
**PERIODIC WAVE THEORIES PROVIDING BEST FIT TO**  
**DYNAMIC FREE SURFACE BOUNDARY CONDITION**  
**(ANALYTICAL THEORIES ONLY)**



**FIGURE 8.**  
**PERIODIC WAVE THEORIES PROVIDING BEST FIT TO**  
**DYNAMIC FREE SURFACE BOUNDARY CONDITION**  
**(ANALYTICAL AND STREAM FUNCTION  $\Psi$  THEORIES)**

function wave theory was calculated for breaking wave conditions and  $h/T^2 = 0.1 \text{ ft/sec}^2$  as shown in Fig. 6. Inspection of this figure indicates that the use of higher order Stream function wave theories would extend the range of best validity of this theory to considerably shallower conditions (Fig. 8).

*Comparison with Stream function theory developed  
by Von Schwind and Reid*

As noted earlier, Von Schwind and Reid<sup>5</sup> have developed a Stream function theory with basic similarities to that employed in the present study. The principal difference between the two theories is that Von Schwind and Reid transform their problem to and carry out their solution in the complex plane. It is noted that their solution in terms of wave length and coefficients is also obtained by iteration. The DFSBC error definition used by Von Schwind and Reid was originally defined by Chappellear<sup>12</sup> and is somewhat different than that employed here (Equation 17) and is

$$e_2(\theta) = \frac{\varepsilon_2(\theta)}{\bar{Q} + h} \quad (17a)$$

It is noted by comparison of Equations (17) and (17a), that the *actual* distribution of DFSBC errors would appear as numerically smaller based on Equation (17a) due to the water depth and Bernoulli constant appearing in the denominator.

Von Schwind and Reid presented distributed DFSBC errors for three sets of wave conditions. Errors were calculated for the same wave conditions using the present theory. Figures 9, 10, and 11 are reproduced from Von Schwind and Reid<sup>5</sup> and the maximum errors obtained by the present theory (indicated University of Florida) are shown for each wave case. The maximum UF errors obtained are so small that it would not be worthwhile to show them graphically. Note that all errors ( $e_2$ ) shown in Figs. 9, 10, and 11 are based on Equation (17a). The reason that the errors obtained by the present theory are smaller than those obtained by Von Schwind and Reid is not known. With a numerical solution, it is possible to obtain a low error (down to some limit) by increasing the order of the theory or by increasing the number of iterations used to obtain the solution. For the three cases shown in Figs. 9-11, the University of Florida waves were seventh order and each solution was obtained by 15 iterations; the corresponding values for the Von Schwind-Reid waves are not known.

*Conclusions Resulting from the Analytical  
Validity Study*

The analytical validity evaluation is based on the degree to which the various theories satisfy the governing equations in the boundary value problem formulation. It is stressed again that there is no

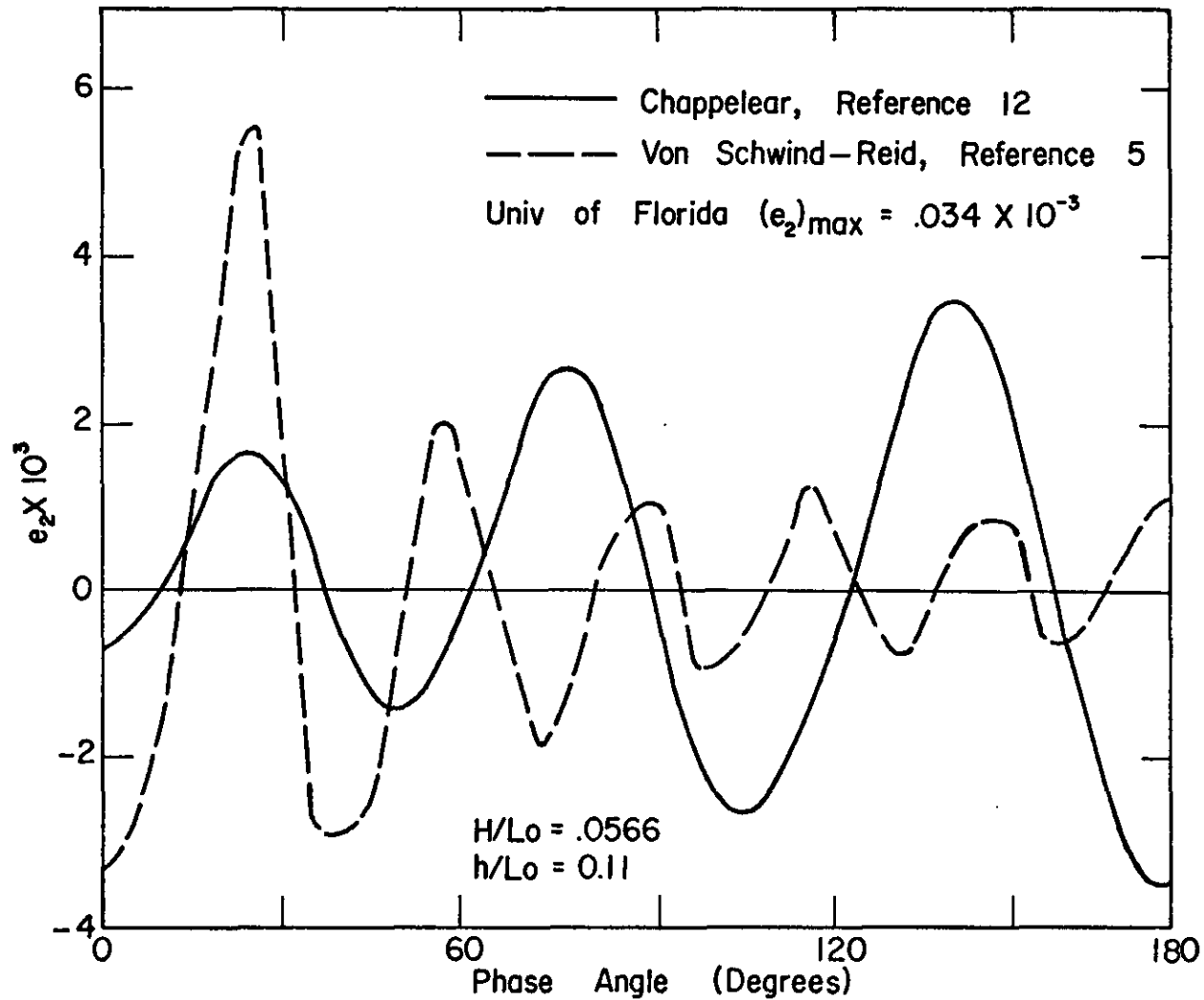


FIGURE 9 COMPARISON OF ERRORS IN DYNAMIC FREE SURFACE BOUNDARY CONDITION FOR THREE NUMERICAL WAVE THEORIES, WAVE NO. 1 (Figure Modified From Reference 5)

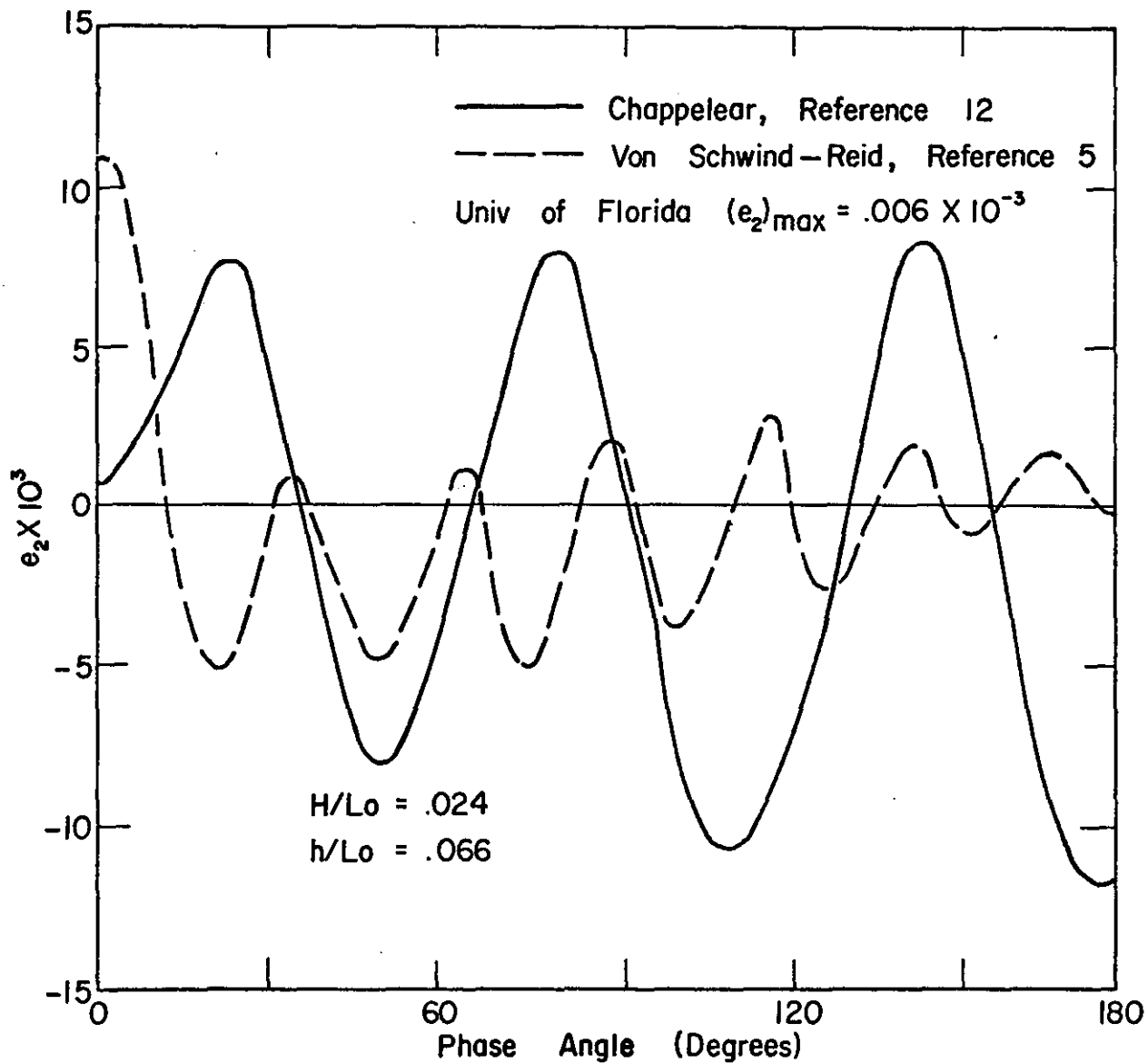


FIGURE 10 COMPARISON OF ERRORS IN DYNAMIC FREE SURFACE BOUNDARY CONDITION FOR THREE NUMERICAL WAVE THEORIES, WAVE NO. 2 (Figure Modified From Reference 5)

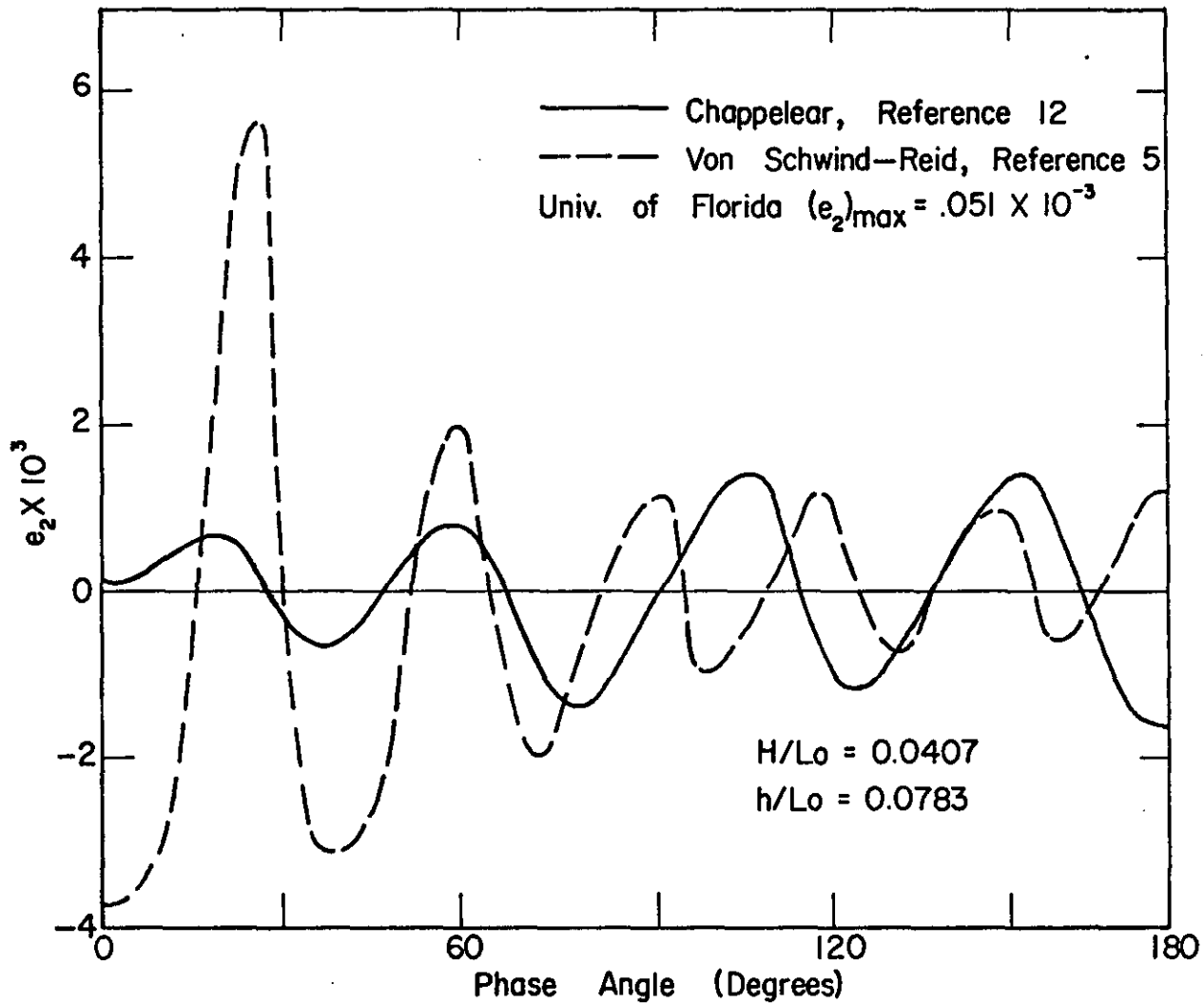


FIGURE 11 COMPARISON OF ERRORS IN DYNAMIC FREE SURFACE BOUNDARY CONDITION FOR THREE NUMERICAL WAVE THEORIES, WAVE NO. 3 (Figure Modified From Reference 5)

guarantee that a theory providing a good analytical validity will necessarily represent well the features of the natural wave phenomenon. The reason, of course, is there there are assumptions (negligible viscosity and capillary effects) introduced into the governing equations which may adversely affect the degree to which the formulation represents real wave motion. The purpose of the analytical validity study, rather, was to attempt to resolve the question of whether the theories developed for the same formulation and for various regions of relative depth do indeed provide the best fit in these regions. Also this study, combined with some additional studies reported later in this report do aid in determining whether the most critical need in wave theory research is in the improvement of the formulation or in the development of improved solutions to the existing formulation.

The results of the analytical validity study have shown that:\*

1. The general status of wave theories for  $h/T^2 > 0.2$  ft/sec<sup>2</sup> for instance, is much more satisfactory than for the smaller values of  $h/T^2$ . In particular, for the larger relative depths, there is reasonable consistency between the fits to the dynamic free surface boundary condition and the maximum drag force as calculated by the various theories including a seventh order Stream function theory. In

---

\*The reader is referred to Reference 1 for reinforcement of statements presented.

shallow water, it is not clear that the boundary condition fit is an appropriate measure of wave theory validity, unless the associated errors are very small. In particular, the Airy wave theory provides a relatively good fit to the boundary conditions in shallow water; however this theory does not represent many of the observed features of shallow water waves including the strong skewness of the wave profile about the mean water level.

2. The Stokes higher order wave theories converge to accurate representations of wave motion in deep water; however, in intermediate and shallow water, the boundary condition fits are relatively poor. Furthermore, no fifth order Stokes theory solution could be found for shallow water waves or the smaller values of the intermediate depth ranges. The limiting value of  $h/T^2$  for which a solution exists, depends on  $H/T^2$  and was in the range of  $0.1 < h/T^2 < 0.5 \text{ ft/sec}^2$  for the conditions examined.
3. Finally, it is observed that the second order Cnoidal theory provided a worse fit to the boundary conditions than the first order Cnoidal theory for all wave conditions examined. There are other versions of Cnoidal theories; the boundary condition fits of these theories have not been evaluated in this study.
4. The Stream function wave theory described in this report provides good analytical validity over a wide range of wave conditions.

#### *Experimental Validity*

As previously described, experimental validity is based on the comparison of theoretical predictions and measured wave phenomena. If it could be generally shown that the theory providing the best analytical validity also provides the best experimental validity, then one could conclude that the formulation is valid and

that errors in the boundary conditions are also good indicators of experimental validity. If the differences between the theory and experiments were of the same order as the estimated experimental error, and if this could be shown to be the situation generally, then the most productive direction in water wave research on this problem would be improved measurements. If however, the disagreement between theory and experiment is much larger than can be attributed to experimental error and, especially if this difference were of considerable engineering significance, then additional efforts on the formulation and solution of water wave theories would be indicated.

The availability of data is inadequate to carry out a comprehensive evaluation of experimental validity over all ranges of relative depth and heights of engineering importance. Le Méhauté et al.,<sup>4</sup> have carried out a measurement program in which distributions over depth of horizontal water particle velocities were measured under the crest phase position of fairly high waves in the shallow and intermediate depth range. The results included measured horizontal water particle velocity distributions for eight cases, and also a vertical water particle velocity distribution for one case, and one measured wave profile. Le Méhauté et al., compared

a number of wave theories with their data, however the Stream function theory was not included; the experimental validity reported in this study was based on a comparison of the Stream function wave theory with the data described earlier. It should be emphasized that the only addition to the paper by Le Méhauté et al., presented in Reference 4 is (1) comparison of the Stream function wave theory with the data and (2) calculations which represent the overall agreement between the data and several of the theories. In the Stream function horizontal velocity component profiles presented, a uniform mass transport velocity has been subtracted out, whereas due to time limitations, the other theoretical velocity distributions were simply plotted from Reference 4. It is not clear whether or not the mass transport term should be subtracted out; although the experiments were conducted in a closed tank, the data were taken before waves reflected from the beach had propagated back to the tank test section and the zero net flow over depth had probably not been established completely.

In all, data for 10 different wave conditions are available. These waves are in the shallow and intermediate relative depth regions, and according to the conventional breaking criteria, the wave heights range from 0.43 to 0.70 of the breaking height. The wave

conditions are shown as points in Fig. 12 where isolines representing various ratios of wave height to breaking wave height are also presented. It is emphasized that the breaking wave height in Fig. 12 is the conventional breaking height: i.e.,  $H/h = 0.78$  in shallow water (McCowan)<sup>10</sup>;  $H/L = 0.142$  in deep water (Michell)<sup>13</sup>; in the intermediate range the breaking limit was first established by Reid and Bretschneider<sup>14</sup> by interpolating on the basis of measured data and is presented in a number of more available references<sup>6,15</sup>. A recent paper by Divoky et al.,<sup>16</sup> reports an experimentally determined shallow water breaking limit of approximately  $H_B/h = 0.60$  to  $0.66$  as compared to the conventional value of  $0.78$ . The recent experiments resulting in the lower value were obtained with a laterally converging wave channel. Certainly it is apparent that more work is needed to better resolve wave breaking limits.

Table B presents the comparison results included in the experimental validity evaluation. The eight comparisons of horizontal water particle velocity are presented in Figs. 13-20; the vertical velocity comparison is presented in Fig. 21; and the wave profile is presented in Fig. 22.

Inspection of Figs. 13-20 indicates that the Stream function theory is in reasonable agreement with the data. It is noteworthy that the shallow water wave

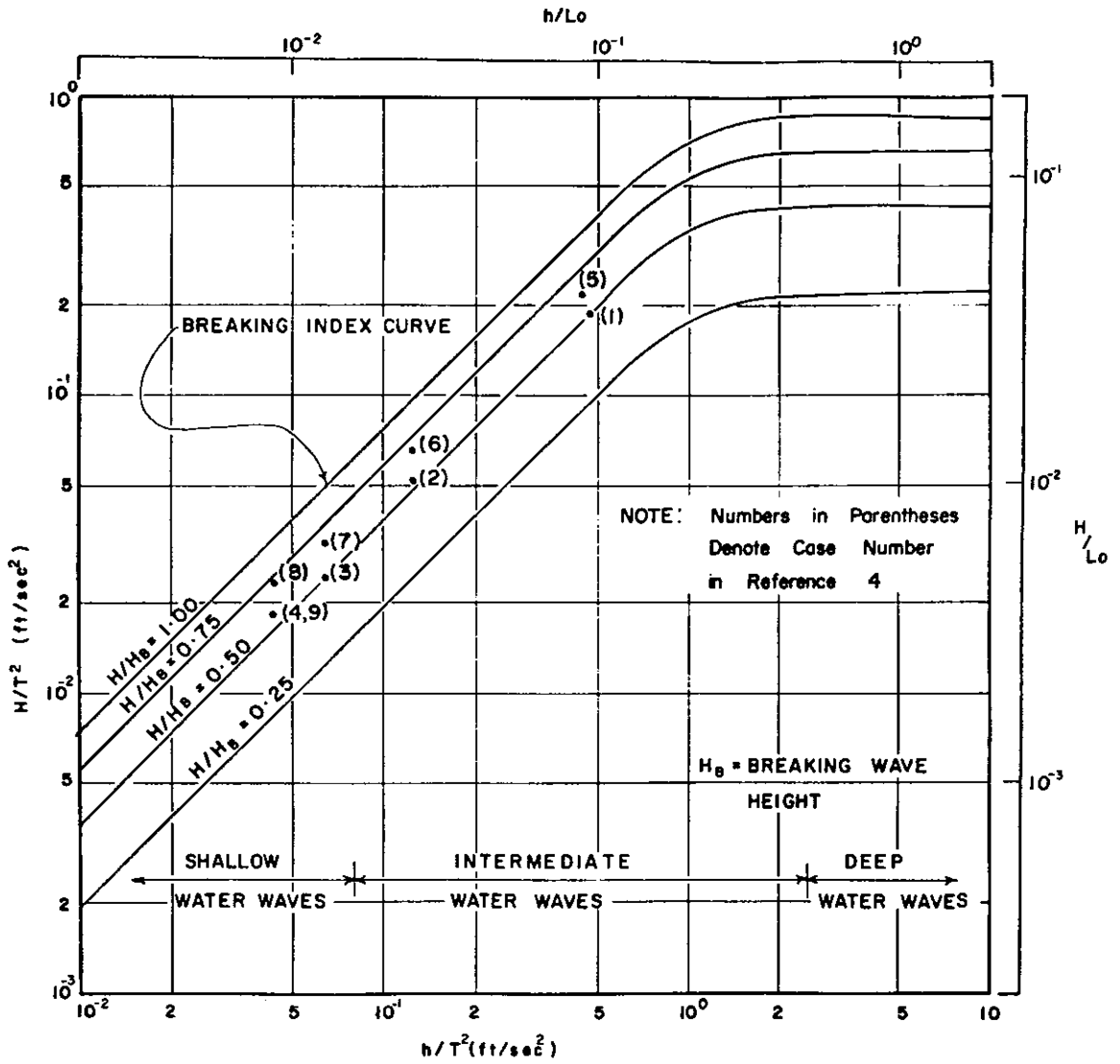


FIGURE 12 EXPERIMENTAL WAVE CHARACTERISTICS

TABLE B  
Experimental Waves; Characteristics and Variables Measured

| Case No. | Wave Characteristics |         |        | Ratio of Wave Height to Breaking Height | Variable Measured                                     | Compared in Figure No. |
|----------|----------------------|---------|--------|---|---|------------------------|
|          | H (ft)               | T (sec) | h (ft) |   |   |                        |
| 1        | 0.255                | 1.16    | 0.587  | 0.56                                    | Horizontal Water Particle Velocity Component at Crest | 13                     |
| 2        | 0.260                | 2.2     | 0.619  | 0.54                                    | Horizontal Water Particle Velocity Component at Crest | 14                     |
| 3        | 0.232                | 3.06    | 0.596  | 0.50                                    | Horizontal Water Particle Velocity Component at Crest | 15                     |
| 4        | 0.241                | 3.58    | 0.556  | 0.56                                    | Horizontal Water Particle Velocity Component at Crest | 16                     |
| 5        | 0.293                | 1.16    | 0.587  | 0.64                                    | Horizontal Water Particle Velocity Component at Crest | 17                     |
| 6        | 0.323                | 2.2     | 0.619  | 0.67                                    | Horizontal Water Particle Velocity Component at Crest | 18                     |
| 7        | 0.293                | 3.06    | 0.595  | 0.64                                    | Horizontal Water Particle Velocity Component at Crest | 19                     |
| 8        | 0.304                | 3.58    | 0.555  | 0.70                                    | Horizontal Water Particle Velocity Component at Crest | 20                     |
| 9        | 0.241                | 3.58    | 0.556  | 0.43                                    | Vertical Water Particle Velocity Component*           | 21                     |
| 10       | 0.271                | 1.6     | 0.586  | 0.60                                    | Wave Profile  | 22                     |

\*Maximum velocity, regardless of phase angle.

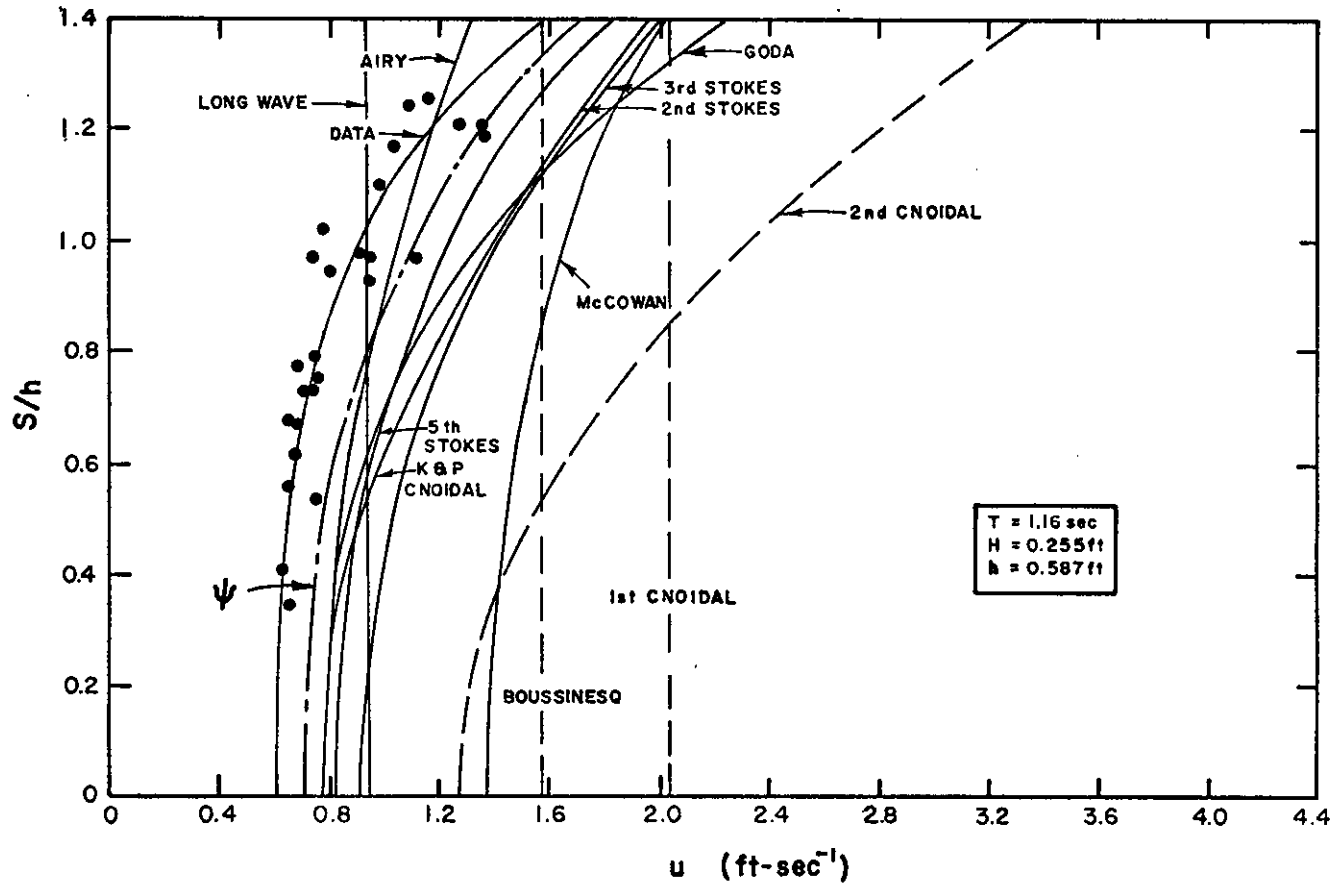


Figure 13 Horizontal Water Particle Velocity Under the Crest, Case I.

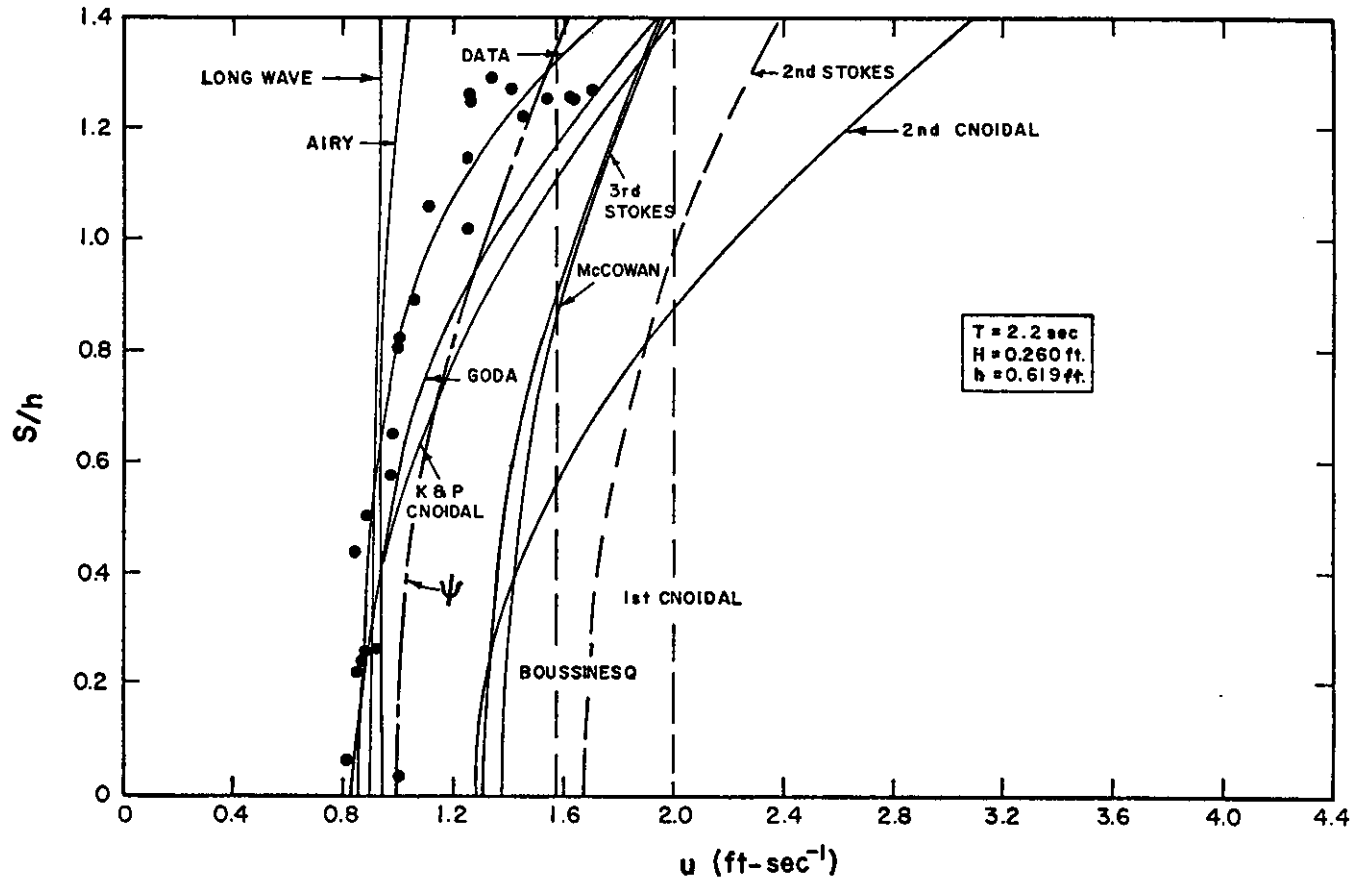


Figure 14 Horizontal Water Particle Velocity Under the Crest , Case 2.

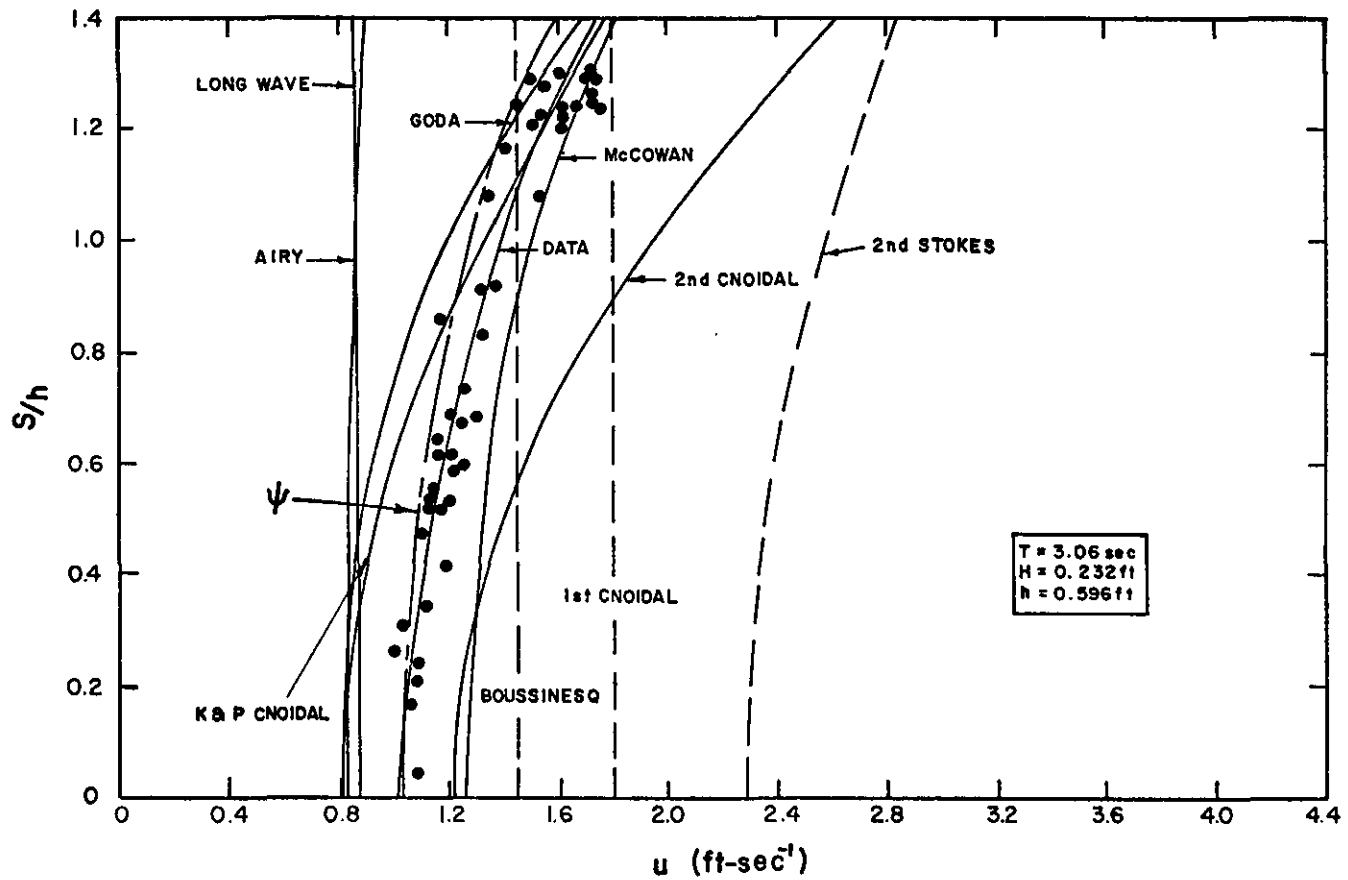


Figure 15 Horizontal Water Particle Velocity Under the Crest, Case 3.

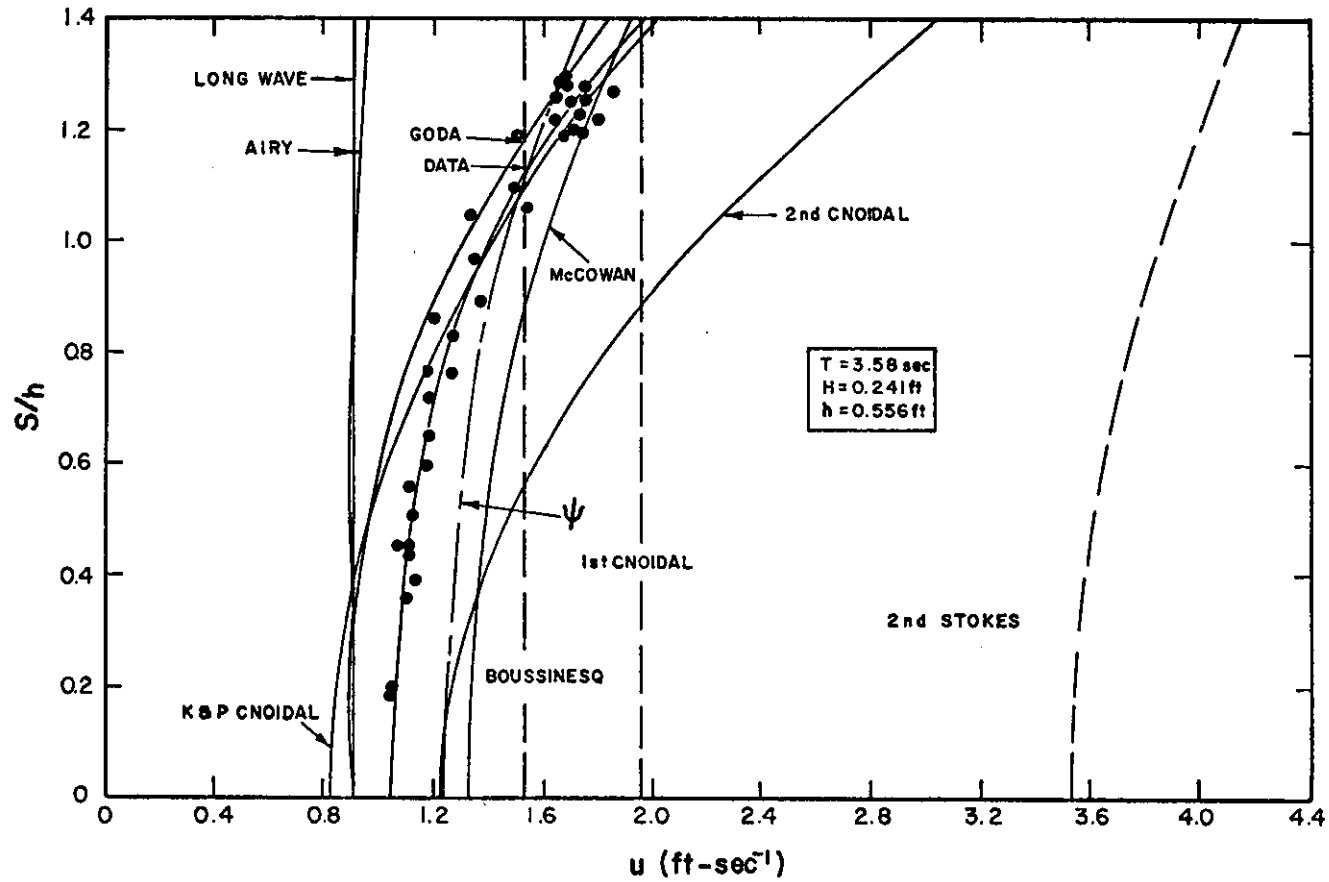


Figure 16 Horizontal Water Particle Velocity Under the Crest, Case 4.

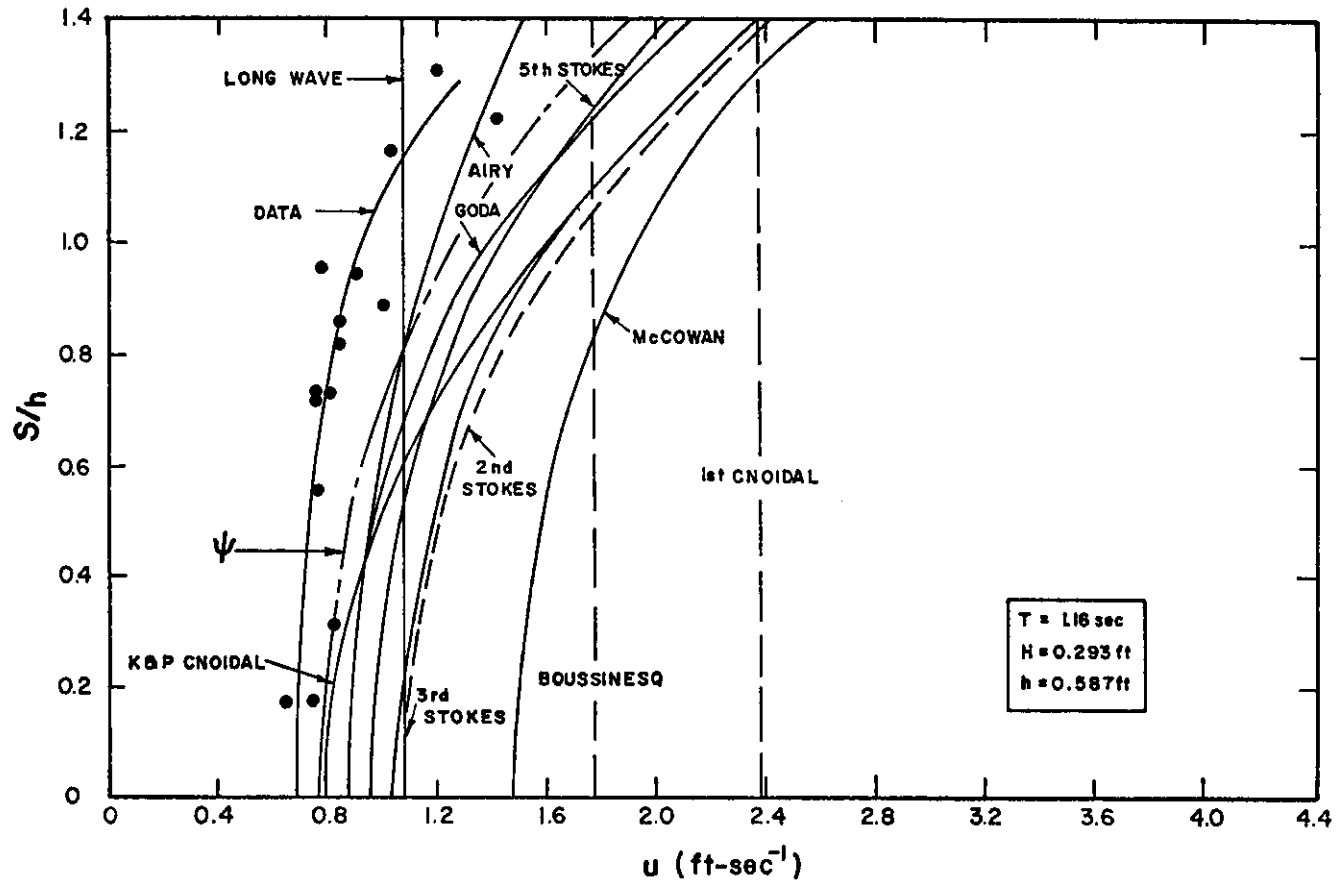


Figure 17 Horizontal Water Particle Velocity Under the Crest, Case 5.

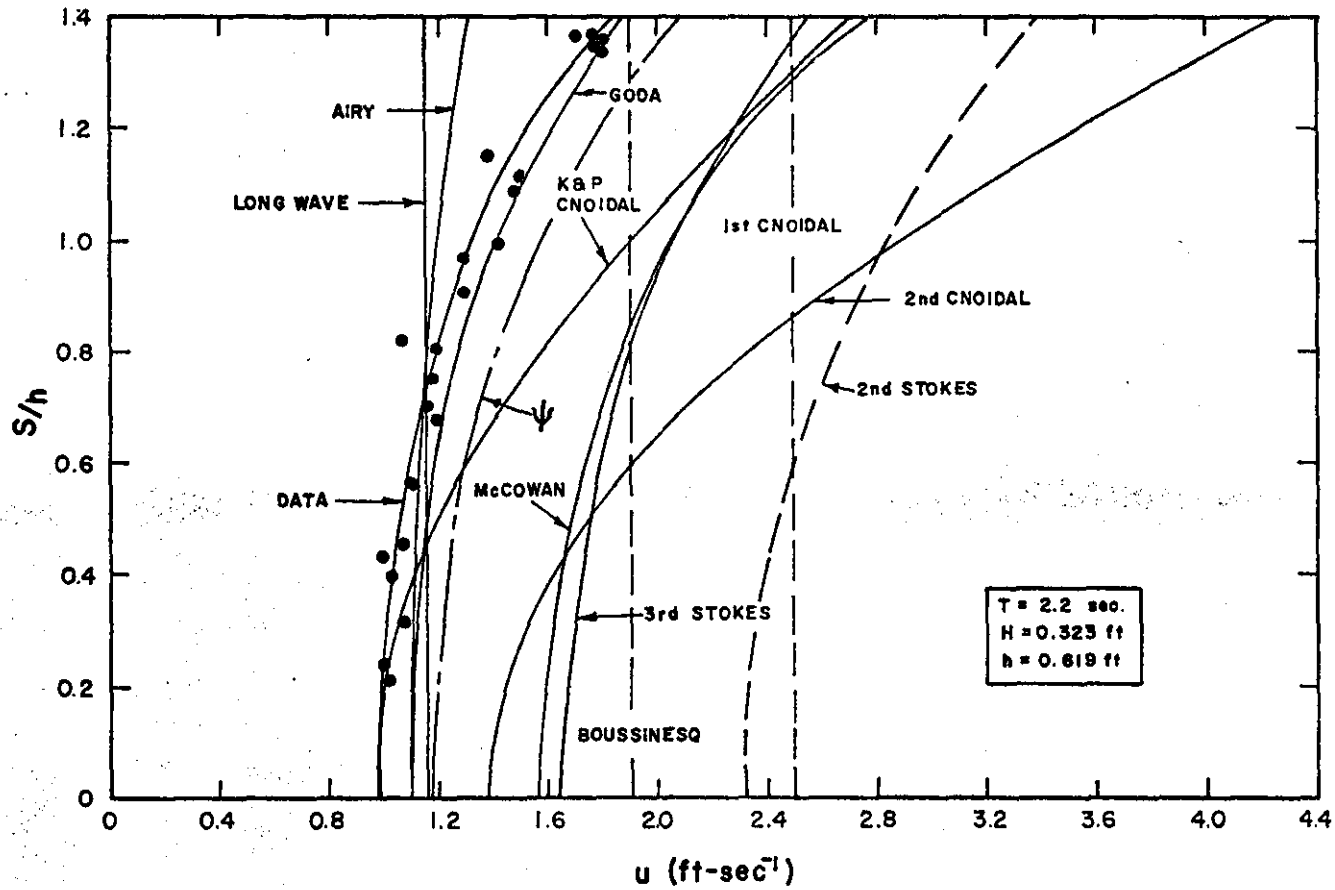


Figure 18 Horizontal Water Particle Velocity Under the Crest, Case 6.

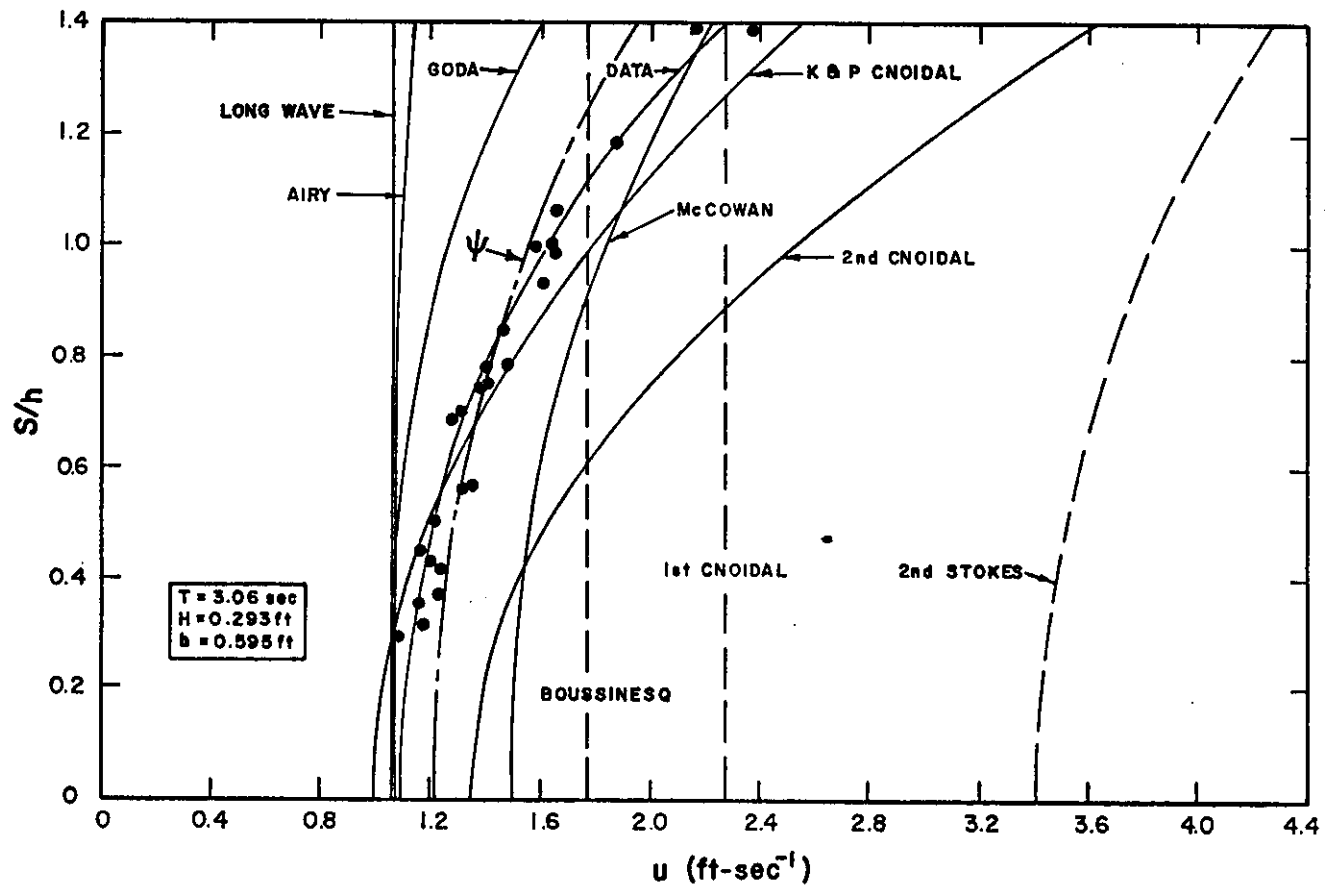


Figure 19 Horizontal Water Particle Velocity Under the Crest, Case 7.

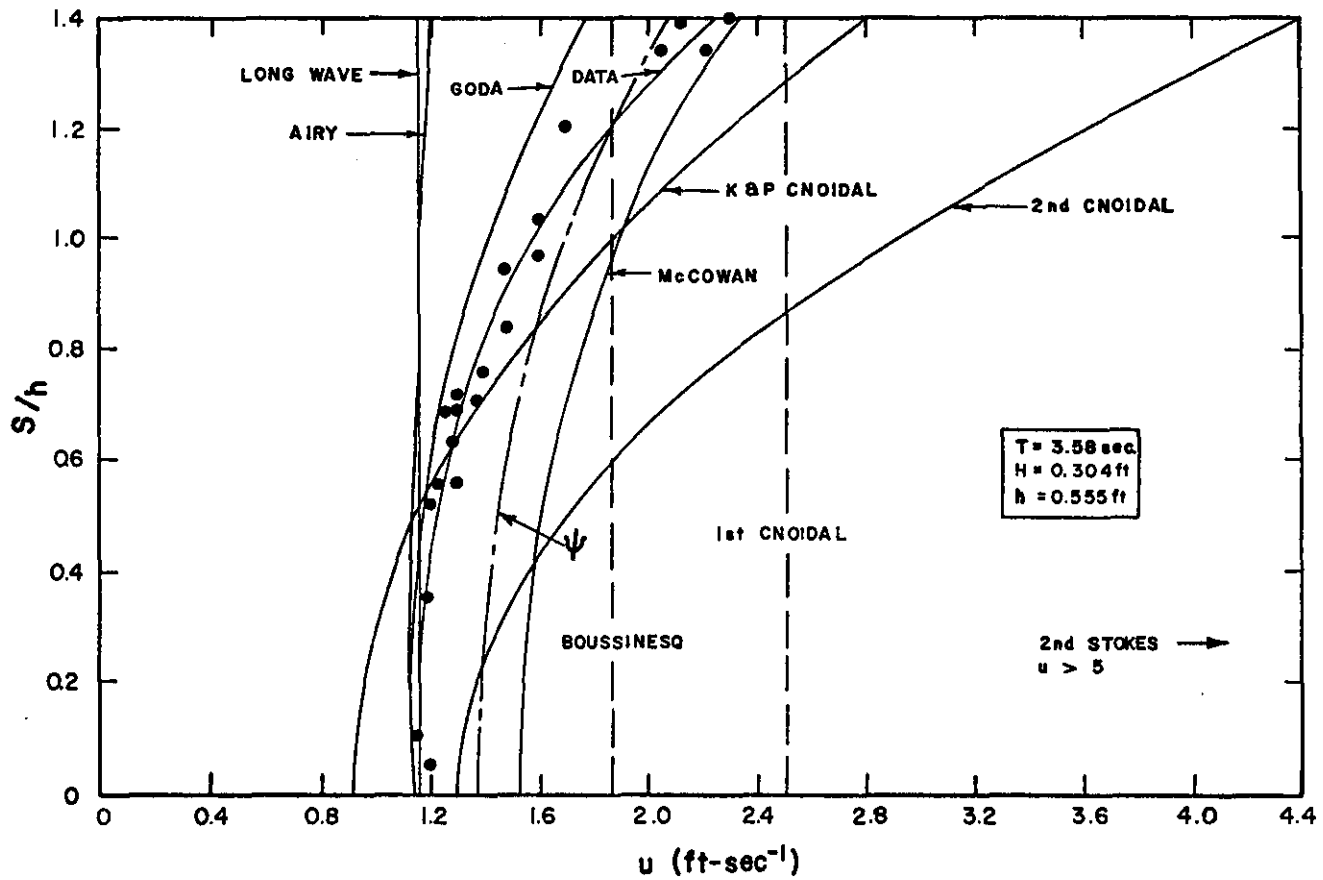


Figure 20 Horizontal Water Particle Velocity Under the Crest, Case 8.

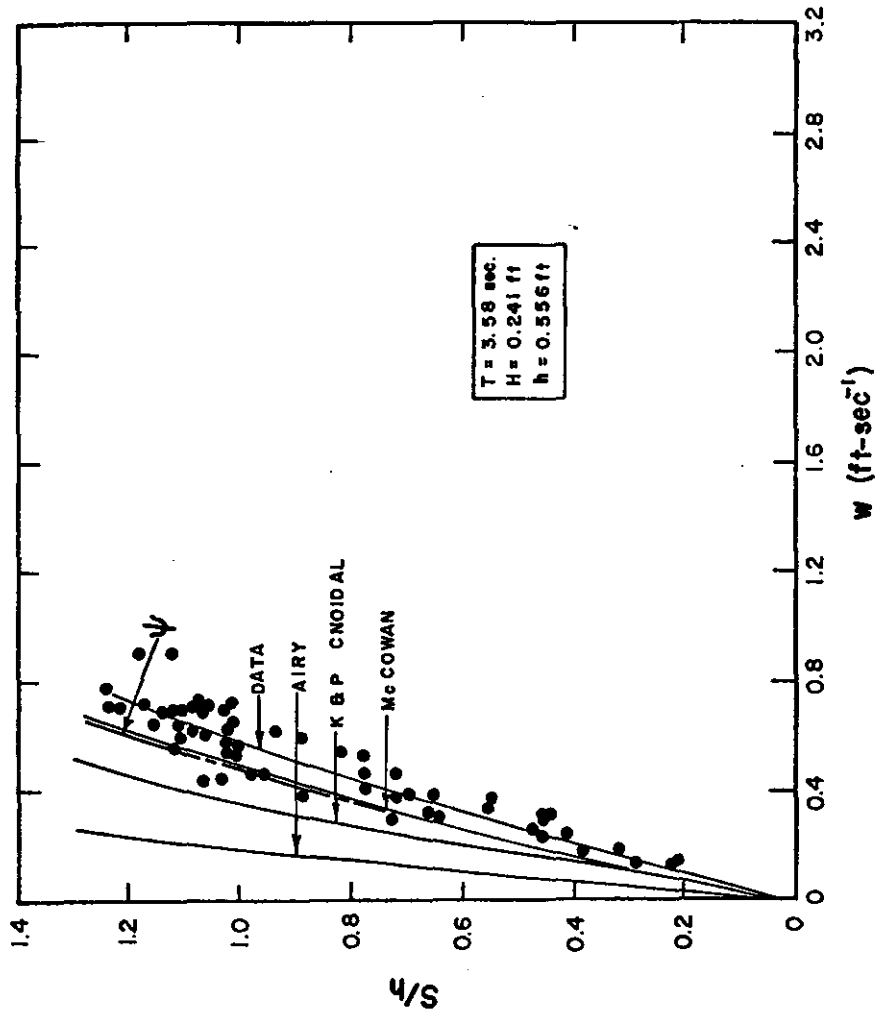


Figure 21 Vertical Water Particle Velocity, Case 9.

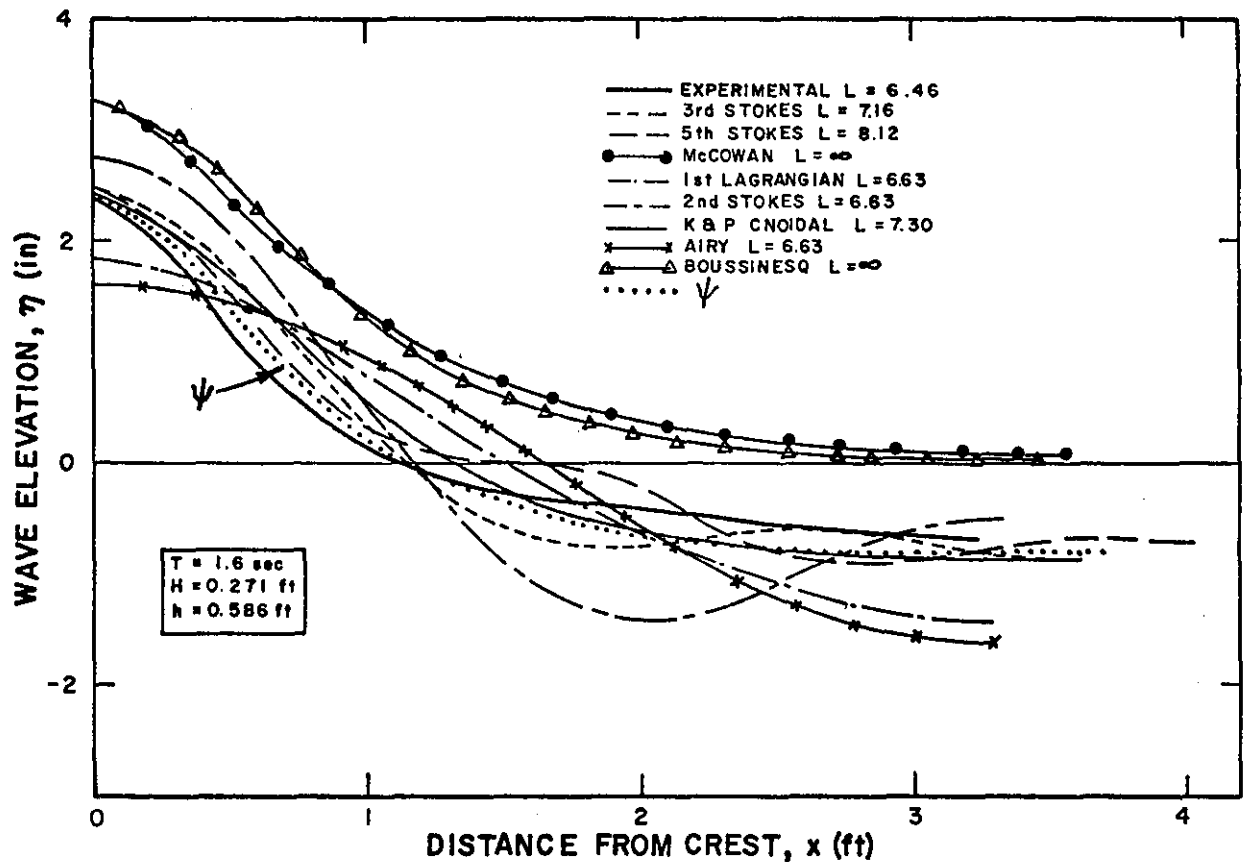


Figure 22 Free Surface Elevation, Case 10.

theories which should provide good fits to the data are so poor. Another interesting feature of the comparison is that the linear (Airy) wave theory agrees better with the data than would be expected. Of the twelve theories included in the comparison, the better agreements with data were provided by the following five theories: Airy, Keulegan and Patterson Cnoidal wave theory, Goda, Long Wave and Stream function. These five theories were then selected for further examination of their agreement with the data. The standard deviations between each of these theories and the data were calculated and are presented in Table C where it is seen that the Stream function theory provided the best fit to the data, followed, in order, by the Goda, Keulegan and Patterson Cnoidal, Airy, and the Long Wave Theories. The Goda "theory" is actually a series representation in which the analytical forms of the terms comprising the series are the same as the hyperbolic and trigonometric functions in the Stokes theories, however the *coefficients* modifying these terms were determined empirically via wave tank experiments. Additional calculations, not presented here, showed that, assuming the data were valid, on the average the Stream function wave theory would overpredict the maximum total drag force on a vertical cylinder by 21%.

Data representing the vertical velocity distribution with depth are available for only one set of

TABLE C

Standard Deviation of Differences Between Horizontal  
Velocities: Measured vs. Predicted

| Case No. | Standard Deviation, $\sigma$ (ft/sec) |       |           |       |               |
|----------|---------------------------------------|-------|-----------|-------|---------------|
|          | Theory                                |       |           |       |               |
|          | $\psi$                                | Airy  | Long Wave | Goda  | K & P Cnoidal |
| 1        | 0.229                                 | 0.232 | 0.328     | 0.413 | 0.396         |
| 2        | 0.139                                 | 0.234 | 0.297     | 0.146 | 0.211         |
| 3        | 0.096                                 | 0.470 | 0.468     | 0.206 | 0.155         |
| 4        | 0.126                                 | 0.442 | 0.453     | 0.134 | 0.136         |
| 5        | 0.245                                 | 0.225 | 0.291     | 0.357 | 0.487         |
| 6        | 0.216                                 | 0.181 | 0.244     | 0.095 | 0.469         |
| 7        | 0.123                                 | 0.493 | 0.513     | 0.316 | 0.188         |
| 8        | 0.183                                 | 0.418 | 0.434     | 0.215 | 0.272         |
| Average  | 0.170                                 | 0.337 | 0.379     | 0.235 | 0.289         |

$$\sigma \equiv \sqrt{\frac{1}{J} \sum_{j=1}^J (u_M - u_T)^2}$$

$u_M$  = measured velocity component

$u_T$  = theoretical velocity component

J = number of levels considered for each case (14 to 15)

wave conditions, see Fig. 21. The McCowan theory provides the best fit to the data, with the next best fit associated with the Stream function wave theory. Differences between the McCowan and Stream function wave theories, however, are quite small and it is probably not justified to draw conclusions from only one set of data. Interpreted in terms of vertical drag forces on a horizontal cylinder, the Stream function would underpredict the forces by 30%.

The one set of wave profile data are compared with the various theories in Fig. 22. Although no detailed comparisons were made, it appears that the Stream function theory is in as good or better agreement than any of the other theories shown.

*Conclusions Resulting from the Experimental  
Validity Study*

Comparisons of Stream function wave theory predictions with measurements of velocity components and one wave form representing intermediate and shallow water waves indicate reasonably good agreement. Interpreted on the basis of maximum horizontal drag force components, the Stream function theory would over predict by an average of 21%. Recognizing that the experimental accuracy is approximately 5%, these results are considered reasonable for engineering applications. The predicted maximum vertical drag forces on a horizontal cylinder would be too

small by 30%; however, this statement is based on a comparison with only one set of data. Good qualitative agreement was found between measured and predicted wave profiles.

Finally, based on the results of both the analytical and experimental validity studies, it is concluded that on the basis of available information, the Stream function wave theory is best suited for engineering design purposes. Based on this conclusion, it was decided to tabulate variables that would be of use in engineering design as calculated from the Stream function wave theory. The next section describes the variables included in the tables.

#### IV. DESCRIPTION OF TABLES

##### *Introduction*

An attempt has been made to include in the tables those variables of greatest present engineering interest and application. In addition, other variables were included which would be relevant to checking the relative analytical validity of other theories or variables which were of scientific interest and could conceivably be required for engineering in the future. Variables have been included which describe the detailed kinematics of the waves and also which represent, e.g., the integrated effect of the flow on a structural member.

It is not possible to assemble in concise tabular form, all variables which could be of engineering use. For example, it is feasible to tabulate the dimensionless drag force for all vertical piling extending from the bottom up to a certain level. It would not be feasible, however, to concisely tabulate the total drag force on members with all possible inclinations relative to a vertical.

Forty sets of dimensionless wave conditions were selected for tabulation. Each case is characterized by values of  $h/L_0$  and  $H/L_0$ . The parameter  $h/L_0$  ranged from

0.002 to 2.0 and covered the relative depth range from shallow to deep water. The parameter  $H/L_0$  included wave steepness ratios: 0.25, 0.5, 0.75 and 1.0 of the breaking wave steepness for each of the ten  $h/L_0$  values tabulated. Figure 23 shows the dimensionless wave conditions selected for tabulation and also indicates the referencing notation for the various cases.

All tabulated variables are presented in dimensionless form. The description of these variables is presented in the following paragraphs and in Tables D, E and F, where generally the following are included: the equation for the variable, the dimensionless form of the variable, an equation number for reference purposes, and the table number in the wave tables. To reduce confusion, it should be noted that the tables presented in this report are denoted by Arabic letters, whereas the wave tables are identified by Roman numerals.

#### *Variables Presented in Tabular Form*

There are three classes of variables that are tabulated: (1) Internal field variables, depending on  $\theta$  and  $S$ , (2) Variables depending on  $\theta$  only, and (3) "Overall" variables which have a single value for the entire wave, for example the wave length.

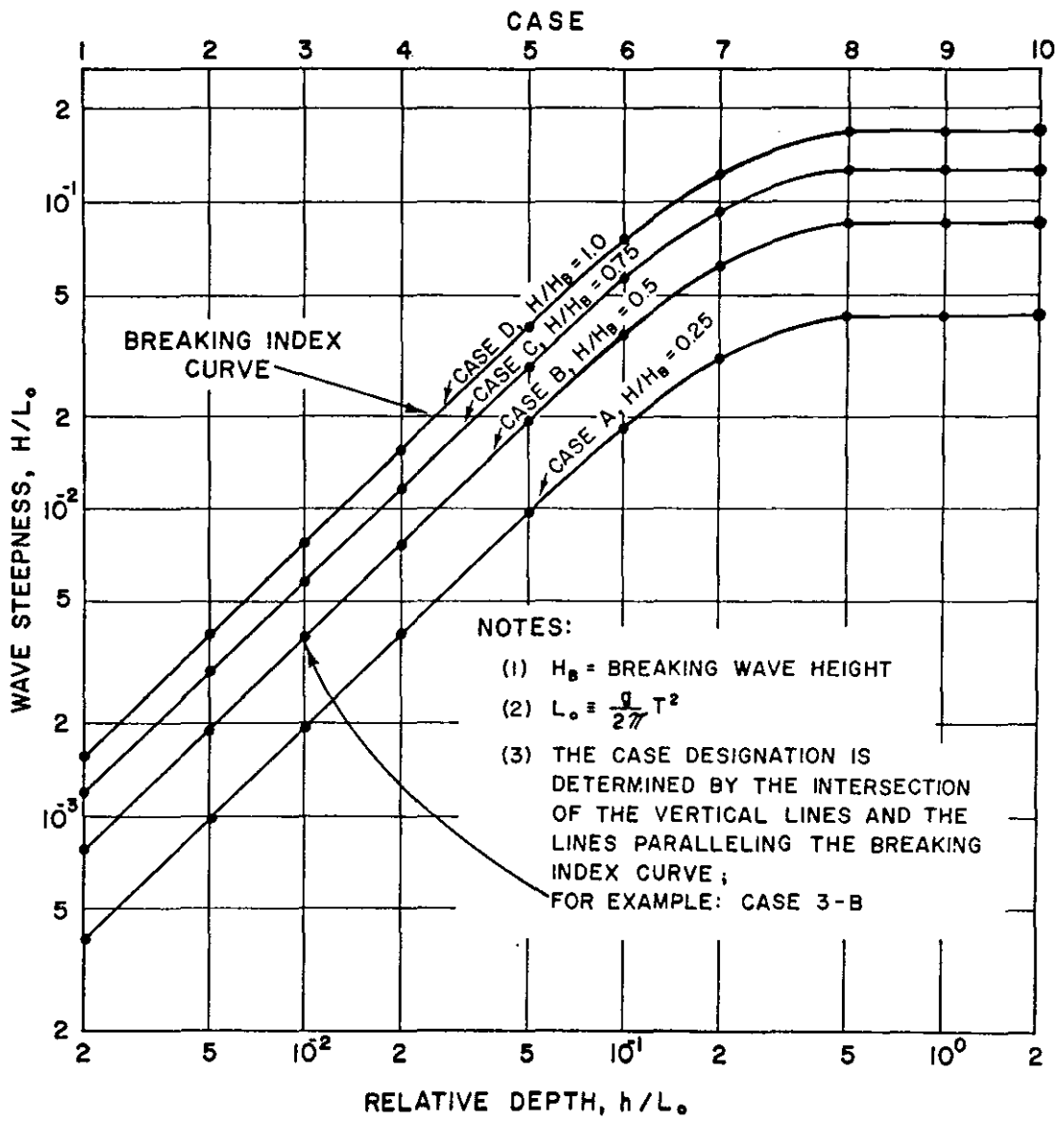


FIGURE 23 WAVE CHARACTERISTICS SELECTED FOR TABULATION

TABLE D  
Internal Field Variables  
(Functions of  $\theta$  and S)

| Variable   | Expression for Variable  | Dimensionless Form                                  | Equation No. | Presented in Table |
|--|--|---|--------------|--------------------|
| Horizontal Water Particle Velocity,<br>$u(\theta, S)$      | $u(\theta, S) = - \sum_{n=1}^{NN} X(n) \left( \frac{2\pi}{L} n \right) \cosh \left( \frac{2\pi}{L} n S \right) \cos n\theta$                           | $\left( \frac{1}{H/T} \right) u$                    | (21)         | I                  |
| Vertical Water Particle Velocity,<br>$w(\theta, S)$        | $w(\theta, S) = - \sum_{n=1}^{NN} X(n) \left( \frac{2\pi}{L} n \right) \sinh \left( \frac{2\pi}{L} n S \right) \sin n\theta$                           | $\left( \frac{1}{H/T} \right) w$                    | (22)         | II                 |
| Horizontal Water Particle Acceleration,<br>$\frac{Du}{Dt}$ | $\frac{Du}{Dt} = (u - C) \frac{\partial u}{\partial x} + w \frac{\partial u}{\partial z}$<br>Note: $C \equiv L/T$                                      | $\left( \frac{1}{H/T^2} \right) \frac{Du}{Dt}$      | (23)         | III                |
| Vertical Water Particle Acceleration,<br>$\frac{Dw}{Dt}$   | $\frac{Dw}{Dt} = (u - C) \frac{\partial w}{\partial x} + w \frac{\partial w}{\partial z}$  | $\left( \frac{1}{H/T^2} \right) \frac{Dw}{Dt}$      | (24)         | IV                 |
| Drag Force Component up to a Level, S,<br>$F_D(\theta, S)$ | $F_D(\theta, S) = \frac{C_D \rho D}{2} \int_0^S u  u  dS'$<br>Note: $C_D$ = drag coefficient; $D$ = piling diameter;<br>$\rho$ = mass density of water | $\left( \frac{2}{C_D \rho D (H/T)^2 h} \right) F_D$ | (25)         | V                  |

TABLE D—Continued

| Variable   | Expression for Variable  | Dimensionless Form  | Equation No. | Presented in Table |
|--|--|---|--------------|--------------------|
| Inertia Force Component up to a Level, S,<br>$F_I(\theta, S)$  | $F_I(\theta, S) = \frac{C_M \rho \pi D^2}{4} \int_0^S \frac{Du}{Dt} ds'$ Note: $C_M$ = inertia coefficient   | $\left[ \frac{4}{C_M \rho \pi D^2 (H/T^2) h} \right] F_I$   | (26)         | VI                 |
| Drag Moment Component up to a Level, S,<br>$M_D(\theta, S)$    | $M_D(\theta, S) = \frac{C_D \rho D}{2} \int_0^S s' u  u  ds'$  | $\left[ \frac{2}{C_D \rho D (H/T)^2 h^2} \right] M_D$       | (27)         | VII                |
| Inertia Moment Component up to a Level, S,<br>$M_I(\theta, S)$ | $M_I(\theta, S) = \frac{C_M \rho \pi D^2}{4} \int_0^S s' \frac{Du}{Dt} ds'$  | $\left[ \frac{4}{C_M \rho \pi D^2 (H/T^2) h^2} \right] M_I$ | (28)         | VIII               |
| Dynamic Pressure Component<br>$P_D(\theta, S)$                 | $P_D(\theta, S) = \gamma \bar{Q} - \frac{\rho}{2} ((u - C)^2 + w^2) + \frac{\rho}{2} C^2$ Note: $\gamma$ = specific weight of water $\equiv \rho g$ ;<br>$\bar{Q}$ is defined in Eq. (17). | $\left[ \frac{2}{\gamma H} \right] P_D$                     | (29)         | IX                 |

TABLE E  
Variables Depending on  $\theta$  Only

| Variable  | Expression for Variable   | Dimensionless Form  | Equation No. | Presented in Table   |
|---|---|---|--------------|--|
| Water Surface Displacement, $\eta(\theta)$                            | $\eta(\theta) = \frac{T}{L} \psi_n - \frac{T}{L} \sum_{n=1}^{NN} X(n) \sinh \left[ \frac{2\pi}{L} n(h+n) \right] \cos(n\theta)$ | $\left( \frac{1}{H} \right) \eta(\theta)$                   | (30)         | I - IX   |
| Total Drag Force Component, $F_D(\theta)$                             | Same as Eq. (25), except upper limit is $h + \eta(\theta)$  | $\left( \frac{2}{C_D \rho D (H/T)^2 H} \right) F_D$         | (31)         | V<br>(labeled "Surface")   |
| Total Inertia Force Component, $F_I(\theta)$                          | Same as Eq. (26), except upper limit is $h + \eta(\theta)$  | $\left( \frac{4}{C_M \rho \pi D^2 (H/T^2) H} \right) F_I$   | (32)         | VI<br>(labeled "Surface")  |
| Total Drag Moment Component, $M_D(\theta)$                            | Same as Eq. (27), except upper limit is $h + \eta(\theta)$  | $\left( \frac{2}{C_D \rho D (H/T)^2 H^2} \right) M_D$       | (33)         | VII<br>(labeled "Surface")                                       |
| Total Inertia Moment Component, $M_I(\theta)$                         | Same as Eq. (28) except upper limit is $h + \eta(\theta)$   | $\left( \frac{4}{C_M \rho \pi D^2 (H/T^2) H^2} \right) M_I$ | (34)         | VIII<br>(labeled "Surface")                                      |
| Kinematic Free Surface Boundary Condition Error, $\epsilon_1(\theta)$ | $\epsilon_1(\theta) = \frac{\partial \eta}{\partial x} - \frac{w}{u - C}$   | Expression given is in dimensionless form                   | (35)         | X<br>Item 1<br>Linear Theory<br>Item 2<br>Stream Function Theory |

TABLE E—Continued

| Variable  | Expression for Variable  | Dimensionless Form                    | Equation No. | Presented in Table   |
|---|--|---------------------------------------|--------------|--|
| Dynamic Free Surface Boundary Condition Error, $\epsilon_2(\theta)$ | $\epsilon_2(\theta) = Q(\theta) - \bar{Q}$ Note: $\bar{Q} \equiv \overline{Q(\theta)}$ | $\left(\frac{1}{H}\right) \epsilon_2$ | (36)         | X<br>Item 3,<br>Linear Theory<br>Item 4,<br>Stream Function Theory |

1  
62  
1

TABLE F  
Overall Variables  
(Do Not Depend on  $\theta$  or S)

| Variable                                      | Expression for Variable   | Dimensionless Form                               | Equation No. | Presented in Table |
|---|---|--|--------------|--------------------|
| Wave Length,<br>L                             | L is determined from Stream function solution<br>(no explicit expression)   | $\left[ \frac{2\pi}{gT^2} \right] L$             | (37)         | XI<br>Item 1       |
| Average Potential Energy,<br>PE               | $PE = \frac{\gamma}{4\pi} \int_0^{2\pi} \eta^2(\theta) d\theta$   | $\left[ \frac{8}{\gamma H^2} \right] PE$         | (38)         | XI<br>Item 2       |
| Average Kinetic Energy,<br>KE                 | $KE = \frac{\rho}{4\pi} \int_0^{2\pi} \int_0^{h+\eta} (u^2 + w^2) dS d\theta$   | $\left[ \frac{8}{\gamma H^2} \right] KE$         | (39)         | XI<br>Item 3       |
| Average Total Energy,<br>TE                   | $TE = PE + KE$  | $\left[ \frac{8}{\gamma H^2} \right] TE$         | (40)         | XI<br>Item 4       |
| Average Total Energy Flux,<br>F <sub>TE</sub> | $F_{TE} = \frac{1}{2\pi} \int_0^{2\pi} \int_0^{h+\eta} u \left( p_D + \rho g z + \frac{\rho}{2} (u^2 + w^2) \right) dS d\theta$ | $\left[ \frac{8}{\gamma H^2 L/T} \right] F_{TE}$ | (41)         | XI<br>Item 5       |
| Group Velocity,<br>C <sub>G</sub>             | $C_G = \frac{F_{TE}}{TE}$   | $\left[ \frac{1}{L/T} \right] C_G$               | (42)         | XI<br>Item 6       |
| Average Momentum<br>M                         | $M = \frac{1}{2\pi} \int_0^{2\pi} \int_0^{h+\eta} \rho u dS d\theta$  | $\left[ \frac{8L/T}{\gamma H^2} \right] M$       | (43)         | XI<br>Item 7       |

TABLE F—Continued

| Variable  | Expression for Variable  | Dimensionless Form   | Equation No. | Presented in Table  |
|---|--|--|--------------|---------------------|
| Average Momentum Flux, in Wave Direction, $F_{m_x}$   | $F_{m_x} = \frac{1}{2\pi} \int_0^{2\pi} \int_0^{h+\eta} (P_D + \rho u^2) \, ds \, d\theta$   | $\left(\frac{8}{\gamma H^2}\right) F_{m_x}$  | (44)         | XI<br>Item 8        |
| Average Momentum Flux, Transverse to Wave Direction<br>$F_{m_y}$  | $F_{m_y} = \frac{1}{2\pi} \int_0^{2\pi} \int_0^{h+\eta} P_D \, ds \, d\theta$  | $\left(\frac{8}{\gamma H^2}\right) F_{m_y}$  | (45)         | XI<br>Item 9        |
| Root-Mean-Square (RMS) and Maximum (Max) Kinematic Free Surface Boundary Condition Errors,<br>$\sqrt{\epsilon_1^2}$ and $ \epsilon_1 _{\max}$ | See Eq. (35)   | Expression Given is in Dimensionless Form  | (46)         | XI<br>Items 10 & 12 |
| RMS and Max Dynamic Free Surface Boundary Condition Errors,<br>$\sqrt{\epsilon_2^2}$ and $ \epsilon_2 _{\max}$                                | See Eq. (36)   | $\left(\frac{1}{H}\right) \sqrt{\epsilon_2^2}$ and<br>$\left(\frac{1}{H}\right)  \epsilon_2 _{\max}$ | (47)         | XI<br>Items 11 & 13 |
| Kinematic Free Surface Breaking Parameter, $\beta_1$  | $\beta_1 = \frac{u}{C}, \text{ u evaluated at } \begin{cases} \theta = 0^\circ \\ S = h + \eta \end{cases}$                            | Expression Given is in Dimensionless Form  | (48)         | XI<br>Item 14       |
| Dynamic Free Surface Breaking Parameter, $\beta_2$  | $\beta_2 = -\frac{1}{g} \frac{Dw}{Dt}, \frac{Dw}{Dt} \text{ evaluated at } \begin{cases} \theta = 0^\circ \\ S = h + \eta \end{cases}$ | Expression Given is in Dimensionless Form  | (49)         | XI<br>Item 15       |

Note: In addition to values tabulated, the results include combined refraction/shoaling effects over idealized bathymetry; these results are presented in graphical form and will be described later.

*Internal Field Variables Depending on  $\theta$  and  $S$*

The internal field variables are tabulated at equally spaced dimensionless distances above the bottom, i.e., at  $S/h$  values of 0, 0.1, 0.2 . . . up to and including the free surface and at  $\theta$  values of  $0^\circ$ ,  $10^\circ$ ,  $20^\circ$ ,  $30^\circ$ ,  $50^\circ$ ,  $75^\circ$ ,  $100^\circ$ ,  $130^\circ$ ,  $180^\circ$ . As an example, see Fig. 24 for a sample presentation of the dimensionless horizontal velocity component field.

A description of the entries presented in Fig. 24 will serve to familiarize the reader with most of the features of the tables. The phase angles ( $\theta$ ) are listed, in degrees, as the first row. The second row lists the dimensionless wave profile ( $\eta/H$ ) at the corresponding phase angles. The percent values listed beneath the  $\eta/H$  values are the differences between the Stream function and Airy theories, defined as

$$\% = \frac{\text{Stream Fn.} - \text{Airy}}{\text{Stream Fn.}} \times 100\%$$

The main body (remaining portion) of the table lists the dimensionless horizontal water particle velocities. The row labeled "Surface" represents the dimensionless velocities evaluated at the free surface; the percentage differences for velocities are calculated as defined above for the profile. The remaining part of the table represents the dimensionless velocities and percentage differences

| CASE 4-D   |                  |                 |                 |                  |                  |                  |                 |                   |                   |
|--|------------------|-----------------|-----------------|------------------|------------------|------------------|-----------------|-------------------|-------------------|
| TABLE I-DIMENSIONLESS HORIZONTAL VELOCITY COMPONENT FIELD...DEFINED IN EQUATION (21) |                  |                 |                 |                  |                  |                  |                 |                   |                   |
| THETA=   | 0.0              | 10.0            | 20.0            | 30.0             | 50.0             | 75.0             | 100.0           | 130.0             | 180.0             |
| ETA/HEIGHT=  | 0.889<br>43.7%   | 0.583<br>15.5%  | 0.284<br>-65.4% | 0.101<br>-326.7% | -0.055<br>681.4% | -0.101<br>227.7% | -0.110<br>21.4% | -0.112<br>-242.4% | -0.111<br>-346.7% |
| SURFACE  | 19.899<br>51.9%  | 12.419<br>24.1% | 5.621<br>-59.5% | 1.840<br>-347.1% | -0.953<br>*****  | -1.636<br>245.1% | -1.789<br>12.9% | -1.799<br>-273.2% | -1.780<br>-386.6% |
| S/DEPTH=1.6  | 18.167<br>100.0% |                 |                 |                  |                  |                  |                 |                   |                   |
| S/DEPTH=1.5  | 16.533<br>100.0% |                 |                 |                  |                  |                  |                 |                   |                   |
| S/DEPTH=1.4  | 15.137<br>36.7%  | 11.986<br>21.4% |                 |                  |                  |                  |                 |                   |                   |
| S/DEPTH=1.3  | 13.942<br>32.3%  | 11.246<br>17.3% |                 |                  |                  |                  |                 |                   |                   |
| S/DEPTH=1.2  | 12.919<br>26.0%  | 10.598<br>13.6% | 5.627<br>-55.3% |                  |                  |                  |                 |                   |                   |
| S/DEPTH=1.1  | 12.043<br>23.9%  | 10.030<br>10.0% | 5.637<br>-52.8% |                  |                  |                  |                 |                   |                   |
| S/DEPTH=1.0  | 11.294<br>19.9%  | 9.535<br>6.6%   | 5.627<br>-51.1% | 2.046<br>-283.0% |                  |                  |                 |                   |                   |
| S/DEPTH=0.9  | 10.655<br>16.1%  | 9.106<br>3.3%   | 5.603<br>-49.9% | 2.266<br>-241.7% | -0.869<br>*****  | -1.630<br>242.0% | -1.788<br>13.2% | -1.799<br>100.0%  | -1.780<br>100.0%  |
| S/DEPTH=0.8  | 10.113<br>12.5%  | 8.736<br>0.3%   | 5.570<br>-46.2% | 2.445<br>-213.2% | -0.733<br>*****  | -1.603<br>242.8% | -1.780<br>13.7% | -1.798<br>-273.2% | -1.783<br>100.0%  |
| S/DEPTH=0.7  | 9.657<br>9.3%    | 8.420<br>-2.5%  | 5.534<br>-48.7% | 2.592<br>-192.7% | -0.614<br>*****  | -1.579<br>243.6% | -1.773<br>14.2% | -1.798<br>-273.1% | -1.785<br>-367.1% |
| S/DEPTH=0.6  | 9.278<br>6.4%    | 8.155<br>-4.9%  | 5.497<br>-48.5% | 2.709<br>-177.7% | -0.510<br>*****  | -1.556<br>244.5% | -1.766<br>14.7% | -1.798<br>-270.1% | -1.787<br>-366.1% |
| S/DEPTH=0.5  | 8.968<br>3.8%    | 7.935<br>-7.0%  | 5.462<br>-48.4% | 2.803<br>-166.5% | -0.423<br>*****  | -1.537<br>245.2% | -1.762<br>15.0% | -1.798<br>-267.5% | -1.788<br>-362.3% |
| S/DEPTH=0.4  | 8.722<br>1.7%    | 7.760<br>-8.6%  | 5.431<br>-48.4% | 2.875<br>-158.3% | -0.351<br>*****  | -1.521<br>245.9% | -1.758<br>15.3% | -1.798<br>-265.4% | -1.789<br>-379.2% |
| S/DEPTH=0.3  | 8.535<br>-0.0%   | 7.626<br>-10.2% | 5.406<br>-48.4% | 2.928<br>-152.5% | -0.296<br>*****  | -1.508<br>246.5% | -1.755<br>15.5% | -1.798<br>-263.7% | -1.790<br>-376.8% |
| S/DEPTH=0.2  | 8.404<br>-1.2%   | 7.531<br>-11.3% | 5.387<br>-48.4% | 2.965<br>-148.5% | -0.256<br>*****  | -1.498<br>247.0% | -1.753<br>15.7% | -1.798<br>-262.6% | -1.791<br>-375.1% |
| S/DEPTH=0.1  | 8.326<br>-2.0%   | 7.475<br>-11.9% | 5.375<br>-48.4% | 2.987<br>-146.2% | -0.233<br>*****  | -1.493<br>247.2% | -1.751<br>15.8% | -1.797<br>-261.9% | -1.791<br>-374.1% |
| S/DEPTH=0.0  | 8.300<br>-2.2%   | 7.456<br>-12.1% | 5.372<br>-48.5% | 2.994<br>-145.5% | -0.225<br>*****  | -1.491<br>247.3% | -1.751<br>15.8% | -1.797<br>-261.7% | -1.791<br>-373.7% |

FIGURE 24. EXAMPLE OUTPUT FOR DIMENSIONLESS HORIZONTAL VELOCITY COMPONENT FIELD

evaluated on a grid of  $(\theta, S/h)$ . The lack of entries for the higher  $S/h$  and higher theta values (right side of page) is a result of the wave profile in the trough region being lower than in the crest region (left side of page). Two additional comments pertaining to the percentage values will complete the description of the sample table. A percentage difference value of exactly 100.0% implies that the Stream function profile occurred at a  $(\theta, S/h)$  value, however, the Airy profile was lower than the particular  $S/h$  at the phase angle,  $\theta$ , i.e., this grid point was not "covered" by the Airy profile. For example, this is the case at  $\theta = 0^\circ$ ,  $S/h = 1.5$  and  $1.6$  and  $\theta = 180^\circ$ ,  $S/h = 0.8$  and  $0.9$ . Finally, the asterisks indicate that the percentage differences were not calculated because the Stream function value was less than 5% of the maximum Stream function value. This avoided the tabulation of very large percentages which would have been the result of division by a small number.

A brief description of each of the tabulated internal field variables is presented below.

*Horizontal water particle velocity component,  $u(\theta, S)$*

The horizontal water particle velocity component,  $u(\theta, S)$ , is defined by Equation (21).\* The values  $u'(\theta, S)$

---

\*The equations for the tabulated functions are presented in Tables D, E and F.

tabulated, are presented (Table I) in the following dimensionless form:

$$u'(\theta, S) = \frac{u(\theta, S)}{(H/T)}$$

*Vertical water particle velocity component,  $w(\theta, S)$*

The vertical water particle velocity component,  $w(\theta, S)$ , is defined by Equation (22). The dimensionless values tabulated (Table II),  $w'(\theta, S)$ , are defined by:

$$w'(\theta, S) = \frac{w(\theta, S)}{(H/T)}$$

*Horizontal water particle acceleration,  $\frac{Du}{Dt}$*

The horizontal water particle acceleration,  $\frac{Du}{Dt}$ , is defined in terms of the velocity components as presented in Equation (23). Note that the tabulated values represent the total (or material, substantial, etc.) acceleration consisting of the sum of the local and advective contributions. The dimensionless values tabulated (Table III),  $\frac{Du'}{Dt}$ , are defined by:

$$\frac{Du'}{Dt} = \frac{1}{(H/T^2)} \frac{Du}{Dt}$$

*Vertical water particle acceleration,  $\frac{Dw}{Dt}$*

The vertical water particle acceleration, defined in Equation (24), is tabulated (Table IV) in the following dimensionless form:

$$\frac{Dw'}{Dt} = \frac{1}{(H/T^2)} \frac{Dw}{Dt}$$

*Drag force component,  $F_D(\theta, S)$*

The drag force component up to a certain elevation,  $S$ , is defined by Equation (25) and tabulated (Table V) in dimensionless form as:

$$F'_D = \left[ \frac{2}{C_D \rho D (H/T)^2 h} \right] F_D$$

*Inertia force component,  $F_I(\theta, S)$*

The inertia force component up to a certain elevation,  $S$ , is defined by Equation (26) and tabulated (Table VI) in dimensionless form as:

$$F'_I = \left[ \frac{4}{C_M \rho \pi D^2 (H/T^2) h} \right] F_I$$

*Drag moment component,  $M_D(\theta, S)$*

The drag moment component about the bottom due to wave pressures acting on a vertical member extending up to an elevation,  $S$ , is presented as Equation (27) and presented (Table VII) in dimensionless form as:

$$M'_D = \left[ \frac{2}{C_D \rho D (H/T)^2 h^2} \right] M_D$$

*Inertia moment component,  $M_I(\theta, S)$*

The inertia moment component about the bottom due to wave pressures acting on a vertical member extending up

to an elevation,  $S$ , is defined in Equation (28) and presented (Table VIII) in dimensionless form as:

$$M'_I = \left[ \frac{4}{C_M \rho \pi D^2 (H/T^2) h^2} \right] M_I$$

*Dynamic pressure component,  $p_D(\theta, S)$*

The dynamic pressure component, defined by Equation (29) is tabulated (Table IX) in dimensionless form as:

$$P'_D = \left[ \frac{2}{\gamma H} \right] P_D$$

This completes the description of the field variables (depending on  $\theta$  and  $S$ ) that are included in the tables.

*Variables Depending on  $\theta$  Only*

*Water surface displacement,  $\eta(\theta)$*

The water surface displacement is defined in Equation (30), and tabulated (Tables I-IX) in dimensionless form as:

$$\eta' = \left[ \frac{1}{H} \right] \eta$$

*Total drag force component,  $F_D(\theta)$*

The total drag force component is defined by Equation (25) with the upper limit taken to be  $h + \eta(\theta)$ ,

and is tabulated (Table V, labeled "SURFACE") in dimensionless form as:

$$F_D' = \left[ \frac{2}{C_D \rho D (H/T)^2 h} \right] F_D$$

*Total inertia force component,  $F_I(\theta)$*

The total inertia force component is defined by Equation (26) with the upper limit taken to be  $h + \eta(\theta)$ , and is tabulated (Table VI, labeled "SURFACE") in dimensionless form as

$$F_I' = \left[ \frac{4}{C_M \rho \pi D^2 (H/T)^2 h} \right] F_I$$

*Total drag moment component,  $M_D(\theta)$*

The total drag moment component is defined by Equation (27) with the upper limit taken to be  $h + \eta(\theta)$  and is tabulated (Table VII, labeled "SURFACE") in dimensionless form as

$$M_D' = \left[ \frac{2}{C_D \rho D (H/T)^2 h^2} \right] M_D$$

*Total inertia moment component,  $M_I(\theta)$*

The total inertia moment component is defined by Equation (28) with an upper limit of  $h + \eta(\theta)$  and is tabulated (Table VIII, labeled "SURFACE") in dimensionless form as:

$$M_I' = \left( \frac{4}{C_M \rho \pi D^2 (H/T^2) h^2} \right) M_I$$

*Kinematic free surface boundary condition error,  $\epsilon_1(\theta)$*

The kinematic free surface boundary condition error is defined by Equation (35). This variable, as defined, is in dimensionless form and is tabulated in Table X:

Item 1, Linear Wave Theory

Item 2, Stream Function Theory

*Dynamic free surface boundary condition error,  $\epsilon_2(\theta)$*

The dynamic free surface boundary condition error is defined by Equation (36) and is tabulated (Table X) in the following dimensionless form:

$$\epsilon_2' = \left( \frac{1}{H} \right) \epsilon_2$$

with:

Item 3, Linear Wave Theory

Item 4, Stream Function Theory

This completes the presentation of variables depending on  $\theta$  only.

*Overall Variables (do not depend on  $\theta$  or  $S$ )*

*Wave length,  $L$*

For the Stream function wave theory, there is no definable expression for the wave length. Rather the wave

length is determined as a part of the numerical solution as described in Appendix I. The dimensionless wave length is presented (Table XI, Item 1) in the following dimensionless form:

$$L' = \left( \frac{2\pi}{gT^2} \right) L$$

*Average potential energy, PE*

The average potential energy is defined by Equation (38) and is tabulated (Table XI, Item 2) in dimensionless form as:

$$PE' = \left( \frac{8}{\gamma H^2} \right) PE$$

Note that the dimensionless form is defined to be 0.5 for the linear (Airy) wave theory.

*Average kinetic energy, KE*

The average kinetic energy is defined by Equation (39), and is also tabulated (Table XI, Item 3) in dimensionless form as:

$$KE' = \left( \frac{8}{\gamma H^2} \right) KE$$

As for the dimensionless potential energy, the dimensionless value for the linear (Airy) wave theory is 0.5.

*Average total energy, TE*

The average total energy is simply the sum of the potential and kinetic energy contributions (Equation (40)) and is tabulated in dimensionless form (Table XI, Item 4) such that the difference from unity is an indication of the deviation from the linear wave theory.

$$TE' = \left( \frac{8}{\gamma H^2} \right) TE$$

*Average total energy flux, F<sub>TE</sub>*

The average total energy flux is defined by Equation (41), and is tabulated (Table XI, Item 5) in dimensionless form as:

$$F'_{TE} = \left( \frac{8}{\gamma H^2} \frac{L}{T} \right) F_{TE}$$

*Group velocity, C<sub>G</sub>*

The group velocity is defined as the ratio of total energy flux to total energy (Equation (42)) and is presented (Table XI, Item 6) in dimensionless form as:

$$C'_G = \left( \frac{1}{L/T} \right) C_G$$

The dimensionless group velocity is defined such that for linear wave theory the shallow and deep water values are 1.0 and 0.5, respectively.

*Average momentum, M*

The total average momentum is defined by Equation (43) and is presented (Table XI, Item 7) in dimensionless form as:

$$M' = \left( \frac{8 L/T}{\gamma H^2} \right) M$$

The dimensionless momentum is defined such that for linear wave theory, the result is unity. Note that mass transport velocity,  $U = \left( \frac{M}{\rho h} \right)$  is proportional to the average momentum.

*Average momentum flux in wave direction,  $F_{m_x}$*

The total average momentum flux in the wave direction is defined by Equation (44) and is tabulated (Table XI, Item 8) in the following dimensionless form:

$$F'_{m_x} = \left( \frac{8}{\gamma H^2} \right) F_{m_x}$$

The above definition reduces to 1.5 and 0.5 for linear wave theory for shallow and deep water waves, respectively.

*Average momentum flux transverse to wave direction,*  
 $F_{m_Y}$

The total average momentum flux in a direction perpendicular to the wave advance direction is defined by Equation (45) and is tabulated (Table XI, Item 9) in the following dimensionless form:

$$F'_{m_Y} = \left[ \frac{8}{\gamma H^2} \right] F_{m_Y}$$

For linear wave theory, the above definition reduces to 0.5 and 0.0 for shallow and deep water waves, respectively.

*Kinematic free surface boundary condition errors,  $\epsilon_1$*

The kinematic free surface boundary condition error is defined in dimensionless form by Equation (35) and the root-mean-square (RMS) and maximum values are tabulated (Table XI, Items 10 and 12) as defined by Equation (46).

*Dynamic free surface boundary condition errors,  $\epsilon_2$*

The dynamic free surface boundary condition error is defined by Equation (36) and is rendered in the following dimensionless form:

$$\epsilon'_2 = \frac{\epsilon_2}{H}$$

The RMS and maximum values are tabulated (Table XI, Items 11 and 13) as defined by Equation (47).

*Kinematic free surface breaking parameter,  $\beta_1$*

The kinematic free surface breaking parameter is tabulated (Table XI, Item 14) as defined by Equation (48) (dimensionless form).

*Dynamic free surface breaking parameter,  $\beta_2$*

The dynamic free surface breaking parameter is tabulated (Table XI, Item 15) as defined by Equation (49) in dimensionless form.

*Variables Presented in Graphical Form—Combined Effect of Shoaling and Refraction*

In addition to developing the tabulated values previously described, the study reported herein included the development of the combined effect of shoaling and refraction for nonlinear waves advancing toward shore with a deep-water direction,  $\alpha_0$ , over bathymetry characterized by straight and parallel contours.

It is recalled that for linear wave theory, it is possible to separate the shoaling and refraction effects, because neither the wave celerity,  $C$  (governing refraction), nor the group velocity,  $C_G$  (governing energy flux), is dependent on the wave height. For nonlinear waves, both celerity and group velocity at a certain

location depend on the wave height as well as the wave period and water depth. The shoaling/refraction effects for nonlinear waves are therefore not separable and the combined effect depends on the deep water wave steepness,  $H_0/L_0$ , as well as the local relative depth.

Because the shoaling-refraction results are not readily presented in tabular form, graphs are presented as Figs. 25, 26, 27, 28, and 29 for deep water wave directions  $\alpha_0$  of  $0^\circ$ ,  $10^\circ$ ,  $20^\circ$ ,  $40^\circ$ , and  $60^\circ$ , respectively. A brief description of the use of these graphs follows. A wave with a deep water direction  $\alpha_0$ , will propagate toward shore such that the local  $\frac{H}{L_0}$  will fall along a curve characterized by the deep water value  $H_0/L_0$ . At any particular relative depth,  $h/L_0$ , the local wave steepness  $H/L_0$  and direction  $\alpha$  are read from the ordinate and interpolated from the appropriate isolines, respectively. The region to the lower right of the line of dots indicates the region where use of the linear theory agrees with the nonlinear results presented within 1% in  $H/L_0$  and  $1^\circ$  in wave direction,  $\alpha$ .

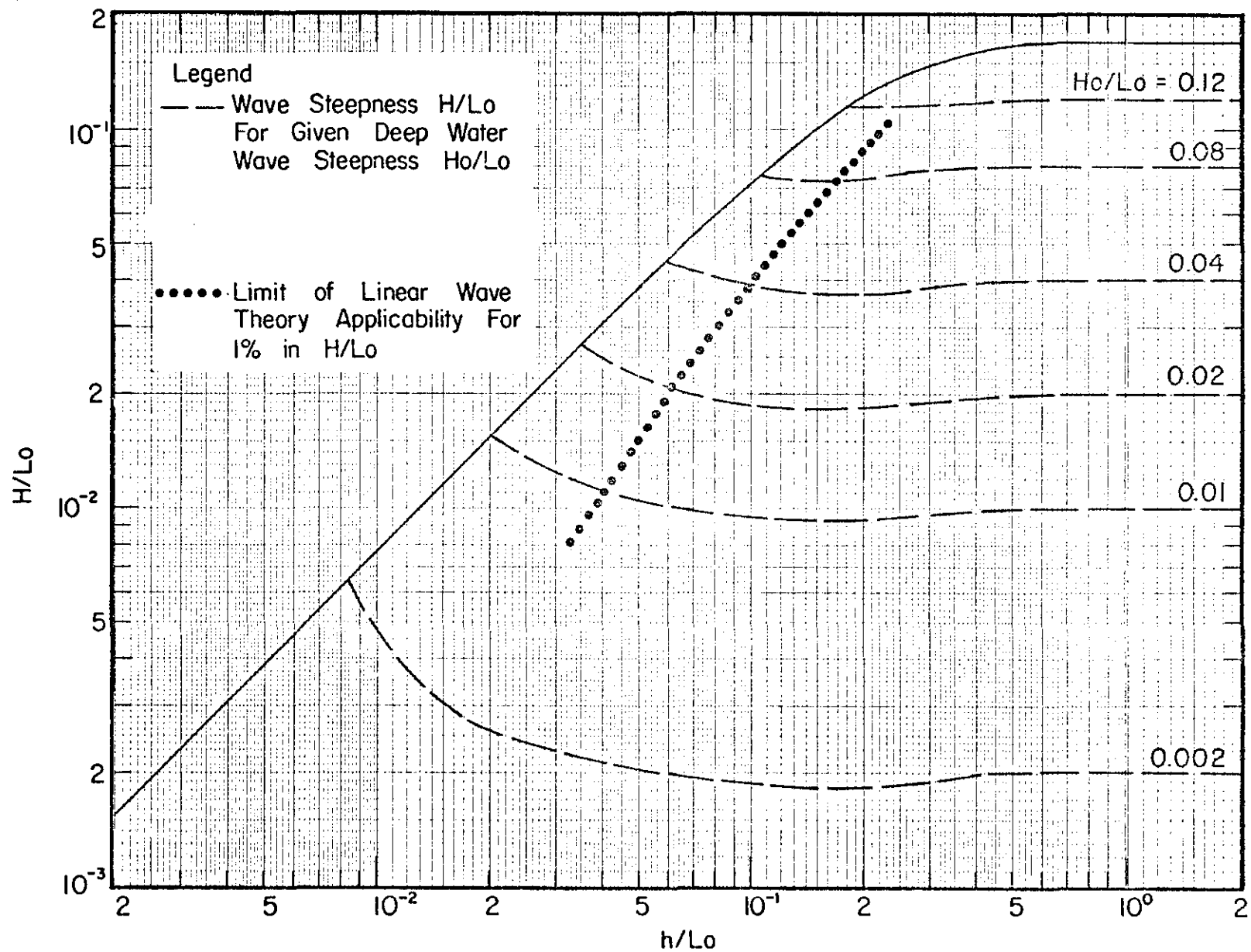


FIGURE 25 COMBINED SHOALING/REFRACTION FOR A DEEP WATER WAVE DIRECTION,  $\alpha_0 = 0^\circ$

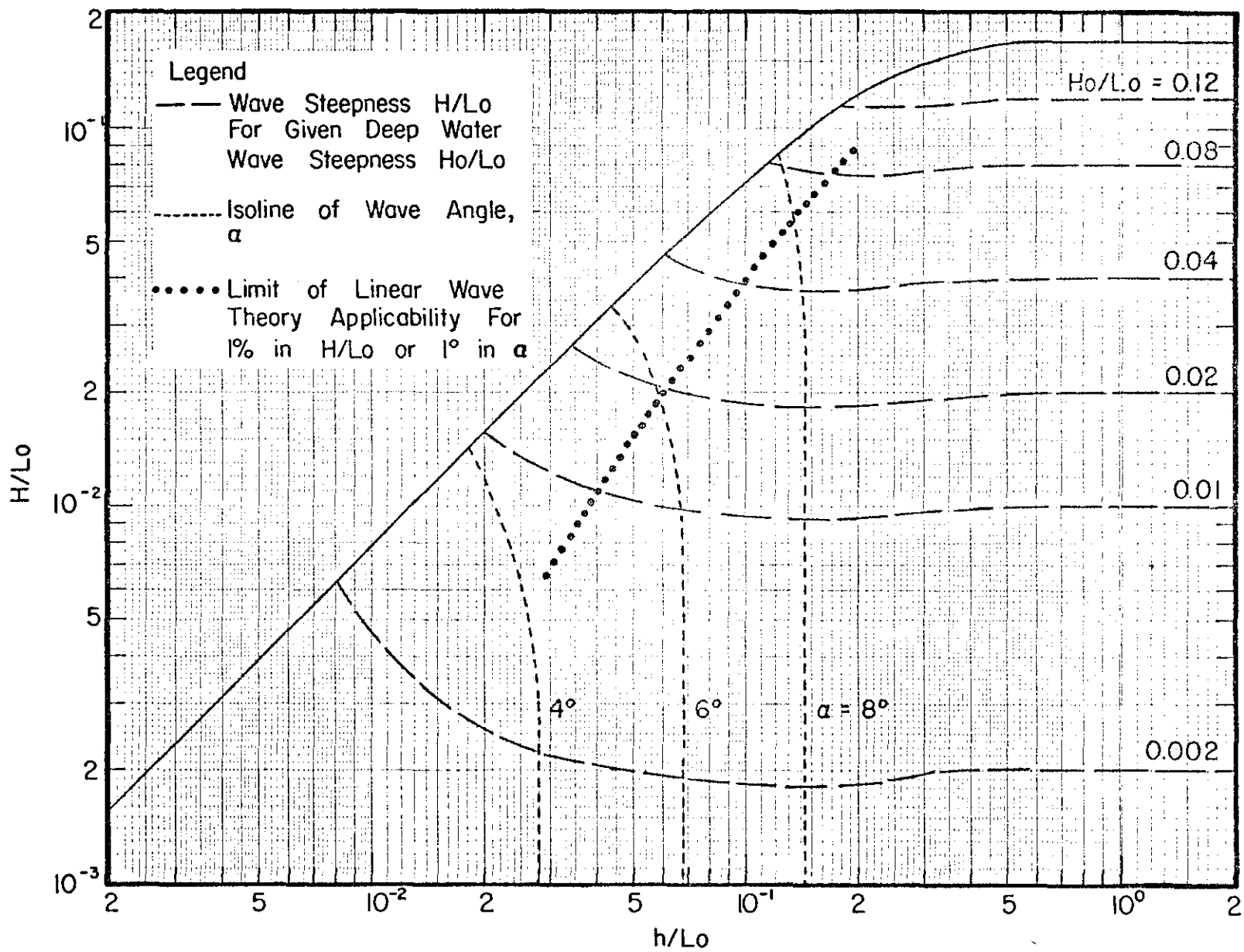


FIGURE 26 COMBINED SHOALING/REFRACTION FOR A DEEP WATER WAVE DIRECTION,  $\alpha_0 = 10^\circ$

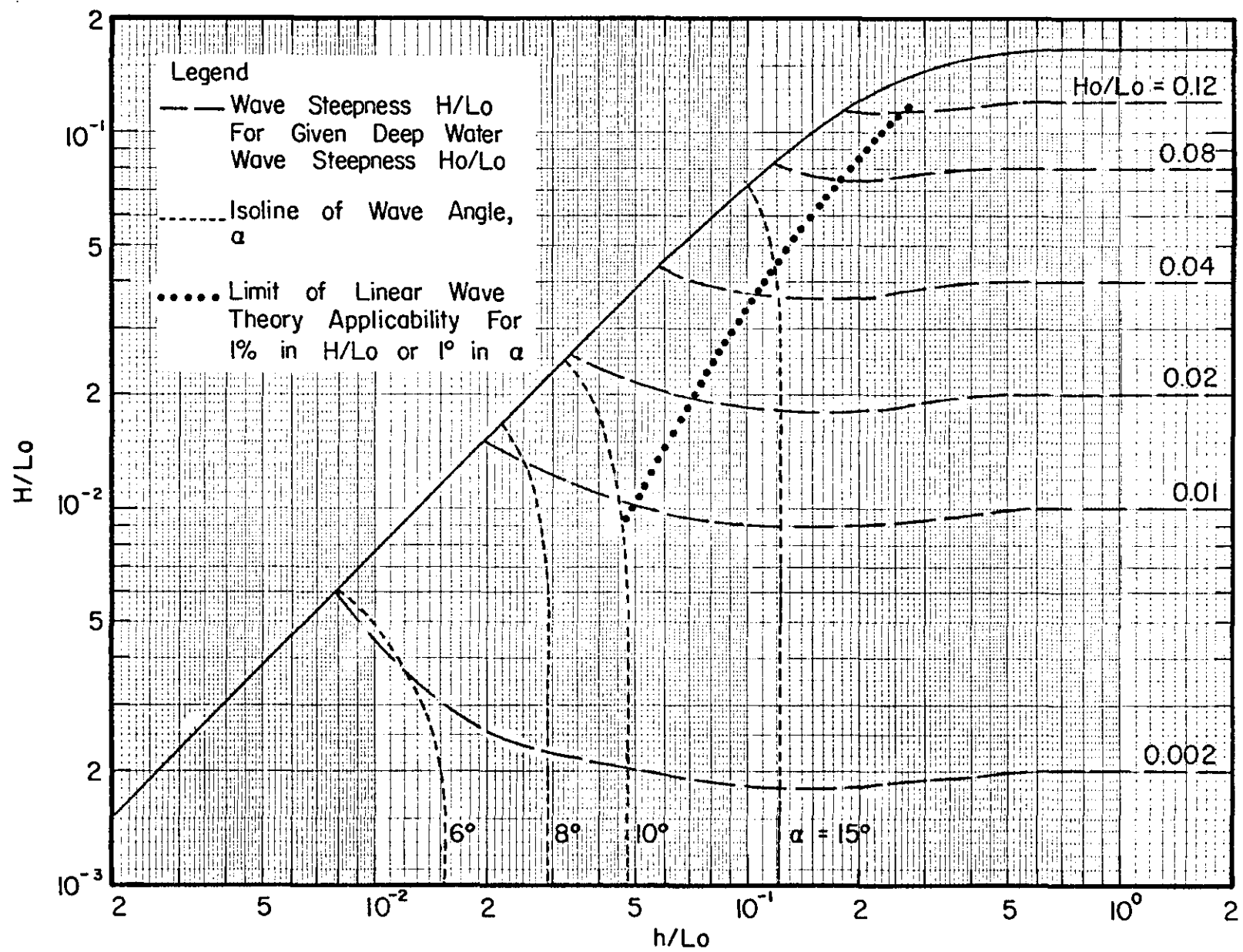


FIGURE 27 COMBINED SHOALING/REFRACTION FOR A DEEP WATER WAVE DIRECTION,  $\alpha_0 = 20^\circ$

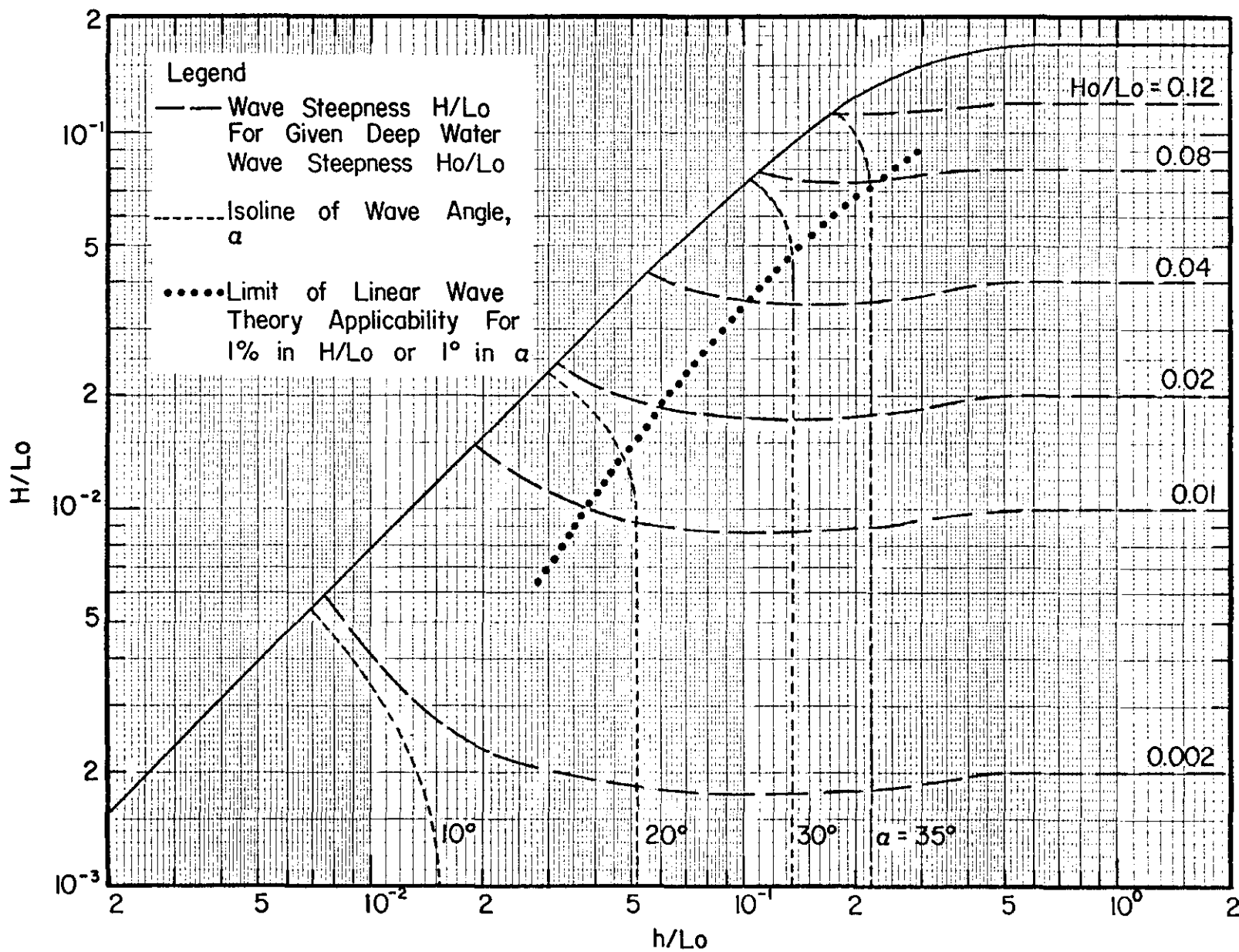


FIGURE 28 COMBINED SHOALING/REFRACTION FOR A DEEP WATER WAVE DIRECTION,  $\alpha_0 = 40^\circ$

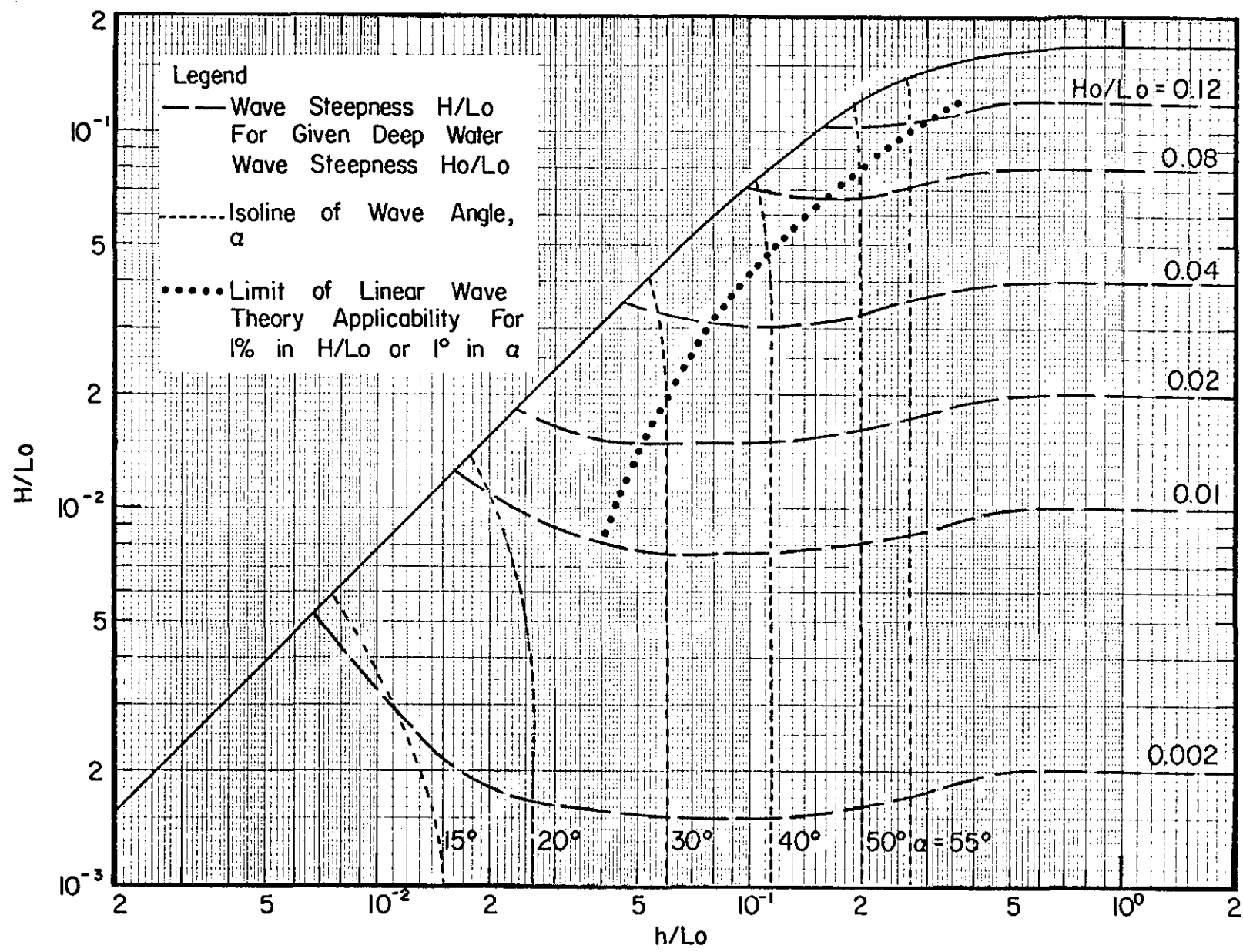


FIGURE 29 COMBINED SHOALING/REFRACTION FOR A DEEP WATER WAVE DIRECTION,  $\alpha_0 = 60^\circ$

## V. EXAMPLES ILLUSTRATING USE OF WAVE TABLES

### *Introduction*

The preceding chapter has described the formats and the various dimensionless parameters included in the wave tables; in order to aid in the application of the tables, examples will be presented illustrating their use. The first example will be a problem of a near-breaking wave interacting with an offshore structure supported by cylindrical piling. This example will utilize those tables which contain the wave profile and the wave forces and moments. Additional examples will then be presented which will illustrate the use of most of the remaining wave tables. Where possible, examples will be selected to parallel problems which may occur in offshore design. It is perhaps worthwhile to note that the tables have a much wider applicability than can be illustrated by the limited number of examples to be presented here. A thorough familiarity of the information summarized in the tables should aid in their understanding and use in many problems involving water wave phenomena. The examples will be presented in the English system of units, however the tables are in dimensionless form and any system could be used readily.

*Example 1 - Deck Elevation and Wave Forces and Moments  
on an Offshore Platform*

Consider the design problem of determining the deck elevation and horizontal wave forces and moments upon individual members of the offshore platform illustrated in Fig. 30. Suppose that the design depth (mean low water + max. tide + storm surge),  $h$ , is 41 ft, and the main structural members of the platform and outriggers are pilings 6 ft in diameter, with piling fenders 3 ft in diameter. The fenders extend from 4.1 ft above the design still water level to a depth of 8.2 ft. The outriggers are 20.5 ft high. Suppose that analysis indicates that the design wave will have a (breaking) height,  $H$ , of 31.78 ft and a period,  $T$ , of 20 sec. The drag and inertia coefficients,  $C_D$  and  $C_M$ , for this structure are assumed to be 1.05 and 1.5, respectively.

To determine which set of tables to use, calculate  $h/L_0$  and  $H/L_0$ , where  $L_0 \equiv gT^2/(2\pi)$ ,

$$\frac{h}{L_0} = \frac{41}{(5.12)(20)^2} = 0.02$$

$$\frac{H}{L_0} = \frac{31.78}{(5.12)(20)^2} = 0.0155$$

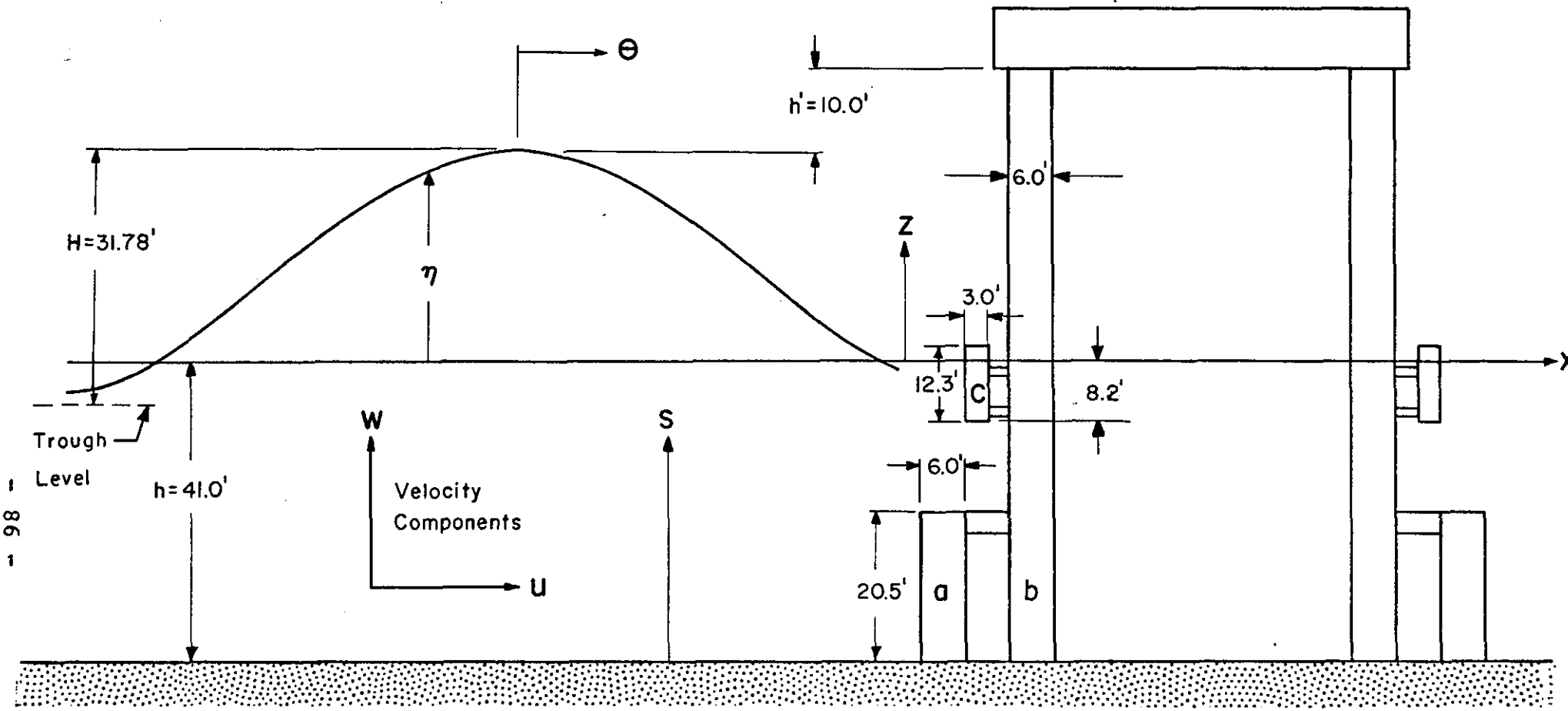


FIGURE 30  
 DEFINITION SKETCH, WAVE APPROACHING PLATFORM.

In this and most subsequent examples in this chapter, the tables for Case 4-D will be utilized (see Fig. 23). A sample table set for Case 4-D is included as Appendix III.

#### *Deck Elevation*

To ensure that the deck is above the design crest elevation; thereby avoiding unnecessarily large horizontal and vertical forces and damage to the platform base, the height of the lower elevation of the deck will be:

$$h'' = h + \eta_{\max} + h'$$

where  $h$  is the design water depth,  $\eta_{\max}$  is the maximum displacement of the wave above design still water level, and  $h'$  is the deck freeboard (say 10 feet for this problem).  $\eta_{\max}$  will occur at zero phase angle ( $\theta = 0^\circ$ ) and from any of the first 9 tables,  $\eta/\text{height} = .89$  for  $\theta = 0^\circ$ . Therefore,  $\eta_{\max} = .89 (H) = 28.3$  ft and  $h'' = h + \eta + h' = 41 + 28.3 + 10 = 79.3$  ft. The platform will be constructed so the lower deck elevation will be 79.3 feet above the bottom.

In determining the forces and moments, it is assumed that the piling are sufficiently far apart to be considered isolated. First, the forces acting upon several structural members will be determined. The total force,  $F_T(\theta, S)$ , will

be a summation of the drag force,  $F_D(\theta, S)$ , and inertia force,  $F_I(\theta, S)$ , components at any particular phase angle. Each component will be presented graphically; the components will then be added to establish the total force, and the maximum force acting upon each member will be obtained from the graph.

*Forces on Member "a"*

In the case of the outrigger, Member a, the drag force is given by:

$$F_D(\theta, S_a) = \frac{C_D \rho D}{2} \int_0^{S_a} u |u| dS'$$

where  $D$  is the piling diameter,  $S_a$  ( $= 20.5'$ ) is the height of the outrigger above bottom, and  $\rho$  = mass density of sea water,  $1.99$  slugs/ft<sup>3</sup>. In order to determine  $F_D(\theta, S_a)$ , select the tabulated dimensionless drag value for the force,  $F_D'(\theta, S_a)$ , at depth  $\frac{S_a}{h} = 0.5$  from Table V and multiply the dimensionless force by:

$$\frac{C_D \rho D (H/T)^2 h}{2}$$

$$\frac{C_D \rho D (H/T)^2 h}{2} = \frac{1.05 (1.99) (6) (31.78/20)^2 41}{2} = \begin{pmatrix} 648.9 \text{ lbs} \\ 0.6489 \text{ kips} \end{pmatrix}$$

The inertia force on Member a is given by:

$$F_I(\theta, S_a) = \frac{C_M \rho \pi D^2}{4} \int_0^{S_a} \frac{Du}{Dt} ds'$$

In order to determine  $F_I(\theta, S_a)$ , select the tabulated value of the dimensionless inertia force,  $F_I'(\theta, S)$ , for a relative depth  $\frac{S_a}{h} = .5$  from Table VI and multiply the dimensionless force by:

$$\frac{C_M \rho \pi D^2 (H/T^2) h}{4} = \begin{cases} 274.9 \text{ lbs} \\ 0.2749 \text{ kips} \end{cases}$$

The total force will be determined by summation of  $F_I(\theta, S_a)$  and  $F_D(\theta, S_a)$  at each phase angle,  $\theta$ . The force calculations are summarized in Table G and the forces are plotted in Figure 31.

*Forces on Member "b"*

Next, consider the horizontal forces acting on the main support piling. In this case, the forces are integrated from 0 to  $h + \eta(\theta)$ . In order to determine  $F_D(\theta)$ , multiply the tabulated value for the dimensionless total drag force,  $F_D'(\theta)$  (indicated "Surface" in Table V) by the same constant as for Member a, i.e.

$$\frac{C_D \rho D (H/T)^2 h}{2} = 0.6849 \text{ kips}$$

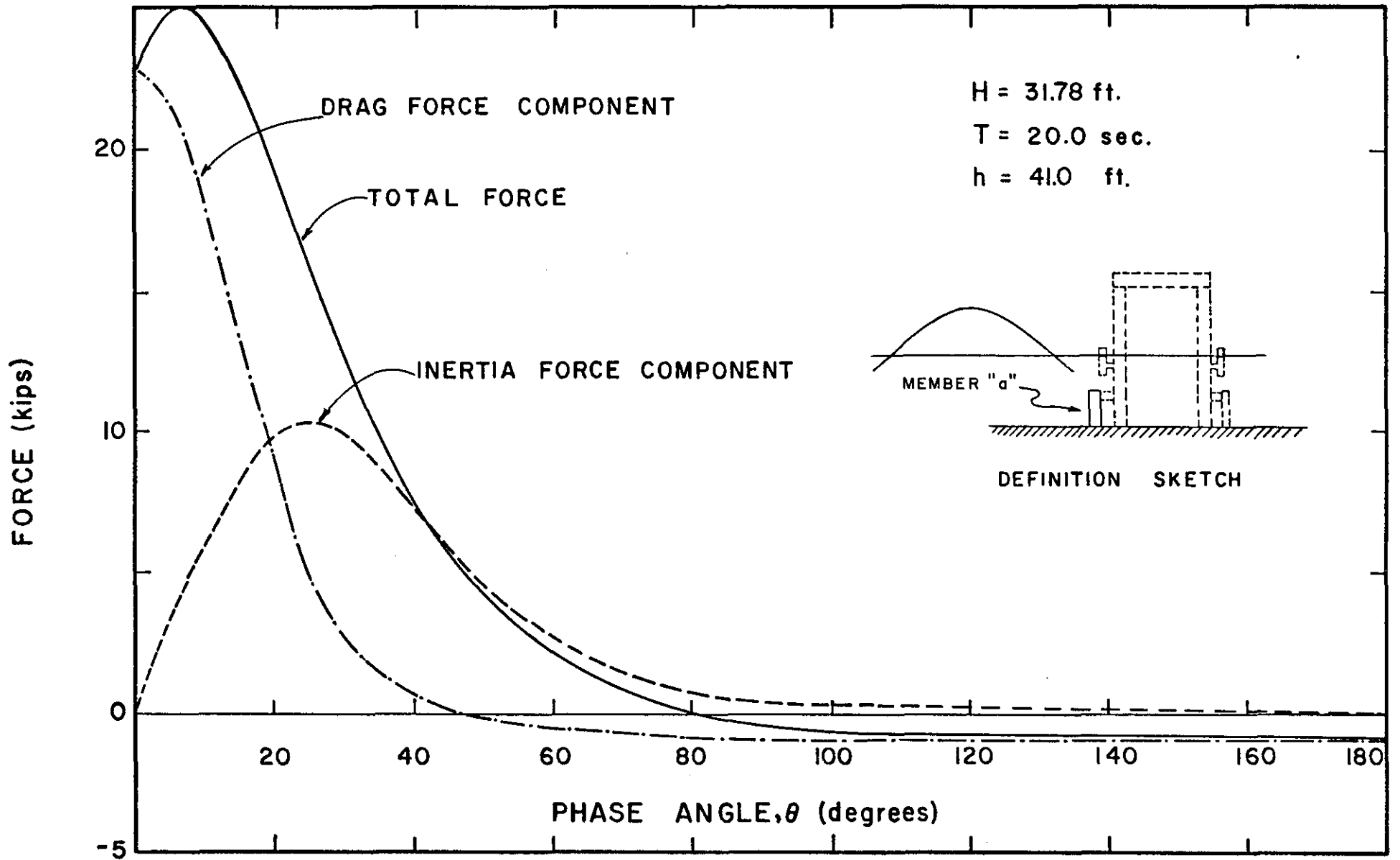


FIGURE 31 HORIZONTAL WAVE FORCES ON MEMBER "a"

TABLE G

## Horizontal Wave Forces on Member "a"

| $\theta$ (°) | 0     | 10    | 20    | 30    | 50     | 75    | 100   | 130   | 180   |
|--------------|-------|-------|-------|-------|--------|-------|-------|-------|-------|
| $F_D'$       | 36.31 | 29.00 | 14.60 | 4.30  | - 0.04 | -1.14 | -1.54 | -1.62 | -1.60 |
| $F_D$ (kips) | 23.56 | 18.81 | 9.47  | 2.79  | - 0.03 | -0.74 | -1.00 | -1.05 | -1.04 |
| $F_I'$       | 0.0   | 22.59 | 36.36 | 36.63 | 17.25  | 3.76  | 0.67  | 0.12  | 0.0   |
| $F_I$ (kips) | 0.0   | 6.21  | 10.00 | 10.07 | 4.74   | 1.03  | 0.18  | 0.03  | 0.0   |
| $F_T$ (kips) | 23.56 | 25.02 | 19.47 | 12.86 | 4.71   | 0.29  | -0.82 | -1.02 | -1.04 |

Similarly,  $F_I(\theta)$  is found by multiplying the tabulated value,  $F_I'(\theta)$ , indicated "Surface" in Table VI by

$$\frac{C_M \rho \pi D^2 (H/T^2) h}{4} = 0.2749 \text{ kips}$$

The calculated forces are summarized in Table H and are plotted in Figure 32.

*Forces on Member "c"*

Finally, consider structural Member c, the fender. The computation for this member is a combination of the two previous methods since it is sometimes over-topped by the wave. The forces are integrated from  $S_{C_1} = 32.8$  ft to

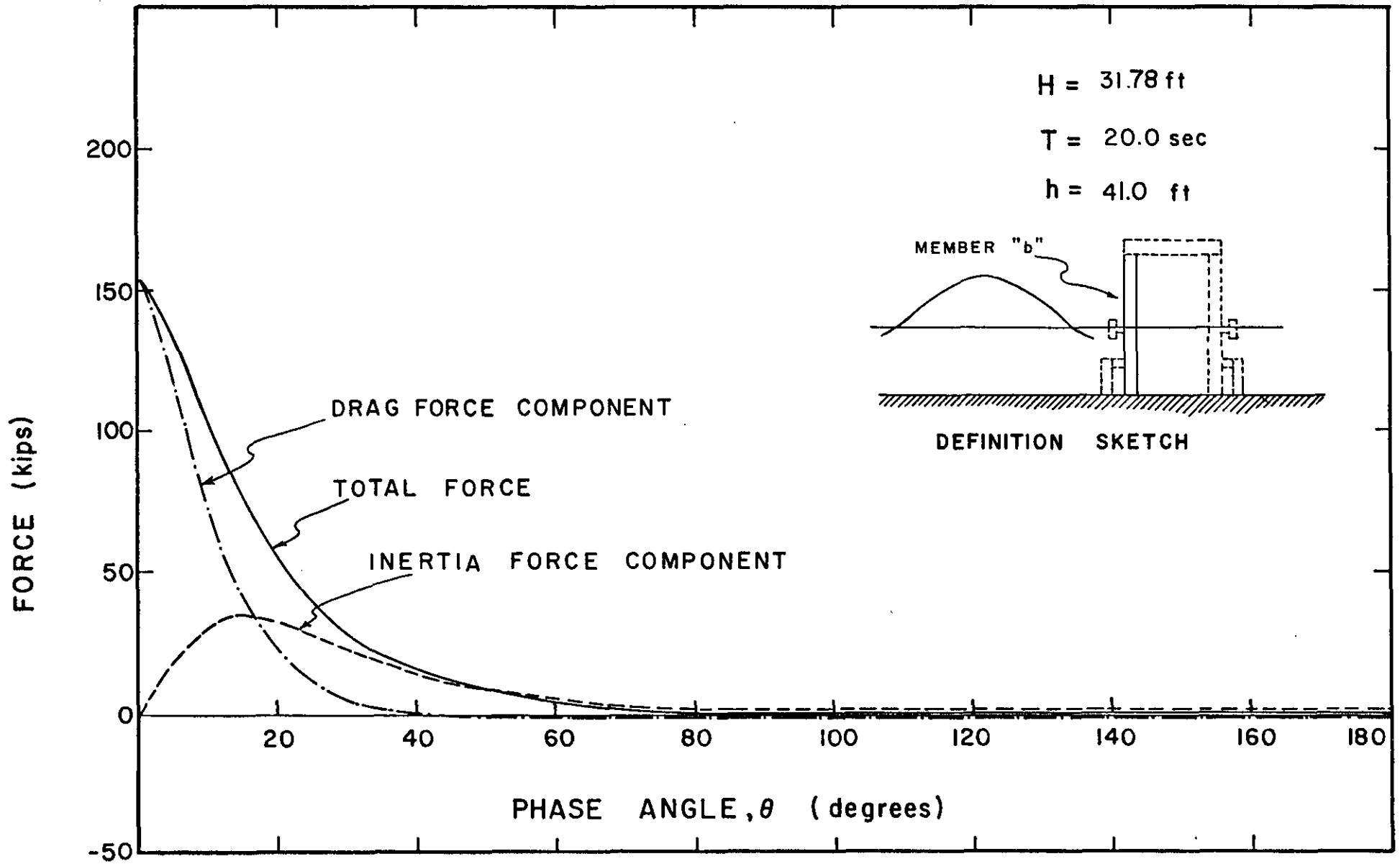


FIGURE 32 HORIZONTAL WAVE FORCES ON MEMBER "b"

TABLE H  
Horizontal Wave Forces on Member "b"

| $\theta$ (°) | 0      | 10     | 20     | 30    | 50     | 75    | 100   | 130   | 180   |
|--------------|--------|--------|--------|-------|--------|-------|-------|-------|-------|
| $F_D'$       | 242.39 | 119.80 | 37.00  | 7.72  | - 0.25 | -2.19 | -2.84 | -2.95 | -2.92 |
| $F_D$ (kips) | 157.3  | 77.7   | 24.0   | 5.0   | - 0.2  | -1.4  | -1.8  | -1.9  | -1.9  |
| $F_I'$       | 0.0    | 112.13 | 113.47 | 84.55 | 30.12  | 6.08  | 1.03  | 0.27  | 0.0   |
| $F_I$ (kips) | 0.0    | 30.8   | 31.2   | 23.2  | 8.3    | 1.7   | 0.3   | 0.1   | 0.0   |
| $F_T$ (kips) | 157.3  | 108.5  | 55.2   | 28.2  | 8.1    | 0.3   | -1.5  | -1.8  | -1.9  |

$S_{C_2} = 45.1$  ft; therefore, the force acting on an imaginary piling up to the bottom of the fender is subtracted from a similar term for the top of the fender. The dimensionless forces are obtained by subtracting the dimensionless force components pertaining to the bottom of the member from those pertaining to the top. If the top of the member is submerged, the value at  $S'_{C_2} = 1.1$  should be used; for times that the top is not submerged, the value indicated "Surface" should be employed for  $S'_{C_2}$ . Note that the selection of the proper value for the member upper elevation follows readily from the tables; the values at  $S'_{C_2} = 1.1$  are used at phase angles where they are

tabulated ( $0 \leq \theta \leq 20^\circ$ ) and the values labeled "Surface" are used for the remaining phase angles ( $30^\circ \leq \theta \leq 180^\circ$ ).

Summarizing, for each phase angle, the net dimensionless force components on Member c are obtained by:

$$F'_{D_N} = F'_{D_U} - F'_{D_L}$$

$$F'_{I_N} = F'_{I_U} - F'_{I_L}$$

where the subscripts N, U and L indicate net, upper and lower, respectively. The dimensionalizing constant for drag force for the member is calculated (recalling that  $D = 3'$ )

$$\frac{C_D \rho D (H/T)^2 h}{2} = 0.3245 \text{ kips}$$

and for the inertia force component

$$\frac{C_M \rho \pi D^2 (H/T^2) h}{4} = 0.0687 \text{ kips}$$

The required calculations are summarized in Table I and the results are shown in Figure 33.

The maximum horizontal wave induced forces are now available for the design wave and may be used in further design analysis. They are summarized in Table J.

TABLE I  
Horizontal Wave Forces on Member "c"

| $\theta$ (°)                          | 0     | 10    | 20    | 30    | 50     | 75    | 100   | 130   | 150   |
|---------------------------------------|-------|-------|-------|-------|--------|-------|-------|-------|-------|
| $F_{D_U}'$                            | 99.73 | 75.87 | 33.17 | 7.72  | - 0.25 | -2.19 | -2.84 | -2.95 | -2.92 |
| $F_{D_L}'$                            | 63.34 | 49.68 | 23.72 | 6.40  | - 0.14 | -1.87 | -2.48 | -2.59 | -2.56 |
| $F_{D_N}' =$<br>$F_{D_U}' - F_{D_L}'$ | 36.39 | 26.19 | 9.45  | 1.32  | - 0.11 | -0.32 | -0.36 | -0.36 | -0.36 |
| $F_D$ (kips)                          | 11.81 | 8.50  | 3.07  | 0.43  | - 0.04 | -0.10 | -0.12 | -0.12 | -0.12 |
| $F_{I_U}'$                            | 0.0   | 65.78 | 96.88 | 84.55 | 30.12  | 6.08  | 1.03  | 0.27  | 0.0   |
| $F_{I_L}'$                            | 0.0   | 40.55 | 62.97 | 60.49 | 26.23  | 5.53  | 0.96  | 0.22  | 0.0   |
| $F_{I_N}' =$<br>$F_{I_U}' - F_{I_L}'$ | 0.0   | 25.23 | 33.91 | 24.06 | 3.89   | 0.55  | 0.07  | 0.05  | 0.0   |
| $F_I$ (kips)                          | 0.0   | 1.73  | 2.33  | 1.65  | 0.27   | 0.04  | 0.0   | 0.0   | 0.0   |
| $F_T$ (kips)                          | 11.81 | 10.23 | 5.40  | 2.08  | 0.23   | -0.06 | -0.11 | -0.11 | -0.12 |

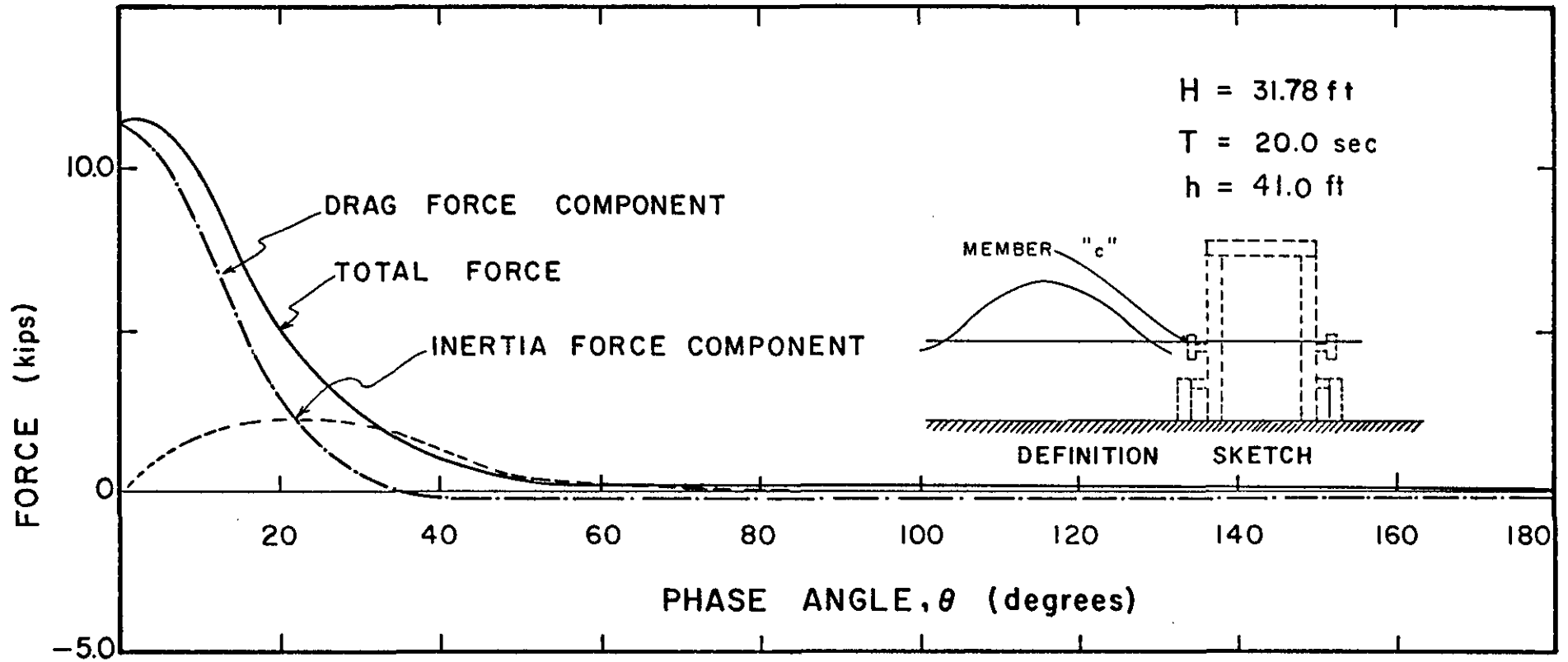


FIGURE 33 HORIZONTAL WAVE FORCES ON MEMBER "c"

TABLE J

Summary of Maximum Wave Forces on  
Several Platform Components

| Member | Phase Angle of<br>Maximum Force,<br>$\theta_m$ (°) | $F_{T_{max}}$ (kips) |
|--------|--|----------------------|
| a      | 7°   | 25.1                 |
| b      | 1°   | 160                  |
| c      | 1°   | 12.3                 |

Note: Phase angles and maximum forces  
obtained by interpolation from  
Figures 31, 32 and 33.

*Moments on Member "a"*

The moments due to the wave forces acting on the structure are also essential in design. For any member, the moment about the mudline is defined as:

$$M_T(\theta) = \int_{S_1}^{S_2} S \, dF_T(\theta, S) = \int_{S_1}^{S_2} S \, dF_D(\theta, S) + \int_{S_1}^{S_2} S \, dF_I(\theta, S)$$

$$= M_D(\theta) + M_I(\theta)$$

where

$$M_D(\theta) = \frac{\rho C_D D}{2} \int_{S_1}^{S_2} S \, u |u| \, ds$$

and

$$M_I(\theta, S) = \frac{C_M \rho \pi D^2}{4} \int_{S_1}^{S_2} S \, \frac{Du}{Dt} \, ds$$

Consider the total moment about the mudline on the outrigger (Member a). In this case  $S_1 = 0$ , and  $S_2 = S_a = 0.5 h$ . To determine the drag moment,  $M_D(\theta)$ , multiply the dimensionless tabulated value for the drag moment,  $M'_D(\theta)$ , listed at depth  $S_a/h = .5$  in Table VII, by

$$\frac{C_D \rho D (H/T)^2 h^2}{2} = \begin{cases} 26606 & \text{for } M_D \text{ in ft-lbs} \\ 26.606 & \text{for } M_D \text{ in ft-kips} \end{cases}$$

Similarly, multiply  $M'_I(\theta)$  listed at depth  $S_a/h = .5$  in Table VIII by

$$\frac{C_M \rho \pi D^2 (H/T^2) h^2}{4} = \begin{cases} 11272 & \text{for } M_I \text{ in ft-lbs} \\ 11.272 & \text{for } M_I \text{ in ft-kips} \end{cases}$$

to obtain  $M_I(\theta)$ . These moments are added to obtain  $M_T(\theta)$ , as shown in Table K and Figure 34.

TABLE K  
Wave Moments (About Mudline) on Member "a"

| $\theta$ (°)    | 0     | 10    | 20    | 30    | 50     | 75     | 100    | 130    | 180    |
|-----------------|-------|-------|-------|-------|--------|--------|--------|--------|--------|
| $M'_D$          | 9.31  | 7.40  | 3.67  | 1.05  | - 0.01 | - 0.29 | - 0.39 | - 0.40 | - 0.40 |
| $M_D$ (ft-kips) | 247.7 | 196.9 | 97.6  | 27.9  | - 0.3  | - 7.7  | -10.4  | -10.6  | -10.6  |
| $M'_I$          | 0.0   | 5.85  | 9.32  | 9.26  | 4.25   | 0.92   | 0.16   | 0.03   | 0.0    |
| $M_I$ (ft-kips) | 0.0   | 65.9  | 105.1 | 104.4 | 47.9   | 10.4   | 1.8    | 0.3    | 0.0    |
| $M_T$ (ft-kips) | 247.7 | 262.8 | 202.7 | 132.3 | 47.6   | + 2.7  | - 8.6  | -10.3  | -10.6  |

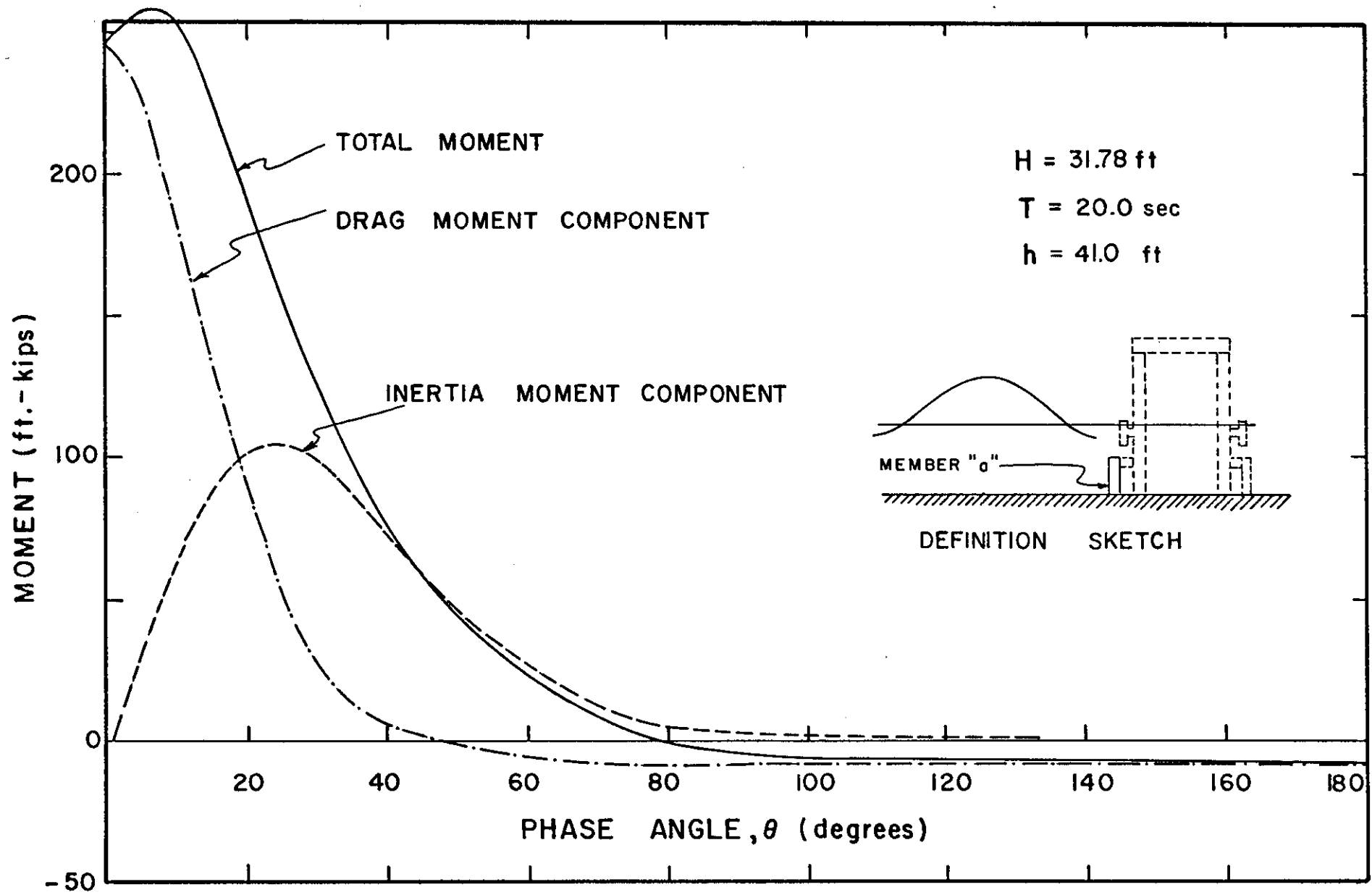


FIGURE 34 WAVE MOMENTS ON MEMBER "d"

Moments on Member "b"

Next consider the moment on the main structural piling (Member b). The limits of integration are from 0 to  $h + \eta(\theta)$ . Therefore, take the tabulated values labeled "Surface" from Table VII,  $\{M'_D(\theta)\}$ , and Table VIII,  $\{M'_I(\theta)\}$ , and multiply by

$$\frac{C_D \rho D (H/T)^2 h^2}{2} = 26.606 \text{ for } M_D \text{ in ft-kips}$$

and

$$\frac{C_M \rho \pi D^2 (H/T^2) h^2}{4} = 11.272 \text{ for } M_I \text{ in ft-kips}$$

in order to obtain  $M_D(\theta)$  and  $M_I(\theta)$ . The two moments are added to obtain  $M_T(\theta)$  as indicated in Table L and plotted in Figure 35.

TABLE L  
Wave Moments (About Mudline) on Member "b"

| $\theta$ (°)    | 0     | 10    | 20   | 30   | 50    | 75    | 100   | 130   | 180   |
|-----------------|-------|-------|------|------|-------|-------|-------|-------|-------|
| $M'_D$          | 268.1 | 102.6 | 23.0 | 3.6  | - 0.2 | - 1.0 | - 1.3 | - 1.3 | - 1.3 |
| $M_D$ (ft-kips) | 7133  | 2730  | 612  | 96   | - 5   | -27   | -35   | -35   | -35   |
| $M'_I$          | 0.0   | 101.7 | 78.5 | 47.5 | 13.5  | 2.5   | 0.4   | 0.1   | 0.0   |
| $M_I$ (ft-kips) | 0.0   | 1146  | 885  | 535  | 152   | 28    | 5     | 1     | 0.0   |
| $M_T$ (ft-kips) | 7133  | 3876  | 1497 | 631  | 147   | 1     | -30   | -34   | -35   |

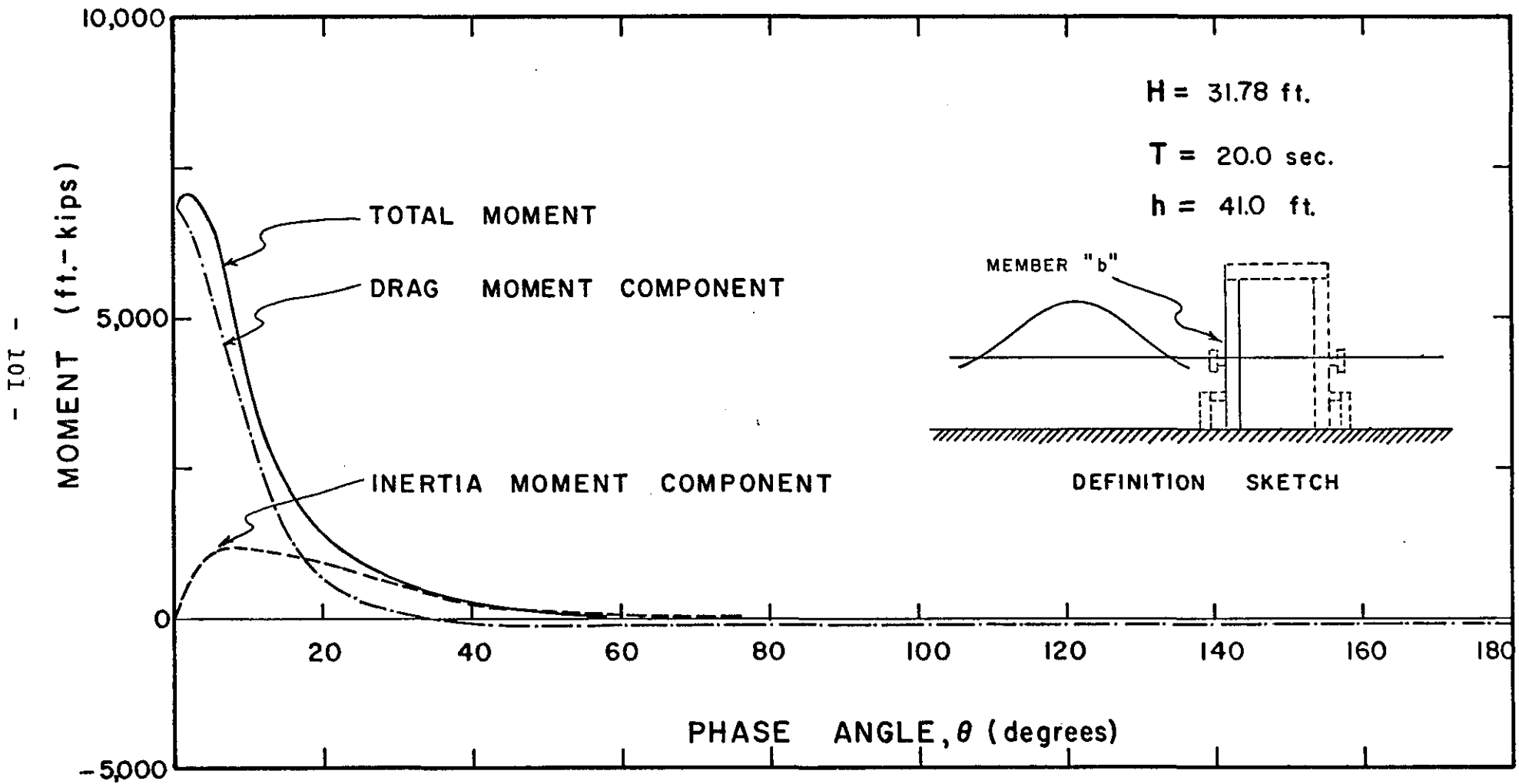


FIGURE 35 WAVE MOMENTS ON MEMBER "b"

Moments on Member "c"

The fender has the same limits of integration for moment calculation as for the force calculation and is determined in a similar manner. However, the tabulated moments,  $M'_D(\theta, S)$  and  $M'_I(\theta, S)$ , are taken from Tables VII and VIII. The total moment acting on the fender is found by:  $M_T(\theta) = M_D(\theta) + M_I(\theta)$ . The calculations are summarized in Table M and are plotted in Figure 36.

TABLE M  
Wave Moments (About Mudline) on Member "c"

| $\theta$ (°)                       | 0     | 10    | 20    | 30    | 50     | 75    | 100   | 130   | 180   |
|------------------------------------|-------|-------|-------|-------|--------|-------|-------|-------|-------|
| $M'_{DU}$                          | 61.94 | 46.01 | 18.59 | 3.63  | - 0.18 | -1.04 | -1.31 | -1.35 | -1.33 |
| $M'_{DL}$                          | 27.04 | 20.94 | 9.61  | 2.40  | - 0.08 | -0.77 | -1.00 | -1.04 | -1.02 |
| $M'_{DN} =$<br>$M'_{DU} - M'_{DL}$ | 34.90 | 25.07 | 8.98  | 1.23  | - 0.10 | -0.27 | -0.31 | -0.31 | -0.31 |
| $M_D$<br>(ft-kips)                 | 464   | 334   | 119   | 16    | - 1    | -4    | -4    | -4    | -4    |
| $M'_{IU}$                          | 0.0   | 41.87 | 59.20 | 47.47 | 13.45  | 2.52  | 0.40  | 0.14  | 0.0   |
| $M'_{IL}$                          | 0.0   | 17.66 | 26.76 | 24.82 | 10.04  | 2.05  | 0.34  | 0.10  | 0.0   |
| $M'_{IN} =$<br>$M'_{IU} - M'_{IL}$ | 0.0   | 24.21 | 32.44 | 22.65 | 3.41   | 0.47  | 0.06  | 0.04  | 0.0   |
| $M_I$<br>(ft-kips)                 | 0.0   | 68    | 91    | 64    | 10     | 1     | 0     | 0     | 0.0   |
| $M_T$<br>(ft-kips)                 | 464   | 402   | 210   | 80    | 9      | -3    | -4    | -4    | -4    |

- 103 -

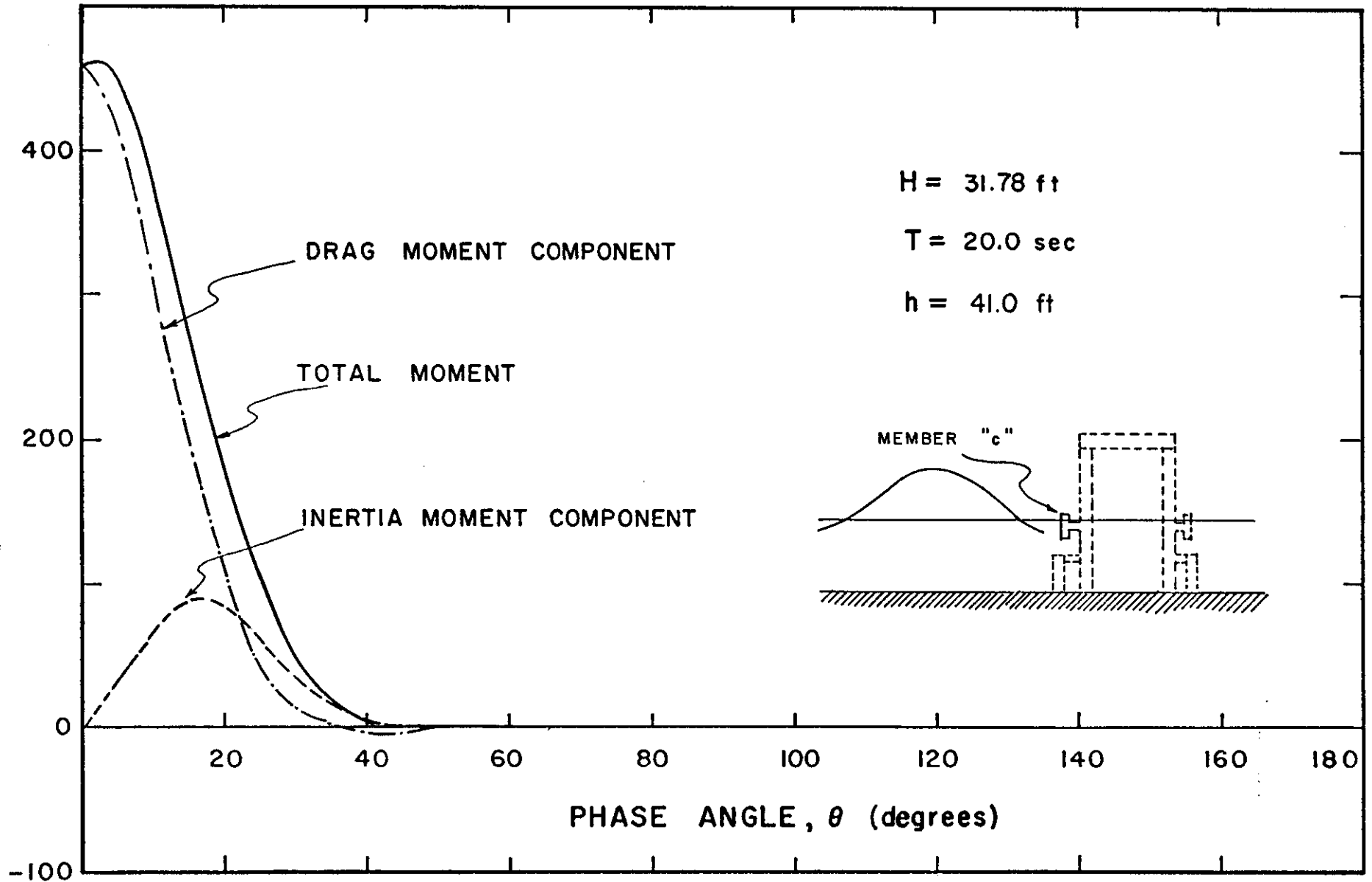


FIGURE 36 WAVE MOMENTS ON MEMBER "c"

The maximum calculated forces and moments on the three platform members due to the design wave are summarized in Table N.

TABLE N  
Summary of Maximum Wave Forces and Moments

| Member | $\theta$ | $F_T(\theta, S)$<br>(kips) | $\theta$ | $M_T(\theta, S)$<br>(ft-kips) |
|--------|----------|----------------------------|----------|-------------------------------|
| a      | 7°       | 25.1                       | 5°       | 267                           |
| b      | 1°       | 160                        | 1°       | 7140                          |
| c      | 1°       | 12.3                       | 1°       | 475                           |

*Example 2 - Wave Characteristics, Kinematics and Pressure Fields*

This example describes the use of the tables for calculating various parameters associated with a periodic wave. These parameters include the wave length and the kinematic and pressure fields.

*Wave Length*

The wave length is presented in dimensionless form in Table XI of the sample output and is determined as follows:

$$L = \frac{gT^2}{2\pi} L'$$

For example, for the same wave considered in Example 1,

$L' = 0.422$  and  $T = 20$  sec. The wave length is therefore:

$$L = 5.12 (20)^2 (0.422) = 864.3 \text{ ft}$$

#### *Wave Profile*

The dimensionless wave profile,  $\eta'(\theta)$ , is tabulated in each of Tables I - IX and is defined as:

$$\eta'(\theta) = \frac{\eta(\theta)}{H}$$

therefore

$$\eta(\theta) = \eta'(\theta) \cdot H$$

The wave profile calculation for Case 4-D is summarized in Table O and is plotted in Figure 37. Note that  $\eta$  is an even function of  $\theta$ .

#### *Water Particle Kinematics*

The water particle kinematics will be calculated for Case 4-D as presented in the sample output. These kinematics will be calculated for mid-depth (i.e., 20.5 ft above the bottom). The dimensionless forms of these variables are presented in Tables I - IV of the sample output. The dimensionless water particle velocities are defined as

$$u'(\theta, S) \equiv \frac{u(\theta, S)}{H/T}$$

and

$$w'(\theta, S) \equiv \frac{w(\theta, S)}{H/T}$$

TABLE O

Calculated Wave Profile, Kinematics, and Dynamic Pressure (All Kinematics and Dynamic Pressure Calculated at Mid-Depth)

| Variable   | Dimensionalizing Constant   | $\theta$ (°)    |                  |               |               |                  |                  |                  |                  |                  |  |
|--|---|-----------------|------------------|---------------|---------------|------------------|------------------|------------------|------------------|------------------|--|
|  |   | 0               | 10               | 20            | 30            | 50               | 75               | 100              | 130              | 180              |  |
| $\eta'$<br>$\eta$ (ft)                                     | $H = 31.78$ ft  | 0.89<br>28.28   | 0.58<br>18.43    | 0.28<br>8.90  | 0.10<br>3.18  | - 0.06<br>- 1.90 | - 0.10<br>- 3.18 | - 0.11<br>- 3.50 | - 0.11<br>- 3.50 | - 0.11<br>- 3.50 |  |
| $u'$<br>$u$ (ft/sec)                                       | $H/T = 31.78/20$<br>$= 1.589$ ft/sec  | 8.97<br>14.25   | 7.94<br>12.62    | 5.46<br>8.68  | 2.80<br>4.45  | - 0.42<br>- 0.67 | - 1.54<br>- 2.45 | - 1.76<br>- 2.80 | - 1.80<br>- 2.86 | - 1.79<br>- 2.84 |  |
| $w'$<br>$w$ (ft/sec)                                       | Same as for $u$ ,<br>$= 1.589$ ft/sec                                       | 0.0<br>0.0      | 1.46<br>2.32     | 2.14<br>3.40  | 1.95<br>3.10  | 0.81<br>1.29     | 0.17<br>0.27     | 0.03<br>0.05     | 0.01<br>0.02     | 0.0<br>0.0       |  |
| $\frac{Du'}{Dt}$<br>$\frac{Du}{Dt}$ (ft/sec <sup>2</sup> ) | $H/T^2 = 31.78/(20)^2$<br>$= 0.07945$<br>ft/sec <sup>2</sup>                | 0.0<br>0.0      | 51.89<br>4.12    | 80.18<br>6.37 | 76.41<br>6.07 | 32.40<br>2.57    | 6.73<br>0.53     | 1.16<br>0.09     | 0.28<br>0.02     | 0.0<br>0.0       |  |
| $\frac{Dw'}{Dt}$<br>$\frac{Dw}{Dt}$ (ft/sec <sup>2</sup> ) | Same as for $\frac{Du}{Dt}$ ,<br>$= 0.07945$<br>ft/sec <sup>2</sup>         | -39.21<br>-3.11 | -25.66<br>- 2.03 | 2.27<br>0.18  | 21.80<br>1.73 | 18.01<br>1.43    | 4.04<br>0.32     | 1.04<br>0.08     | 0.04<br>0.00     | - 0.28<br>- 0.02 |  |
| $p'_D$<br>$p_D$ (lb/ft <sup>2</sup> )                      | $\frac{\gamma H}{2} = \frac{(64)(31.78)}{2}$<br>$= 1017$ lb/ft <sup>2</sup> | 1.030<br>1048   | 0.930<br>946     | 0.673<br>684  | 0.372<br>378  | - 0.035<br>-36   | - 0.189<br>-192  | - 0.221<br>-225  | - 0.226<br>-230  | - 0.225<br>-229  |  |

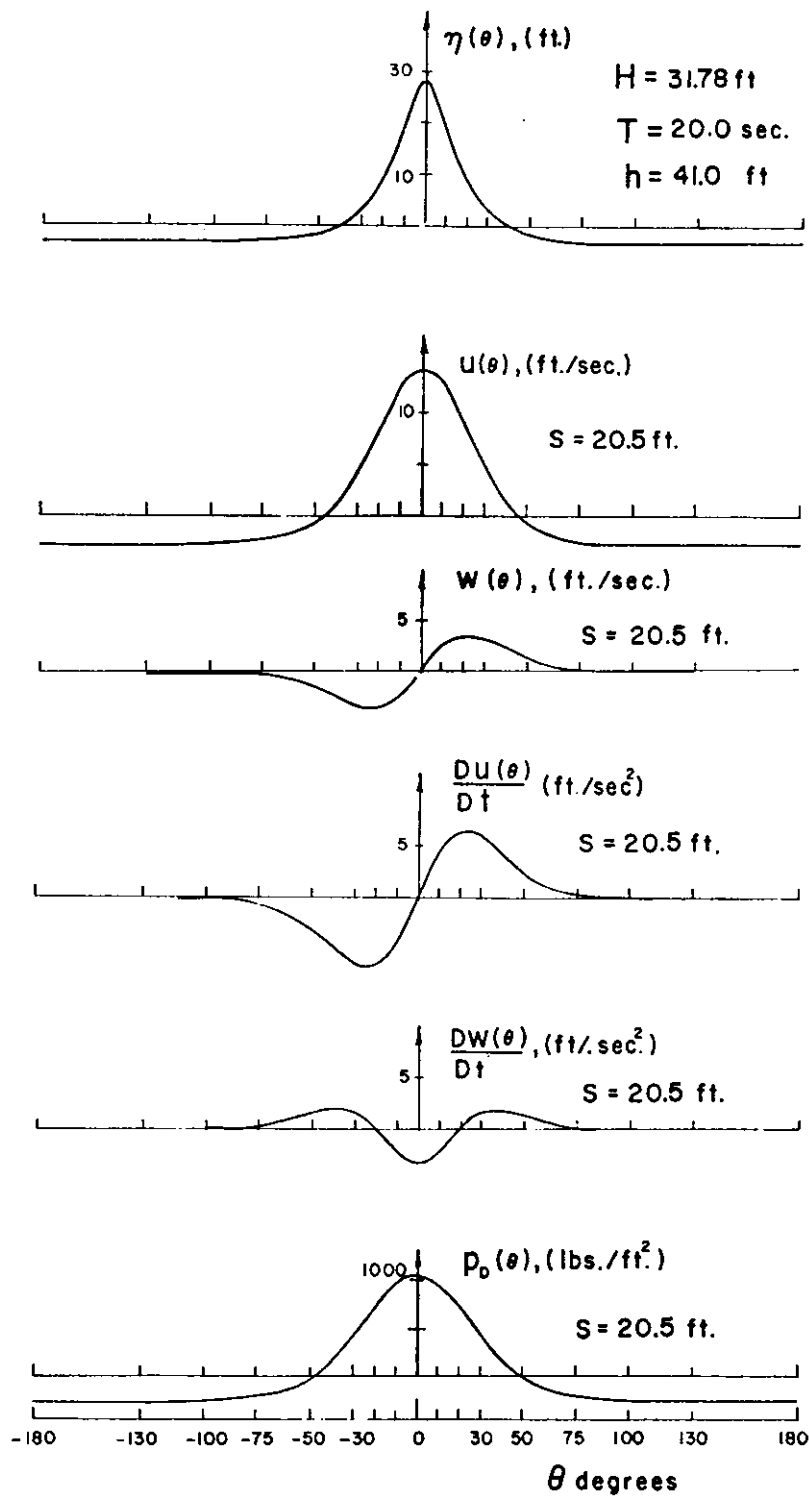


FIGURE 37 EXAMPLE CALCULATIONS OF WAVE PROFILE, KINEMATICS AND DYNAMIC PRESSURE

and the dimensionless water particle total accelerations are defined as

$$\left(\frac{Du}{Dt}\right)' \equiv \frac{\frac{Du}{Dt}}{H/T^2}$$

and

$$\left(\frac{Dw}{Dt}\right)' \equiv \frac{\frac{Dw}{Dt}}{H/T^2}$$

Note that these are functions of  $\theta$  and  $S$ , however, for convenience, the dependence has not been indicated in the above expressions. The calculations of the water particle velocities and accelerations over the range  $0^\circ < \theta < 180^\circ$ , are also summarized in Table O and plotted in Figure 37.

It will be noted that in the tables of wave functions, the variables are only presented for phase angles ranging between zero degrees and 180 degrees. All of the variables are either symmetrical or anti-symmetrical about a phase angle of zero degrees. The variables that are symmetrical include: the water surface profile, the horizontal component of water particle velocity and the vertical component of water particle acceleration. The anti-symmetrical variables include the vertical component of velocity and the horizontal component of water particle acceleration.

#### *Dynamic Pressure*

The dynamic pressure was also calculated at a distance of 20.5 ft above the bottom. The dimensionless

form of this variable is

$$p_D' = \frac{p_D}{\frac{\gamma H}{2}}$$

and is presented in Table IX of the sample output. The calculations are summarized in Table O of this report and presented in graphical form in Figure 37. Note that  $p_D$  is an even function of  $\theta$ .

### *Example 3 - Free Surface Boundary Condition Errors*

The free surface boundary condition errors and the reason for examining and tabulating these errors have been described in Section II. By way of illustrating the use of tables to calculate the free surface boundary condition errors, both the distributed errors on the free surface and the root mean square and maximum errors as gross measures of these errors will be presented. The distributed kinematic and dynamic free surface boundary condition errors are presented in Table X, Items 1-4 of the sample output and the root mean square errors and maximum errors are presented in Table XI, Items 10-13.

### *Distributed Boundary Condition Errors*

The calculations of the distributed boundary condition errors are presented in Table P and Figure 38 of this report. It is noted that the kinematic free surface boundary condition errors as defined and presented in the

TABLE P

## Free Surface Boundary Condition Errors

| $\theta$ (°) | 0 | 10 | 20 | 30 | 50 | 75 | 100 | 130 | 180 |
|--------------|---|----|----|----|----|----|-----|-----|-----|
|--------------|---|----|----|----|----|----|-----|-----|-----|

a) KFSBC Error, Linear Wave Theory, Table X, Item (1)

|                            |     |       |       |       |       |       |        |        |     |
|----------------------------|-----|-------|-------|-------|-------|-------|--------|--------|-----|
| $\epsilon_1' = \epsilon_1$ | 0.0 | 0.035 | 0.064 | 0.081 | 0.079 | 0.032 | -0.018 | -0.042 | 0.0 |
|----------------------------|-----|-------|-------|-------|-------|-------|--------|--------|-----|

b) KFSBC Errors, Stream Function Theory, Table X, Item (2)

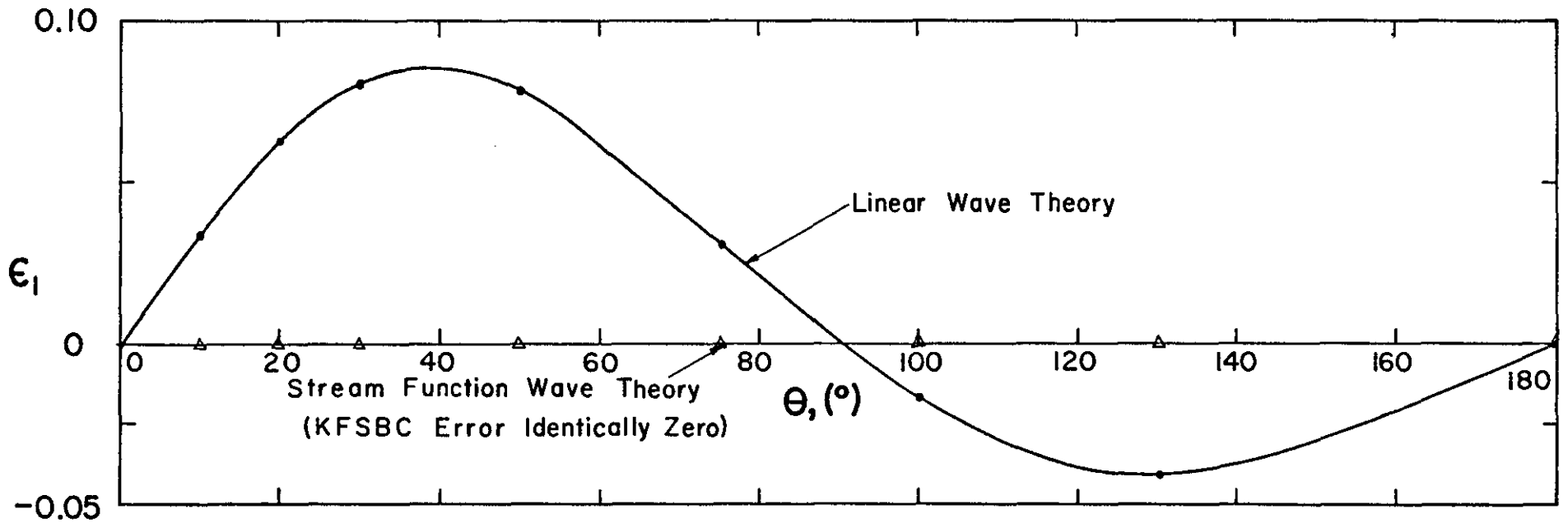
|                            |     |     |     |     |     |     |     |     |     |
|----------------------------|-----|-----|-----|-----|-----|-----|-----|-----|-----|
| $\epsilon_1' = \epsilon_1$ | 0.0 | 0.0 | 0.0 | 0.0 | 0.0 | 0.0 | 0.0 | 0.0 | 0.0 |
|----------------------------|-----|-----|-----|-----|-----|-----|-----|-----|-----|

c) DFSBC Errors, Linear Wave Theory, Table X, Item (3)

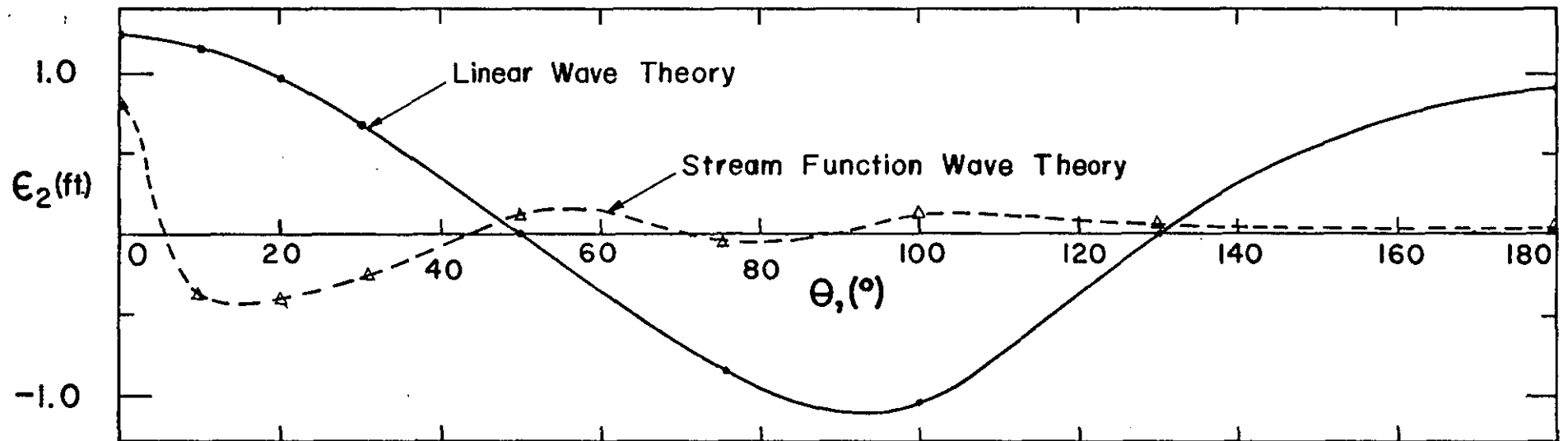
|                              |        |        |        |        |         |         |         |        |        |
|------------------------------|--------|--------|--------|--------|---------|---------|---------|--------|--------|
| $\epsilon_2' = \epsilon_2/H$ | 0.0385 | 0.0366 | 0.0309 | 0.0222 | -0.0007 | -0.0265 | -0.0331 | 0.0004 | 0.0284 |
| $\epsilon_2$ (ft)            | 1.224  | 1.163  | 0.982  | 0.706  | -0.022  | -0.842  | -1.052  | 0.013  | 0.903  |

d) DFSBC Error, Stream Function Wave Theory, Table X, Item (4)

|                              |        |         |         |         |        |        |        |       |        |
|------------------------------|--------|---------|---------|---------|--------|--------|--------|-------|--------|
| $\epsilon_2' = \epsilon_2/H$ | 0.0289 | -0.0112 | -0.0108 | -0.0039 | 0.0007 | 0.0002 | 0.0020 | .0013 | 0.0003 |
| $\epsilon_2$ (ft)            | 0.918  | -0.356  | -0.343  | -0.124  | 0.022  | 0.006  | 0.064  | 0.041 | 0.010  |



a) Distribution of Kinematic Free Surface Boundary Condition Error



b) Distribution of Dynamic Free Surface Boundary Condition Error

FIGURE 38 FREE SURFACE BOUNDARY CONDITION ERRORS

wave tables (Table X, Items 1 and 2) are in dimensionless form. However, the dynamic free surface boundary condition errors (Table X, Items 3 and 4 of wave tables) are dimensional as illustrated in the sample calculations accompanying Table P. The calculations of the root-mean-square (RMS) and maximum kinematic dynamic free surface boundary condition errors are presented below.

*Overall Kinematic Free Surface Boundary Condition Errors*

The RMS kinematic free surface boundary condition errors are presented as Item 10 in Table XI, i.e.

$$\sqrt{\epsilon_1^2} = .0475 \quad (\text{Linear Wave Theory})$$

$$\sqrt{\epsilon_1^2} = 0.0 \quad (\text{Stream Function Wave Theory})$$

The maximum KFSBC error is obtained from Item 12 of Table XI,

$$|\epsilon_1|_{\max} = 0.0856 \quad (\text{Linear Wave Theory})$$

$$|\epsilon_1|_{\max} = 0.0 \quad (\text{Stream Function Wave Theory})$$

*Overall Dynamic Free Surface Boundary Condition Errors*

The RMS DFSBC errors are presented in dimensionless form as Item 11 in Table XI, i.e.

$$\left. \begin{aligned} \sqrt{\epsilon_2^2}/H &= 0.0241 \\ \sqrt{\epsilon_2^2} &= 0.765 \text{ ft} \end{aligned} \right\} \quad (\text{Linear Wave Theory})$$

$$\left. \begin{aligned} \sqrt{\epsilon_2^2}/H &= 0.0048 \\ \sqrt{\epsilon_2^2} &= 0.153 \text{ ft} \end{aligned} \right\} \text{(Stream Function Wave Theory)}$$

The maximum DFSBC errors, obtained from Table XI, Item 13 are

$$\left. \begin{aligned} \frac{|\epsilon_2|_{\max}}{H} &= 0.0385 \\ |\epsilon_2|_{\max} &= 1.224 \text{ ft} \end{aligned} \right\} \text{(Linear Wave Theory)}$$

$$\left. \begin{aligned} \frac{|\epsilon_2|_{\max}}{H} &= 0.0289 \\ |\epsilon_2|_{\max} &= 0.918 \text{ ft} \end{aligned} \right\} \text{(Stream Function Wave Theory)}$$

With regard to interpretation of the boundary condition errors, in accordance with the discussion in Section II, if the boundary condition errors for any given theory were found to be generally better than for the Stream function theory, then it could be concluded that at least the analytical validity of that wave theory would be better and as discussed earlier, there is some evidence to indicate that the analytical wave theory is a good indicator of the experimental validity (or of the wave phenomenon in nature).

*Example 4 - Calculation of Energy, Momentum, and Energy and Momentum Fluxes*

The tabulations of average potential, kinetic, and total energy and energy fluxes and average momentum and

momentum fluxes are presented in Table XI. The calculation of these quantities in dimensional form is relatively straightforward and will simply be presented without discussion.

*Average Potential Energy (Table XI, Item 2)*

$$PE' = \frac{PE}{(\gamma H^2/8)} = 0.213$$

$$PE = 0.213(8080) = 1721 \text{ ft-lb/ft}^2$$

*Average Kinetic Energy (Table XI, Item 3)*

$$KE' = \frac{KE}{(\gamma H^2/8)} = 0.254$$

$$KE = 0.254(8080) = 2052 \text{ ft-lb/ft}^2$$

*Total Energy (Table XI, Item 4)*

$$TE' = \frac{TE}{(\gamma H^2/8)} = 0.467$$

$$TE = 0.467(8080) = 3773 \text{ ft-lb/ft}^2$$

*Energy Flux (Table XI, Item 5)*

$$F'_{TE} = \frac{F_{TE}}{\left[ \frac{\gamma H^2}{8} \frac{L}{T} \right]} = 0.447$$

$$F_{TE} = 0.447(349166) = 156077 \text{ ft-lbs/(ft-sec)}$$

*Group Velocity (Table XI, Item 6)*

$$C_G' = \frac{C_G}{(L/T)} = 0.957$$

$$C_G = 0.957(43.21) = 41.36 \text{ ft/sec}$$

*Average Momentum (Table XI, Item 7)*

$$M' = \frac{M}{\left(\frac{\gamma H^2}{8} \frac{T}{L}\right)} = 0.505$$

$$M = 0.505(187) = 94.42 \text{ lb-sec/ft}^2$$

*Average Momentum Flux in Wave Direction (Table XI, Item 8)*

$$F'_{m_x} = \frac{F_{m_x}}{\left(\frac{\gamma H^2}{8}\right)} = 0.603$$

$$F_{m_x} = 0.603(8080) = 4872 \text{ lb/ft}$$

The average momentum flux has been recognized in recent years as an important dynamic quantity and is related to wave set-up within the surf zone and also is an important factor in the longshore transport of littoral material.

*Average Momentum Flux Transverse to Wave Direction (Table XI, Item 9)*

$$F'_{m_y} = \frac{F_{m_y}}{\left(\frac{\gamma H^2}{8}\right)} = 0.156$$

$$F_{m_y} = 0.156(8080) = 1260$$

From the momentum flux components presented it is possible to obtain any component of the radiation stress tensor.<sup>17</sup>

#### *Example 5 - Free Surface Breaking Parameters*

The free surface breaking parameters as defined by Equations (48) and (49) are based on two stability considerations. The kinematic free surface breaking parameter is

defined in terms of the speed of a water particle on the surface at the crest relative to the wave form speed. If this parameter should equal unity, then the wave is regarded as being unstable due to kinematic considerations. The dynamic free surface breaking parameter is defined as the ratio of the vertical acceleration of a water particle on the surface at the wave crest relative to the acceleration of gravity. The interpretation is that if this parameter should equal unity, then the pressure immediately under the crest would be zero and if the parameter should exceed unity, then according to the equations of motion, the pressure beneath the wave crest would be negative which is unrealistic and would indicate an unstable water surface.

It should be noted that the theory employed in the study is composed of a finite series of terms; in order to adequately define an instability formally, it may be necessary to extend the representation to include an infinite number of terms. The results presented here with regard to the free surface breaking parameters, should be interpreted accordingly. For the sample output (Case 4-D), it is seen (Table XI, Item 14) that the kinematic free surface breaking parameters for the linear and Stream function representations are 0.429 and 0.733, respectively. The corresponding values (Table XI, Item 15) for the dynamic free surface breaking parameter are 0.0409 and

0.286, respectively. The wave height associated with this case is approximately 0.78 of the depth and according to the McCowan criterion, the wave would be breaking.

*Example 6 - Combined Shoaling/Refraction*

The reader is reminded that the shoaling/refraction results were not tabulated, but are presented for various deep water directions in graphical form as Figures 25, 26, 27, 28 and 29 of this report.

*Example 6-a*

Consider a deep water wave propagating over bathymetry characterized by straight and parallel contours; the deep-water wave conditions considered are:

$$H_0 = 11.52 \text{ ft}$$

$$T = 15 \text{ sec}$$

$$\alpha_0 = 40^\circ$$

Suppose that we wish to find the wave height and direction in a water depth of 30 ft and also the wave height, water depth and wave direction at breaking. Figure 28 is applicable for a deep water wave direction of  $40^\circ$ . The deep water wave length  $L_0$  is calculated as

$$L_0 = \frac{g}{2\pi} T^2 = \frac{32.17}{6.2832} (15)^2 = 1152 \text{ ft}$$

therefore

$$\frac{H_0}{L_0} = 0.01$$

and for  $h = 30$  ft

$$\frac{h}{L_0} = \frac{30}{1152} = 0.0260$$

The line for  $H_0/L_0 = 0.01$  is simply followed to the left to the intersection with  $h/L_0 = 0.0260$ . At this intersection,

$$\frac{H}{L_0} = 0.0119$$

$$H = (0.0119)(1152) = 13.71 \text{ ft}$$

$$\alpha \approx 17^\circ$$

The second part of the example requires the breaking depth, height and angle. For this, the  $H_0/L_0 = 0.01$  curve intersects the breaking curve at

$$\frac{h_B}{L_0} = 0.0190$$

therefore

$$\frac{H_B}{L_0} = 0.0147$$

$$\alpha_B = 17^\circ$$

therefore

$$H_B = 0.0147(1152) = 16.9 \text{ ft}$$

$$h_B = 0.0190(1152) = 21.9 \text{ ft}$$

*Example 6-b*

Suppose that a wave is observed in intermediate depth water and it is desired to determine the height at any other depth such as deep water, breaking or any depth of interest. For this example, the values of  $H/L_0$  and  $h/L_0$  are calculated from the observed wave height and period and water depth. If the observed direction corresponds to one of the graphs available, then one proceeds as before in Example 6-a. If the observed point is not in accordance with any of the graphs available, then an interpolative procedure is required. As an example, consider the following observed wave characteristics

$$H = 20 \text{ ft}$$

$$h = 60 \text{ ft}$$

$$T = 12 \text{ sec}$$

$$\alpha = 11^\circ$$

and it is desired to calculate the wave height and direction in a water depth of 40 ft. From the observed information

$$L_0 = 737.3$$

$$H/L_0 = 0.0271$$

$$h/L_0 = 0.0814 \text{ (} h = 60 \text{ ft)}$$

$$h/L_0 = 0.0542 \text{ (} h = 40 \text{ ft)}$$

Examining the available figures, it is seen that the deep water wave direction is in the range  $10^\circ < \alpha_0 < 20^\circ$ .

As a close approximation, the problem is solved for  $\alpha_0 = 10^\circ$  and  $\alpha_0 = 20^\circ$  and the desired results obtained by interpolation. For  $\alpha_0 = 10^\circ$ , from Figure 26, a line passing through  $H/L_0 = 0.0271$ ,  $h/L_0 = 0.0814$  is sketched with the same approximate shape as those for  $H_0/L_0 = 0.02$  and  $0.04$  to determine  $H/L_0 = 0.033$  and  $\alpha = 6.2^\circ$  for  $h/L_0 = 0.0542$ . The corresponding values for  $\alpha_0 = 20^\circ$  are  $H/L_0 = 0.031$  and  $\alpha = 12^\circ$ . The procedure is shown graphically in Figure 39 for  $\alpha_0 = 10^\circ$ . Because for  $\alpha_0 = 10^\circ$  and  $20^\circ$ , the  $\alpha$  values corresponding to  $h/L_0 = 0.0814$  and  $H/L_0 = 0.0271$  are  $6.8$  and  $13^\circ$ , respectively and the desired  $\alpha$  for these conditions is  $11^\circ$ , the values of  $H/L_0$  and  $\alpha$  for  $h = 40$  ft may be determined by linear interpolation as

$$\frac{H}{L_0} = 0.033 + \frac{(.031 - .033)}{(13^\circ - 6.8^\circ)} (11^\circ - 6.8^\circ) = 0.032$$

or

$$H = (737.3)(0.032) = 23.6 \text{ ft}$$

and

$$\alpha = 6.2^\circ + \frac{(12^\circ - 6.2^\circ)}{(13^\circ - 6.8^\circ)} (11^\circ - 6.8^\circ) = 10.1^\circ$$

As a final remark in the discussion of the shoaling/refraction results, it should be noted that dissipative mechanisms such as percolation and bottom friction are not included in these results and in many cases these latter

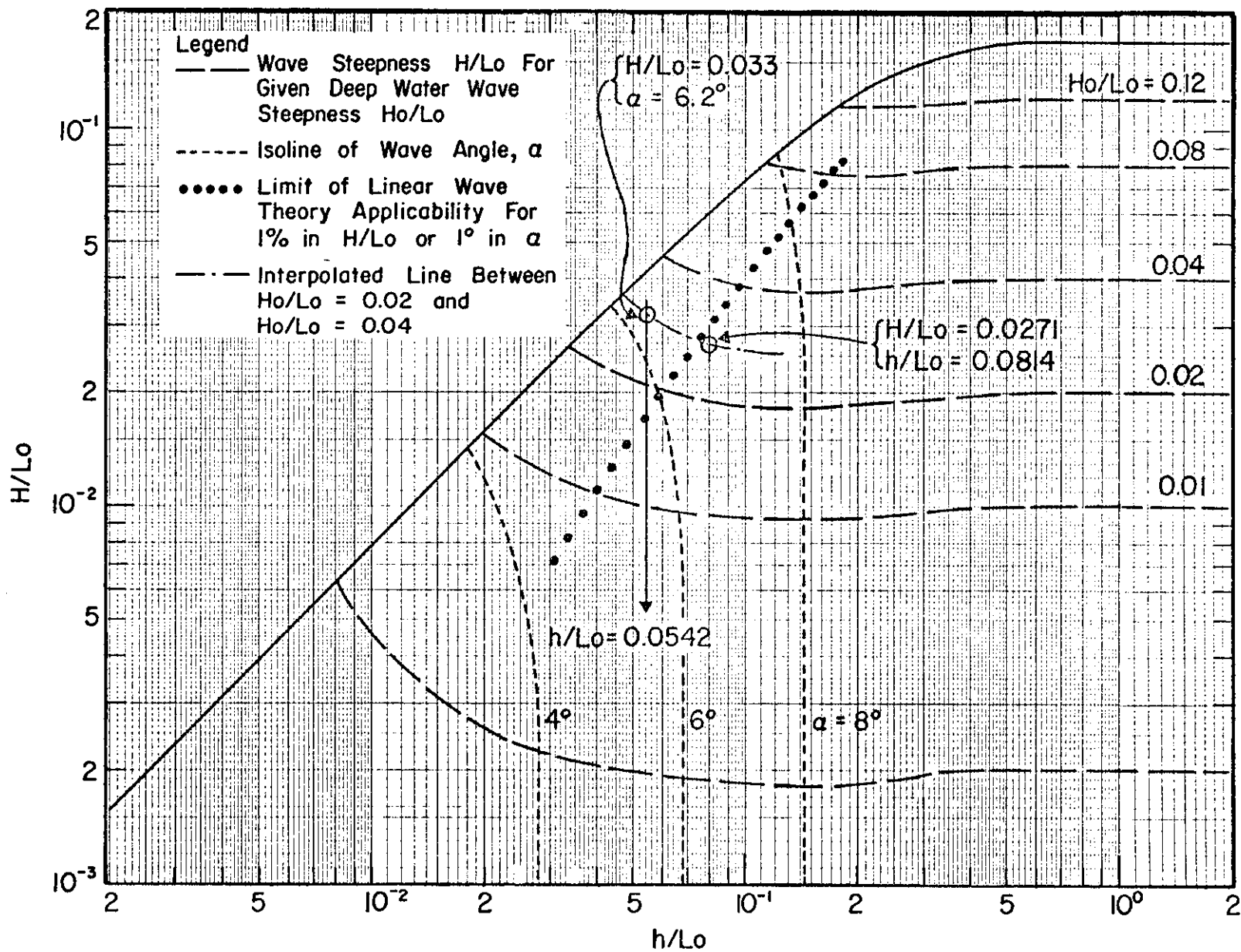


FIGURE 39 EXAMPLE 6-b, SHOALING/REFRACTION FOR  $\alpha_0 = 10^\circ$ .  
 INTERPOLATION FROM  $h/L_0 = 0.0814$  AND  $H/L_0 = 0.0271$  TO  
 $h/L_0 = 0.0542$

effects will be of greater significance than the nonlinear effects on the celerity and group velocity which represent the difference between the results presented here and the linear wave theory.

*Example 7 - Use of Tables for Nontabulated Wave Conditions*

Most of the previous examples have been presented for wave conditions which were available as one of the 40 tabulated cases, i.e., Case 4-D. It is anticipated that the tabulations will be used primarily for preliminary design and therefore that the 40 cases may provide adequate information for this purpose without interpolation. Final design of, for example, a platform supported by battered piling would probably be carried out by establishing a Stream function or other wave theory representation for the particular wave conditions selected for design.

On occasion, it may be desired to interpolate between the cases presented in the tables for wave conditions that are substantially different than one of the 40 cases. Several numerical and graphical interpolation methods were explored with a goal of obtaining a simple method which yielded reasonably accurate results. Because most wave variables of interest are nonlinear, numerical schemes which utilized linear interpolation proved to be inaccurate. The best procedure was found to be a rather simple graphical procedure which generally yields results within 5%.

### Method

The method utilizes the tabulated parameters of interest for the  $H/H_B$  values above and below the value of interest at the two lower and two higher  $h/L_0$  tabulated values; in all for each parameter desired, the interpolated value is based on values of that parameter for eight tabulated wave conditions. The method is outlined in the following paragraphs and illustrated by two examples.

Suppose that the wave height, period and water depth selected for design are  $H_D$ ,  $T_D$ , and  $h_D$ , respectively. The design wave steepness and relative depth are calculated as:

$$\begin{aligned} \text{Wave Steepness:} & \quad \frac{H_D}{L_{0D}} \\ \text{Relative Depth:} & \quad \frac{h_D}{L_{0D}} \end{aligned}$$

where

$$L_{0D} = \frac{g}{2\pi} T_D^2$$

The relative depth and wave steepness are plotted on Figure 40 to establish which wave cases should be used for design. For the example shown  $H/L_{0D} = 0.086$  and  $h/L_{0D} = 0.313$ . This point falls between  $H/H_B$  values denoted as "B" and "C" (i.e. 50% and 75% of breaking heights, respectively) and between tabulated  $h/L_0$  values denoted as Cases 7 and 8. The interpolation would therefore be based

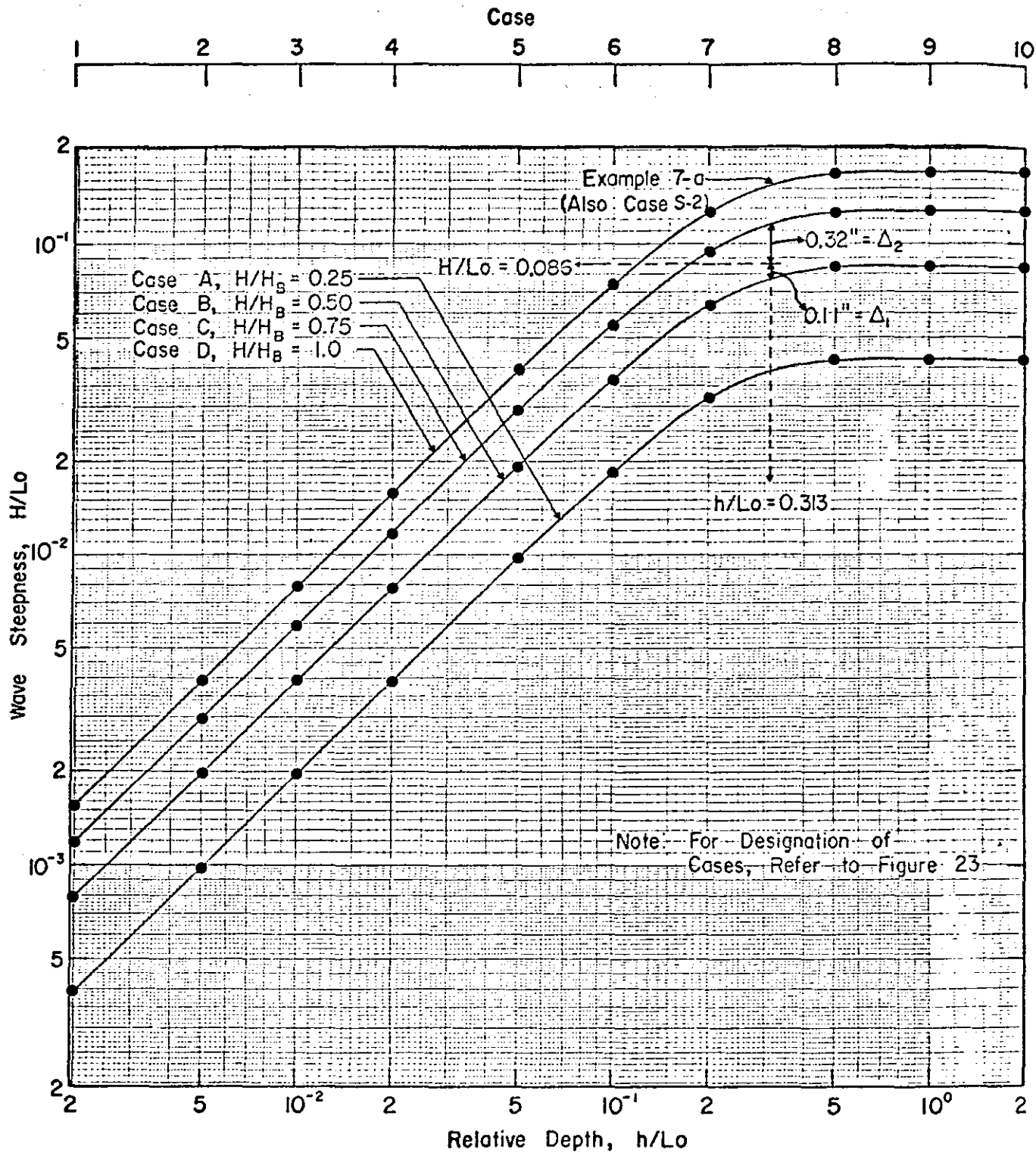


FIGURE 40 INTERPOLATION AID

on the tabulated parameter of interest for Cases 6-B, 6-C, 7-B, 7-C, 8-B, 8-C, 9-B and 9-C.

The interpolation proceeds as follows. An auxiliary plot is made of the variable of interest, e.g. the total dimensionless drag force at  $\theta = 0^\circ$  (denoted  $F'_D(0^\circ, \text{Surf.})$ ). This plot provides a continuous distribution of  $F'_D(0^\circ, \text{Surf.})$  versus  $h/L_0$  for relative breaking heights B and C. Interpolated  $F'_D$  values are then obtained from the auxiliary plot for the  $h/L_0$  design value (0.313). The interpolation for the design wave steepness requires measuring (Figure 40) the vertical linear distance from the B and C lines to the design  $h/L_0$  of interest; denote these values,  $\Delta_1$  and  $\Delta_2$ , respectively. Weighting factors,  $W$ , are then established as

$$W_L = \frac{\Delta_2}{\Delta_1 + \Delta_2} \quad (50)$$

$$W_U = \frac{\Delta_1}{\Delta_1 + \Delta_2}$$

The interpolated  $F'_D$  value is finally determined as

$$(F'_D)_D = W_L (F'_D)_L + W_U (F'_D)_U$$

where the subscripts, D, L and U outside the parentheses denote: "Design," "Lower" (Case B), and "Upper" (Case C), respectively.

*Example 7-a - Numerical Illustration of Interpolation Procedure*

Consider the following wave conditions selected for design

$$H_D = 44 \text{ ft}$$

$$T_D = 10 \text{ sec}$$

$$h_D = 160 \text{ ft}$$

which yield

$$L_{0D} = \frac{g}{2\pi} T^2 = 512 \text{ ft}$$

$$\frac{h_D}{L_{0D}} = 0.313$$

$$\frac{H_D}{L_{0D}} = 0.0859$$

and suppose that we require the maximum dimensionless drag force on a piling that extends from the bottom up above the crest level. This maximum value would occur at  $\theta = 0^\circ$  and is the value labeled "SURFACE" in the tabulations. Plotting of the wave steepness and relative depth on Figure 40 indicates that the design values are spanned by Cases 7-B, 7-C, 8-B and 8-C. In accordance with the preceding section the values of  $F'_D$  ( $0^\circ$ , Surf.) for Cases 6-B, 6-C, 7-B, 7-C, 8-B, 8-C, 9-B and 9-C are required for interpolation and are summarized in Table Q.

The values in Table Q are presented as an auxiliary plot in Figure 41. Interpolation at the design  $h/L_0$  of 0.313 yields the following values of  $F'_D$  for relative breaking of 50% and 75% respectively.

$$\text{Relative Breaking of 50\% (Line B): } (F'_D)_L = 4.90$$

$$\text{Relative Breaking of 75\% (Line C): } (F'_D)_U = 6.10$$

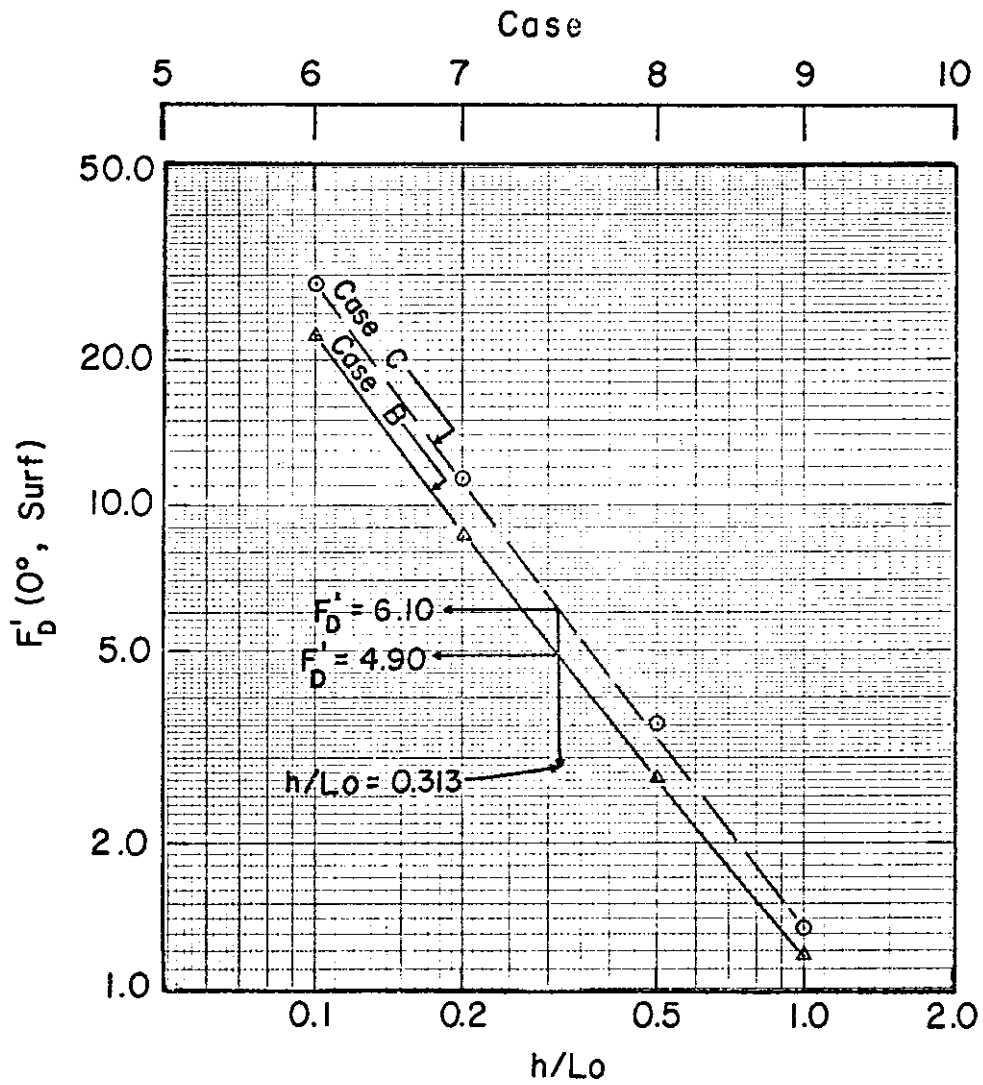


FIGURE 41 AUXILIARY PLOT OF  $F_D'$  FOR EXAMPLE 7-a

TABLE Q

Summary of  $F'_D(0^\circ, \text{Surf.})$  Required for Example 7-a

| Case | $F'_D(0^\circ, \text{Surf.})$ |
|------|-------------------------------|
| 6-B  | 22.37                         |
| 6-C  | 28.79                         |
| 7-B  | 8.60                          |
| 7-C  | 11.31                         |
| 8-B  | 2.71                          |
| 8-C  | 3.53                          |
| 9-B  | 1.33                          |
| 9-C  | - 1.72                        |

In order to interpolate to the design  $H/L_0$ , the distances  $\Delta_1$  and  $\Delta_2$  are measured from Figure 40. For this example, these are found to be

$$\Delta_1 = 0.11 \text{ in}$$

$$\Delta_2 = 0.32 \text{ in}$$

The weighting values are then (Eq. 50)

$$W_L = \frac{\Delta_2}{\Delta_1 + \Delta_2} = 0.744$$

$$W_U = \frac{\Delta_1}{\Delta_1 + \Delta_2} = 0.256$$

and the interpolated value of  $F'_D$  is

$$\begin{aligned}
(F'_D)_D &= W_L(F'_D)_L + W_U(F'_D)_U \\
&= (0.744)(4.90) + (0.256)(6.10) \\
&= 5.21
\end{aligned}$$

In order to evaluate this interpolated value, a Stream function solution was developed for the conditions of interest and  $F'_D$  from the actual solution was found to be 5.04 or a difference of about 3.4%.

More comprehensive evaluations of the accuracy of the interpolation method are presented in the next example.

*Example 7-b - Assessment of the Interpolation Method*

In order to present a more extensive evaluation of the accuracy of the interpolation method, two special cases (one shallow water and one deep water) were selected for evaluation. The wave characteristics for these two cases are presented in Table R.

TABLE R  
Wave Characteristics Selected for Accuracy  
Evaluation of Interpolation Method

| Case                   | Wave Height,<br>H(ft) | Wave Period,<br>T(sec) | Water Depth,<br>h(ft) |
|------------------------|-----------------------|------------------------|-----------------------|
| S-1<br>(Shallow Water) | 19                    | 20                     | 30                    |
| S-2<br>(Deep Water)    | 44                    | 10                     | 160                   |

Using the procedure described, interpolated values of a number of quantities of interest were developed and compared with values obtained by Stream function solutions at the wave conditions of interest. Table S presents a summary of the percentage differences between the solution and interpolated values.

As an overall statement regarding the interpolation, it is noted that Table S indicates that the procedure presented generally provides results which are within 5%, however, differences up to 10% could occur. One final comment concerning the consistency of the tabulated values is in order. In preparing the auxiliary plots, it was usually found that a line could be drawn through the four points within 2 to 3%, except for the breaking wave height,  $H/H_B = 1.0$  in which case the maximum deviations could amount to  $\pm 5\%$ . The probable explanation for this deviation is that: (1) the calculated wave heights for the tabulated cases were allowed to deviate from the desired values by 1%, and (2) the different orders to represent different cases could cause a difference in kinematics of 1 to 2%. The effects noted above could conceivably amount to deviations of  $\pm 5\%$  for those variables which are inherently nonlinear, e.g. drag forces or wave breaking parameters.

This completes the section illustrating the use of the wave tables. It should be recognized, however, that only the more simple examples have been presented and that

TABLE S

Summary of Percentage Differences Between Values  
Determined by Stream Function Solutions  
and by Interpolation

| Dimensionless Variable <sup>a</sup>   | Percentage Difference <sup>b</sup> |               |
|---|------------------------------------|---------------|
|   | Case S-1                           | Case S-2      |
| $u'(0^\circ, 0.5)$ ; Horiz. Vel. Comp., Zero Phase Angle, Mid-Depth                   | +3.9%                              | <1%           |
| $F'_D(0^\circ, \text{Surf})$ , Max. Drag Force Component, Acting Over Entire Depth    | +6.7%                              | +3.4%         |
| $F'_I(10^\circ, \text{Surf})$ , Inertia Force Component                               | +1.3%                              | Not Evaluated |
| $F'_I(75^\circ, \text{Surf})$ , Inertia Force Component                               | Not Evaluated                      | -3.9%         |
| $M'_D(0^\circ, \text{Surf})$ , Max. Drag Moment Component About Mudline               | +4.5%                              | +3.6%         |
| $M'_I(10^\circ, \text{Surf})$ , Inertia Moment Component                              | +2.2%                              | Not Evaluated |
| $M'_I(75^\circ, \text{Surf})$ , Inertia Moment Component                              | Not Evaluated                      | -3.7%         |
| $p'_D(0^\circ, 0.5)$ , Dynamic Pressure Component, Zero Phase Angle, Mid-Depth        | <1%                                | -2.4%         |
| $p'_D(180^\circ, 0.5)$ , Dynamic Pressure Component, Trough Phase Position, Mid-Depth | <1%                                | -2.8%         |
| $L'$ , Wave Length  | 1.1%                               | <1%           |
| $TE'$ , Total Energy  | -4.6%                              | -3.7%         |

TABLE S—Continued

| Dimensionless Variable <sup>a</sup>                     | Percentage Difference <sup>b</sup> |          |
|---|------------------------------------|----------|
|   | Case S-1                           | Case S-2 |
| $F'_{TE}$ , Total Energy Flux                           | -4.2%                              | +3.5%    |
| $M'$ , Momentum   | -4.1%                              | -2.2%    |
| $F'_{m_x}$ , Momentum Flux in Wave Direction            | -3.7%                              | -2.6%    |
| $F'_{m_y}$ , Momentum Flux Transverse to Wave Direction | -1.7%                              | <1%      |
| KFSBP, Kinematic Free Surface Breaking Parameter        | 8.4%                               | +4.4%    |
| DFSBP, Dynamic Free Surface Breaking Parameter          | 1.4%                               | <1%      |

<sup>a</sup>Refer to Tables D, E, and F for a more complete description of the dimensionless variables.

$$b\% \text{ Diff.} \equiv \frac{\text{Interp. Value} - \text{Stream Fn. Soln.}}{\text{Stream Fn. Soln.}} \times 100\%$$

the tables can be effectively applied to the solution of situations which are considerably broader and more complex than those examined in this section.

## VI. SUMMARY

This report presents the results of an investigation which has demonstrated that the Stream function wave theory provides a generally better representation of periodic wave phenomena than other wave theories examined. As a result of this indication, tables have been prepared, based on the Stream function wave theory and including parameters which should be an aid in preliminary offshore design. The tables also include parameters which are presently of greatest interest to researchers.

Because of its simplicity, the linear wave theory is widely used for many calculations over all ranges of relative depth. This study has identified that, for a number of variables, there are substantial differences between the linear and Stream function wave theories. Although this point has not been amplified in this report, inspection of the tables will substantiate this conclusion. The identification of these differences should be of assistance in planning experimental programs to provide definitive research results.

If the set of tables is extensively applied, as is hoped, undoubtedly the users will note shortcomings, omissions or develop recommendations directed toward the improved usefulness, applicability or efficiency of the tables. The

author would welcome information of this type in order that future work may benefit by as wide a range of user's needs as possible.

## VII. REFERENCES

1. Dean, R. G., "Relative Validity of Water Wave Theories," *Proceedings, ASCE Specialty Conference on Civil Engineering in The Oceans*, San Francisco, pp. 1-30, 1968. (Also published in *Waterways and Harbors Journal*, American Society of Civil Engineers, p. 105-119, February, 1970).
2. Dean, R. G., "Breaking Wave Criteria: A Study Employing a Numerical Wave Theory," *Proceedings Eleventh International Conference on Coastal Engineering*, London, Chap. 8, p. 108-123, 1968.
3. Dean, R. G., and B. Le Méhauté, "Experimental Validity of Water Wave Theories," Paper presented at the 1970 ASCE Structural Engineering Conference, Portland, Oregon, April 8, 1970.
4. Le Méhauté, B., D. Divoky and A. Lin, "Shallow Water Waves: A Comparison of Theory and Experiment," *Proceedings Eleventh International Conference on Coastal Engineering*, Chap. 7, pp. 86-107, 1968.
5. Von Schwind, J.J. and R. O. Reid, "Characteristics of Gravity Waves of Permanent Form," *Journal of Geophysical Research*, Vol. 77, No. 3, pp. 420-433, January, 1972.
6. Ippen, A. T. (Editor), *Estuary and Coastline Hydrodynamics*, McGraw-Hill, Inc., Chaps. 1 and 2, pp. 1-132, 1966.
7. Le Méhauté, B. and L. M. Webb, "Periodic Gravity Waves Over a Gentle Slope at a Third Order of Approximation," *Proceedings Ninth Conference on Coastal Engineering*, Chap. 2, pp. 23-40, 1964.
8. Skjelbreia, L. and J. A. Hendrickson, "Fifth Order Gravity Wave Theory," *Proceedings Seventh Conference on Coastal Engineering*, Chap. 10, pp. 184-196, 1961.
9. Laitone, E. V., "The Second Approximation to Cnoidal and Solitary Waves," *Journal of Fluid Mechanics*, V. 9, Part 3, pp. 430-444, November, 1960.

10. Munk, W. H., "The Solitary Wave and Its Application to Surf Problems," *Annals New York Academy of Science*, v. 51, pp. 376-424, 1949.
11. Dean, R. G., "Stream Function Representation of Nonlinear Ocean Waves," *Journal of Geophysical Research*, Vol. 70, No. 18, pp. 4561-4572, September, 1965.
12. Chappellear, J. E., "Direct Numerical Calculation of Wave Properties," *Journal of Geophysical Research*, Vol. 66, No. 2, pp. 501-508, February, 1961.
13. Michell, J. H., "On the Highest Waves in Water," *Philosophical Magazine*, Vol. 36, No. 5, pp. 430-435, 1893.
14. Reid, R. O. and C. L. Bretschneider, "Surface Waves and Offshore Structures," *Texas A and M Research Foundation*, Technical Report, October, 1953.
15. Bretschneider, C. L., "Selection of Design Waves for Offshore Structures," *Transactions, American Society of Civil Engineers*, Paper No. 3026, 1960.
16. Divoky, D., B. Le Méhauté and A. Lin, "Breaking Waves on Gentle Slopes," *Journal of Geophysical Research*, Vol. 75, No. 9, pp. 1681-1692, March, 1970
17. Bowen, A. J., "The Generation of Longshore Currents on a Plane Beach," *Journal of Marine Research*, Vol. 27, No. 2, p. 209, May, 1969.

**APPENDIXES**

APPENDIX I

NUMERICAL SOLUTION OF STREAM FUNCTION PARAMETERS

## *Introduction*

This appendix outlines the method of determining numerical values for the parameters in the general form of the Stream function solution. The numerical solution requires the use of a reasonably high speed, large memory computer.

### *Review of Problem Formulation*

The problem of a two-dimensional, periodic wave propagating in water of uniform depth has been discussed in Section II of the main body of this report. If the water is incompressible and the motion irrotational, then the following boundary value problem can be established for an "arrested" wave system.

Differential Equation (DE):

$$\nabla^2 \psi = 0 \quad (\text{I-1})$$

Boundary Conditions { Bottom Boundary Condition (BBC):

$$w = 0, \quad z = -h \quad (\text{I-2})$$

Kinematic Free Surface Boundary Condition (KFSBC):

$$\frac{\partial \eta}{\partial x} = \frac{w}{u - C}, \quad z = \eta(x) \quad (\text{I-3})$$

Boundary  
Conditions

Dynamic Free Surface Boundary Condition (DFSBC):

$$\eta + \frac{1}{2g} \left[ (u - C)^2 + w^2 \right] - \frac{C^2}{2g} = Q, \quad z = \eta(x) \quad (\text{I-4})$$

Motion is periodic in x with spatial periodicity of the wave length, L. (I-5)

Equations (I-1) - (I-5) represent the common formulation for all of the classical nonlinear water wave problems in which it is assumed that the wave propagates without change of form and a reference coordinate system has been chosen which travels with the wave form. For a specified wave height, water depth and wave period, the goal then is to determine as exact as possible a solution to the formulation.

### *Stream Function Solution*

The general form of the Stream function solution is

$$\psi(x, z) = \frac{L}{T} z + \sum_{n=1}^{NN} X(n) \sinh \left[ \frac{2\pi n}{L} (h + z) \right] \cos \left[ \frac{2\pi n}{L} x \right] \quad (I-6)$$

The water displacement,  $\eta$ , is determined by setting  $z = \eta$  in Equation (I-6).

$$\eta = \frac{T}{L} \psi_{\eta} - \frac{T}{L} \sum_{n=1}^{NN} X(n) \sinh \left[ \frac{2\pi n}{L} (h + \eta) \right] \cos \left[ \frac{2\pi n}{L} x \right] \quad (I-7)$$

where  $\psi_{\eta}$  is the (constant) value of the Stream function on the free surface. The velocity components are defined by:

$$u - C = - \frac{\partial \psi}{\partial z} \quad (\text{I-8})$$

$$w = + \frac{\partial \psi}{\partial x} \quad (\text{I-9})$$

In continuing the quest to determine a solution which satisfies Equations (I-1) to (I-5) as faithfully as possible, it is noted that for arbitrary values of:  $\psi_\eta$ ,  $L$ , and the  $X(n)$ 's, the Stream function solution *exactly* satisfies all of the requirements of the formulation except the DFSBC, Equation (I-4). All of the effort can therefore be directed to determining these "free" variables such that they represent the specified wave height and also "best" satisfy Equation (I-4). The approach that is employed is numerical iteration, in which a trial solution is regarded as available and at each step of the iteration, the "free" variables are modified to improve the solution.

As a preliminary step, an error is defined in the one-remaining unsatisfied boundary condition

$$E = \frac{1}{J} \sum_{j=1}^J (Q_j - \bar{Q})^2 \quad (\text{I-10})$$

where the  $Q_j$ 's represent equally spaced (in  $\theta$ ) values of the quantity in Equation (I-4), and  $\bar{Q}$  represents the average of the  $Q_j$ 's. If, for example,  $J = 41$ , and the free variables could be adjusted so that  $E$  was very small,

then the associated solution would provide a good fit to the complete formulation at these 41 points, and computations have shown that the fit at other phase angles would be comparably good. The problem therefore has evolved into one of minimizing the total error  $E$ . The procedure used is a least squares procedure, which requires formally that

$$\frac{\partial E}{\partial L} = 0 \quad (I-11)$$

$$\frac{\partial E}{\partial X(n)} = 0 \quad (I-12)$$

(the parameter  $\psi_n$  is not determined by the least squares procedure, but is selected such that the mean water level is not changed by the other variables selected; this will be discussed later.) Examination of Equations (I-11) and (I-12) further will indicate that the usual least squares procedure is not applicable, because the error is not defined as a quadratic function of the unknowns; this problem then falls in the category of a nonlinear least squares problem.

The problem was linearized as follows. Suppose that at the  $k$ th iteration, a trial solution is available. The objective is to select changes in the unknowns such

that the errors will be reduced. If this were a linear least squares problem, only one iteration would be required. Expressing the quantity  $Q$  in terms of small changes in the unknowns (to be determined at the  $k$ th iteration).

$$Q_j^{k+1} = Q_j^k + \sum_{n=1}^{NN} \frac{\partial Q_j^k}{\partial X(n)} \Delta X(n) + \frac{\partial Q_j^k}{\partial L} \Delta L \quad (\text{I-13})$$

where

$$\frac{\partial Q}{\partial X(n)} = \frac{\partial Q}{\partial \eta} \frac{\partial \eta}{\partial X(n)} + \frac{\partial Q}{\partial u} \frac{\partial u}{\partial X(n)} + \frac{\partial Q}{\partial w} \frac{\partial w}{\partial X(n)} \quad (\text{I-14})$$

$$\frac{\partial Q}{\partial L} = \frac{\partial Q}{\partial \eta} \frac{\partial \eta}{\partial L} + \frac{\partial Q}{\partial u} \frac{\partial u}{\partial L} + \frac{\partial Q}{\partial w} \frac{\partial w}{\partial L} + \frac{\partial Q}{\partial C} \frac{\partial C}{\partial L} \quad (\text{I-15})$$

where the  $\frac{\partial Q}{\partial \eta}$ ,  $\frac{\partial Q}{\partial u}$  are obtained from Equation (I-4) and the  $\frac{\partial \eta}{\partial X(n)}$ ,  $\frac{\partial u}{\partial X(n)}$ , etc. are obtained from Equations (I-7), (I-8), etc.

Rewriting the least squares procedure in terms of the unknowns:  $\Delta L$  and  $\Delta X(n)$

$$\frac{\partial E}{\partial \Delta L} = 0 \quad (\text{I-16})$$

$$\frac{\partial E}{\partial \Delta X(n)} = 0, \quad n = 1 \dots NN \quad (\text{I-17})$$

Equations (I-16) and (I-17) represent a set of  $NN + 1$  linear simultaneous equations in terms of the  $NN + 1$  unknowns. After each iteration, the water surface is recalculated, by iteration, from Equation (I-7) and  $\psi_\eta$  is redetermined such that

$$\int_0^L \eta \, dx = 0 \quad (I-18)$$

which can be expressed in integral form as

$$\psi_\eta = \frac{2}{L} \int_0^{L/2} X(n) \sinh \left[ \frac{2\pi n}{L} (h + \eta) \right] \cos \left[ \frac{2\pi n}{L} x \right] dx \quad (I-19)$$

where, in the computations, a Simpson's rule approximation to Equation (I-19) is used.

One complete iteration comprises a simultaneous solution for  $\Delta L$  and the  $\Delta X(n)$ 's and a redetermination of  $\psi_\eta$ . Successive iterations involve exactly the same procedure, and the iterations can be terminated when successive reductions in the error  $E$  are small. Numerical instabilities can occur, especially near breaking wave conditions and, one effective procedure in these cases, is to apply only a fraction of the  $\Delta L$  and  $\Delta X(n)$ 's specified by the least squares solution.

One final comment should be directed toward the problem of establishing the desired wave height. Although it is possible to develop more sophisticated procedures which converge on the wave height, the procedure followed here was simply to conduct successive runs until the wave height was within an acceptable limit (1%) of the desired height.

APPENDIX II

DEVELOPMENT OF COMBINED SHOALING/REFRACTION COEFFICIENTS

### *Introduction*

This appendix describes briefly the method employed to calculate the combined shoaling/refraction coefficients.

### *Background*

The shoaling/refraction coefficients developed are valid for a bathymetry characterized by straight and parallel bottom contours and for a wave system which suffers no energy losses. The two principles employed are Snell's Law and the concept that there is no energy flux across a wave ray, see Fig. II-1.

Snell's Law governs refraction and relates the wave propagation speed,  $C$ , to the wave direction,  $\alpha$ ,

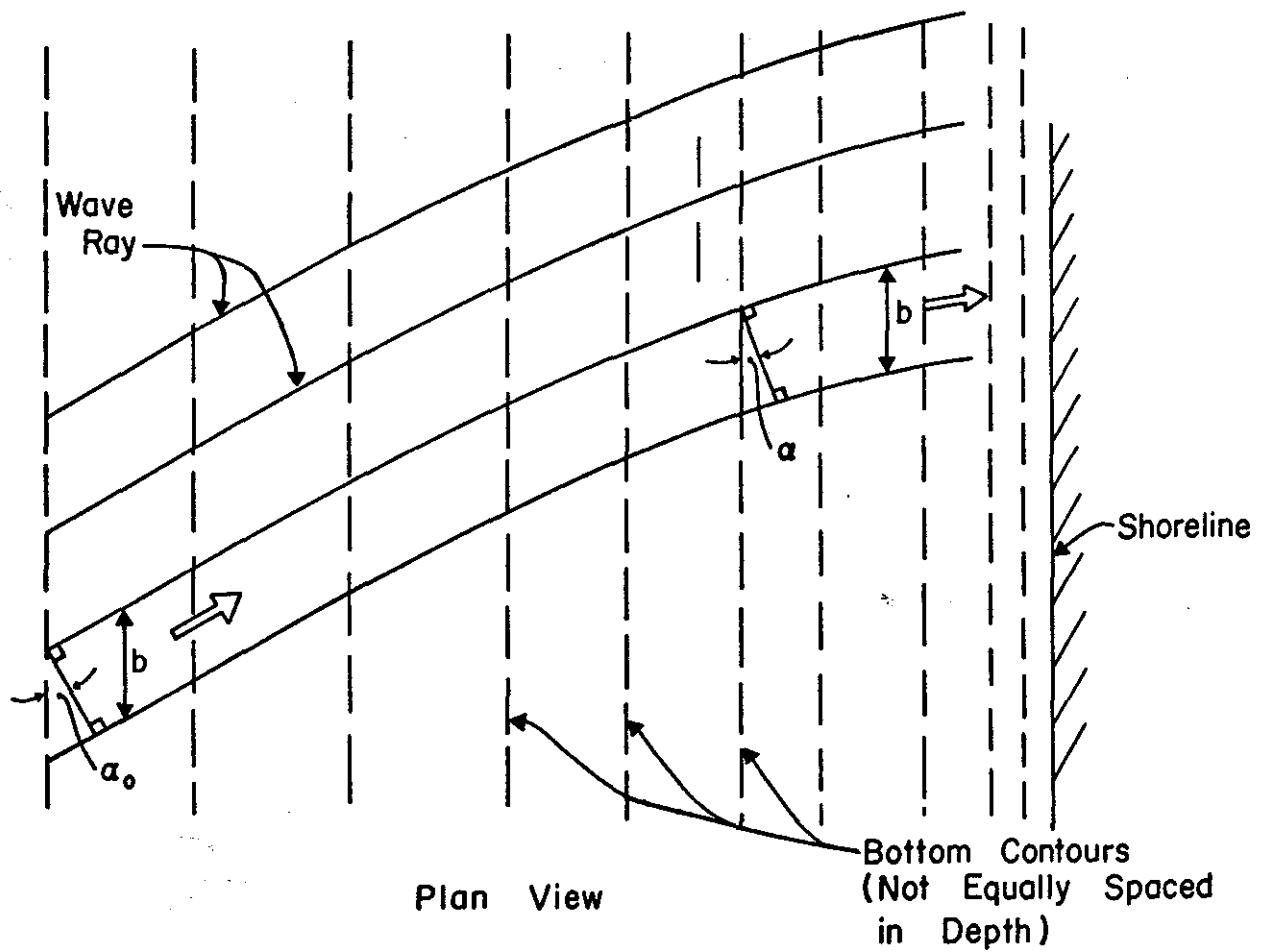
$$\frac{\sin \alpha_1}{C_1} = \text{Const}_1 = \frac{\sin \alpha_2}{C_2} \quad (\text{II-1})$$

in which the subscripts pertain to any arbitrary depths.

The requirement that no energy is propagated across wave rays may be written as

$$\left( F_{\text{TE}} \cos \alpha \right)_1 = \left( F_{\text{TE}} \cos \alpha \right)_2 = \text{Const}_2 \quad (\text{II-2})$$

in which  $F_{\text{TE}}$  represents the energy flux per unit width in the direction of wave propagation and the  $\cos \alpha$  term



Refraction Over Bathymetry Characterized By  
Straight and Parallel Contours

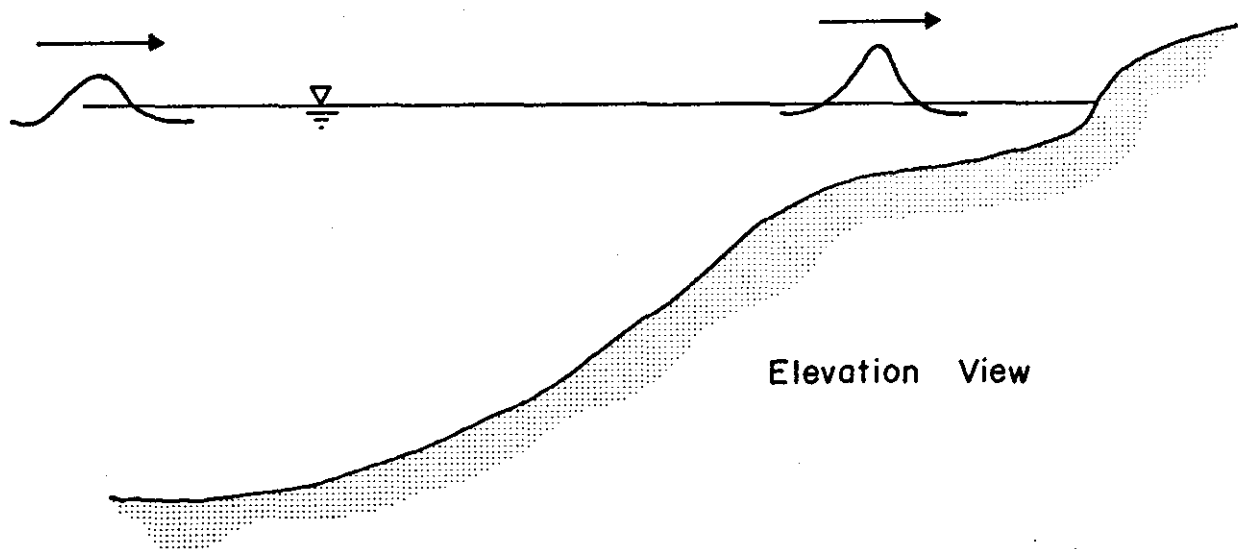


FIGURE II-1 DEFINITION SKETCH FOR SHOALING/  
REFRACTION CONSIDERATIONS

represents the width between adjacent wave rays. The  $F_{TE}$  term could be expressed as the product of the wave energy density,  $E_{TE}$ , and the group velocity,  $C_G$ , although this will not be helpful in the effort here. In the case of linear wave theory, it is possible to separate the refraction and shoaling effects because neither the celerity,  $C$ , (governing refraction) nor the group velocity,  $C_G$  (governing shoaling) depend on wave height. For our case, inspection of Equations (II-1) and (II-2) will show that the two phenomena are coupled through the dependency of  $C$  and  $C_G$  on the wave height.

#### *Method*

The method employed here utilizes the dimensionless energy flux,  $F'_{TE}$  (Table XI, Item 5) and the dimensionless wave length,  $L'$  (Table XI, Item 1),

where

$$F'_{TE} = \frac{F_{TE}}{\gamma \frac{H^2}{8} \frac{L}{T}}$$

$$L' = \frac{L}{(gT^2/2\pi)}$$

Equation (II-1) can be rewritten in terms of the dimensionless quantities as

$$\frac{2\pi}{gT_1} \frac{\sin \alpha_1}{L'_1} = \frac{2\pi}{gT_2} \frac{\sin \alpha_2}{L'_2} = \text{Const}_1 \quad (\text{II-3})$$

However since the period is conserved, i.e.,  $T_1 = T_2$

$$\frac{\sin \alpha_1}{L'_1} = \frac{\sin \alpha_2}{L'_2} = \text{Const}_3 \quad (\text{II-4})$$

The energy flux relationship, Equation (II-2) can be expressed as

$$\frac{\gamma}{8T} \left( \frac{gT^2}{2\pi} \right)^3 \left( \frac{H}{L_0} \right)^2 F'_{TE} L' \cos \alpha = \text{Const}_2$$

or recognizing that the period is conserved

$$\left( \frac{H}{L_0} \right)^2 F'_{TE} L' \cos \alpha = \text{Const}_4 \quad (\text{II-5})$$

Equations (II-4) and (II-5) describe the shoaling/refraction process in terms of available dimensionless parameters and were solved as described in the following paragraphs.

#### *Solution*

It was found convenient to characterize a particular incoming deep water wave by the direction,  $\alpha_0$ , and deep water steepness,  $H_0/L_0$ . The problem is to

determine wave steepnesses at other relative depths  $h/L_0$  such that Equations (II-4) and (II-5) are satisfied recalling that  $L'$  and  $F'_{TE}$  both depend on  $h/L_0$  and  $H/L_0$ . For each relative depth,  $h/L_0$ , four values of  $L'$  and  $F'_{TE}$  are available (for  $H/H_B = 0.25, 0.5, 0.75$  and  $1.0$ , c.f. Figure 23) whereas a continuous distribution is required for the purpose here. For each relative depth,  $h/L_0$ , continuous distributions were obtained by fitting straight lines between the four available points; for  $H/H_B = 0$ , it was assumed that the simple linear wave theory applied, see Figure II-2 for an example for  $h/L_0 = 0.02$ .

For given  $H_0/L_0$  and  $\alpha_0$ , the constants in Equations (II-4) and (II-5) are defined. The wave steepness  $H/L_0$  and direction  $\alpha$  at any relative depth are determined by iteration of the two following equations.

$$\alpha^{k+1} = \sin^{-1} \left[ (L')^k \frac{\sin \alpha_0}{L'_0} \right] \quad (\text{II-6})$$

$$\frac{H}{L_0}^{k+1} = \left[ \frac{(H_0/L_0)^2 (F'_{TE})_0 L'_0 \cos \alpha_0}{(F'_{TE})^k (L')^k \cos \alpha^k} \right]^{1/2} \quad (\text{II-7})$$

in which the superscript  $k+1$  denotes the  $(k+1)$  *th* iteration and applies to the improved estimates of  $\alpha$  and  $H/L_0$ . Once these estimates are known, the parameters with the  $k$

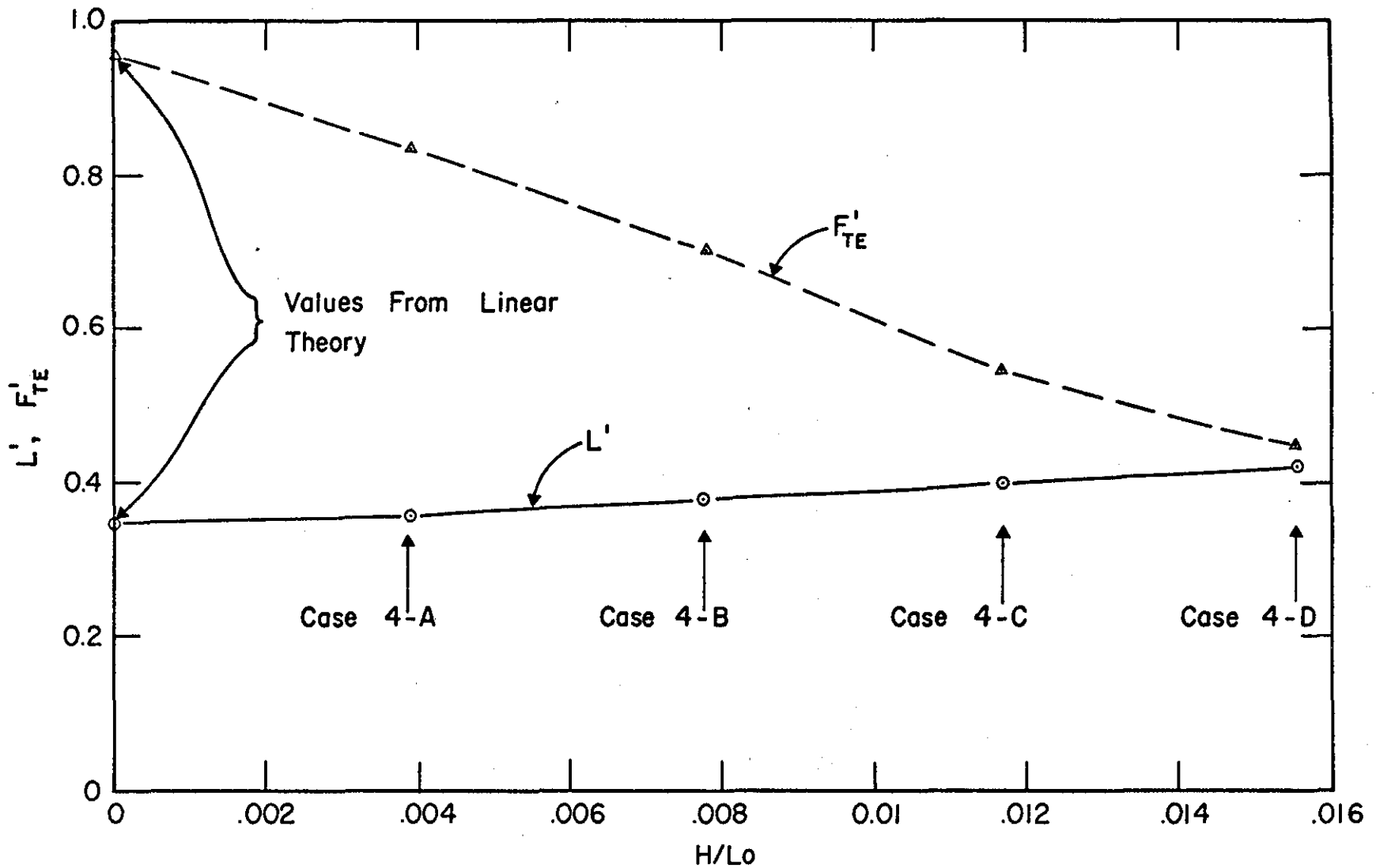


FIGURE II-2 VARIATION OF  $F'_{TE}$  AND  $L'$  AS EMPLOYED IN SHOALING/ REFRACTION DEVELOPMENT FOR  $h/L_0 = 0.02$

subscripts on the right hand sides of Equations (II-8) and (II-9) are calculated and improved estimates of  $\alpha$  and  $H/L_0$  are determined, etc. The procedure was initiated in deep water and the wave steepness and direction calculated at the remaining nine values of relative depth advancing shoreward or until breaking was indicated. At each relative depth, the iteration converged very rapidly with three or four iterations usually sufficient. For the first iteration at a relative depth, the initial value for wave steepness was taken as the final value for the preceding (greater) relative depth.

The shoaling/refraction results are presented in graphical form, for  $\alpha_0 = 0^\circ, 10^\circ, 20^\circ, 40^\circ$  and  $60^\circ$  in Figs. 25, 26, 27, 28 and 29, respectively. A description of these tables is presented in Section IV and two examples illustrating their application are given in Section V.

APPENDIX III

SAMPLE SET OF WAVE TABLES FOR CASE 4-D

CASE 4-D

11TH ORDER STREAM FUNCTION WAVE THEORY

DEFINITIONS

H = WAVE HEIGHT  
T = WAVE PERIOD  
DPT = WATER DEPTH  
LO = DEEP WATER WAVE LENGTH. CALCULATED FROM LINEAR WAVE THEORY,  $LO=(G/6.28318)*T**2$   
L = WAVE LENGTH  
PSI = VALUE OF STREAM FUNCTION ON THE FREE SURFACE  
G = GRAVITATIONAL CONSTANT  
X(N) = NTH STREAM FUNCTION COEFFICIENT

WAVE CHARACTERISTICS

H/LO = 0.015553      DPT/LO = 0.020000  
H/DPT = 0.777652  
L/LO = 0.422461      PSI/(G\*H\*T) = -0.002296

LISTING OF DIMENSIONLESS STREAM FUNCTION COEFFICIENTS

X( 1)/(H\*T\*G) = -0.342656E-01  
X( 2)/(H\*T\*G) = -0.123281E-01  
X( 3)/(H\*T\*G) = -0.499486E-02  
X( 4)/(H\*T\*G) = -0.201883E-02  
X( 5)/(H\*T\*G) = -0.788826E-03  
X( 6)/(H\*T\*G) = -0.298070E-03  
X( 7)/(H\*T\*G) = -0.998972E-04  
X( 8)/(H\*T\*G) = -0.343591E-04  
X( 9)/(H\*T\*G) = -0.105353E-04  
X(10)/(H\*T\*G) = -0.304493E-05  
X(11)/(H\*T\*G) = -0.465501E-06



CASE 4-D

TABLE II-DIMENSIONLESS VERTICAL VELOCITY COMPONENT FIELD...DEFINED IN EQUATION (22)

| THETA=      | 0.0            | 10.0           | 20.0            | 30.0             | 50.0             | 75.0             | 100.0           | 130.0             | 180.0             |
|-------------|----------------|----------------|-----------------|------------------|------------------|------------------|-----------------|-------------------|-------------------|
| ETA/HEIGHT= | 0.889<br>43.7% | 0.593<br>15.5% | 0.284<br>-65.4% | 0.101<br>-326.7% | -0.055<br>681.4% | -0.101<br>227.7% | -0.110<br>21.4% | -0.112<br>-242.4% | -0.111<br>-348.7% |
| SURFACE     | 0.0<br>*****   | 7.078<br>89.1% | 6.715<br>77.8%  | 4.576<br>53.4%   | 1.430<br>-112.8% | 0.273<br>*****   | 0.046<br>*****  | 0.012<br>*****    | -0.000<br>*****   |
| S/DEPTH=1.6 | 0.0<br>*****   | 6.539<br>88.2% | 6.534<br>80.1%  | 5.719<br>74.3%   | 4.186<br>62.5%   | 3.706<br>62.0%   | 3.244<br>61.8%  | 2.799<br>61.8%    | 2.370<br>60.8%    |
| S/DEPTH=1.5 | 0.0<br>*****   | 5.635<br>87.2% | 4.855<br>66.4%  | 4.178<br>65.6%   | 3.586<br>84.1%   | 3.065<br>84.1%   | 2.601<br>83.4%  | 2.189<br>82.7%    | 1.809<br>82.2%    |
| S/DEPTH=1.4 | 0.0<br>*****   | 4.855<br>86.4% | 4.178<br>65.6%  | 3.586<br>84.1%   | 3.065<br>84.1%   | 2.601<br>83.4%   | 2.189<br>82.7%  | 1.809<br>82.2%    | 1.463<br>81.7%    |
| S/DEPTH=1.3 | 0.0<br>*****   | 4.178<br>65.6% | 3.586<br>84.1%  | 3.065<br>84.1%   | 2.601<br>83.4%   | 2.189<br>82.7%   | 1.809<br>82.2%  | 1.463<br>81.7%    | 1.142<br>81.3%    |
| S/DEPTH=1.2 | 0.0<br>*****   | 3.586<br>84.1% | 3.065<br>84.1%  | 2.601<br>83.4%   | 2.189<br>82.7%   | 1.809<br>82.2%   | 1.463<br>81.7%  | 1.142<br>81.3%    | 0.841<br>80.9%    |
| S/DEPTH=1.1 | 0.0<br>*****   | 3.065<br>84.1% | 2.601<br>83.4%  | 2.189<br>82.7%   | 1.809<br>82.2%   | 1.463<br>81.7%   | 1.142<br>81.3%  | 0.841<br>80.9%    | 0.553<br>80.7%    |
| S/DEPTH=1.0 | 0.0<br>*****   | 2.601<br>83.4% | 2.189<br>82.7%  | 1.809<br>82.2%   | 1.463<br>81.7%   | 1.142<br>81.3%   | 0.841<br>80.9%  | 0.553<br>80.7%    | 0.274<br>80.4%    |
| S/DEPTH=0.9 | 0.0<br>*****   | 2.189<br>82.7% | 1.809<br>82.2%  | 1.463<br>81.7%   | 1.142<br>81.3%   | 0.841<br>80.9%   | 0.553<br>80.7%  | 0.274<br>80.4%    | 0.0<br>*****      |
| S/DEPTH=0.8 | 0.0<br>*****   | 1.809<br>82.2% | 1.463<br>81.7%  | 1.142<br>81.3%   | 0.841<br>80.9%   | 0.553<br>80.7%   | 0.274<br>80.4%  | 0.0<br>*****      | 0.0<br>*****      |
| S/DEPTH=0.7 | 0.0<br>*****   | 1.463<br>81.7% | 1.142<br>81.3%  | 0.841<br>80.9%   | 0.553<br>80.7%   | 0.274<br>80.4%   | 0.0<br>*****    | 0.0<br>*****      | 0.0<br>*****      |
| S/DEPTH=0.6 | 0.0<br>*****   | 1.142<br>81.3% | 0.841<br>80.9%  | 0.553<br>80.7%   | 0.274<br>80.4%   | 0.0<br>*****     | 0.0<br>*****    | 0.0<br>*****      | 0.0<br>*****      |
| S/DEPTH=0.5 | 0.0<br>*****   | 0.841<br>80.9% | 0.553<br>80.7%  | 0.274<br>80.4%   | 0.0<br>*****     | 0.0<br>*****     | 0.0<br>*****    | 0.0<br>*****      | 0.0<br>*****      |
| S/DEPTH=0.4 | 0.0<br>*****   | 0.553<br>80.7% | 0.274<br>80.4%  | 0.0<br>*****     | 0.0<br>*****     | 0.0<br>*****     | 0.0<br>*****    | 0.0<br>*****      | 0.0<br>*****      |
| S/DEPTH=0.3 | 0.0<br>*****   | 0.274<br>80.4% | 0.0<br>*****    | 0.0<br>*****     | 0.0<br>*****     | 0.0<br>*****     | 0.0<br>*****    | 0.0<br>*****      | 0.0<br>*****      |
| S/DEPTH=0.2 | 0.0<br>*****   | 0.0<br>*****   | 0.0<br>*****    | 0.0<br>*****     | 0.0<br>*****     | 0.0<br>*****     | 0.0<br>*****    | 0.0<br>*****      | 0.0<br>*****      |
| S/DEPTH=0.1 | 0.0<br>*****   | 0.0<br>*****   | 0.0<br>*****    | 0.0<br>*****     | 0.0<br>*****     | 0.0<br>*****     | 0.0<br>*****    | 0.0<br>*****      | 0.0<br>*****      |
| S/DEPTH=0.0 | 0.0<br>*****   | 0.0<br>*****   | 0.0<br>*****    | 0.0<br>*****     | 0.0<br>*****     | 0.0<br>*****     | 0.0<br>*****    | 0.0<br>*****      | 0.0<br>*****      |

TABLE III-DIMENSIONLESS HORIZONTAL ACCELERATION COMPONENT FIELD.....DEFINED IN EQUATION (23)

| THETA=      | 0.0            | 10.0             | 20.0             | 30.0             | 50.0             | 75.0             | 100.0           | 130.0             | 180.0             |
|-------------|----------------|------------------|------------------|------------------|------------------|------------------|-----------------|-------------------|-------------------|
| ETA/HEIGHT= | 0.050<br>43.7% | 0.583<br>15.5%   | 0.284<br>-65.4%  | 0.101<br>-320.7% | -0.055<br>681.4% | -0.101<br>227.7% | -0.110<br>21.4% | -0.112<br>-242.4% | -0.111<br>-348.7% |
| SURFACE     | 0.0<br>*****   | 167.815<br>95.8% | 145.513<br>90.4% | 89.353<br>76.4%  | 22.552<br>-55.7% | 4.026<br>*****   | 0.460<br>*****  | 0.490<br>*****    | -0.000<br>*****   |
| S/DEPTH=1.6 | 0.0<br>*****   |                  |                  |                  |                  |                  |                 |                   |                   |
| S/DEPTH=1.5 | 0.0<br>*****   |                  |                  |                  |                  |                  |                 |                   |                   |
| S/DEPTH=1.4 | 0.0<br>*****   | 135.086<br>95.5% |                  |                  |                  |                  |                 |                   |                   |
| S/DEPTH=1.3 | 0.0<br>*****   | 134.031<br>94.9% |                  |                  |                  |                  |                 |                   |                   |
| S/DEPTH=1.2 | 0.0<br>*****   | 116.203<br>94.3% | 142.544<br>90.6% |                  |                  |                  |                 |                   |                   |
| S/DEPTH=1.1 | 0.0<br>*****   | 101.379<br>93.6% | 125.328<br>85.8% |                  |                  |                  |                 |                   |                   |
| S/DEPTH=1.0 | 0.0<br>*****   | 89.966<br>92.8%  | 117.723<br>85.0% | 87.724<br>77.6%  |                  |                  |                 |                   |                   |
| S/DEPTH=0.9 | 0.0<br>*****   | 78.402<br>92.0%  | 107.624<br>88.2% | 85.399<br>77.4%  | 24.251<br>-36.3% | 4.194<br>*****   | 0.492<br>*****  | 0.480<br>*****    | -0.000<br>*****   |
| S/DEPTH=0.8 | 0.0<br>*****   | 69.695<br>91.1%  | 96.922<br>87.4%  | 82.971<br>77.1%  | 26.879<br>-21.2% | 4.944<br>*****   | 0.702<br>*****  | 0.413<br>*****    | -0.000<br>*****   |
| S/DEPTH=0.7 | 0.0<br>*****   | 62.499<br>90.3%  | 91.511<br>86.5%  | 80.595<br>76.7%  | 29.087<br>-10.6% | 5.621<br>*****   | 0.880<br>*****  | 0.359<br>*****    | -0.000<br>*****   |
| S/DEPTH=0.6 | 0.0<br>*****   | 56.617<br>89.4%  | 85.292<br>85.8%  | 78.381<br>76.4%  | 30.914<br>-3.0%  | 6.218<br>*****   | 1.032<br>*****  | 0.316<br>*****    | -0.000<br>*****   |
| S/DEPTH=0.5 | 0.0<br>*****   | 51.885<br>88.5%  | 80.180<br>85.0%  | 76.409<br>76.0%  | 32.395<br>2.7%   | 6.731<br>*****   | 1.158<br>*****  | 0.283<br>*****    | -0.000<br>*****   |
| S/DEPTH=0.4 | 0.0<br>*****   | 48.176<br>87.8%  | 76.096<br>84.3%  | 74.735<br>75.7%  | 33.502<br>6.8%   | 7.156<br>*****   | 1.260<br>*****  | 0.258<br>*****    | -0.000<br>*****   |
| S/DEPTH=0.3 | 0.0<br>*****   | 45.369<br>87.1%  | 72.988<br>83.8%  | 73.599<br>75.4%  | 34.440<br>9.7%   | 7.491<br>*****   | 1.339<br>*****  | 0.239<br>*****    | -0.000<br>*****   |
| S/DEPTH=0.2 | 0.0<br>*****   | 43.450<br>86.6%  | 70.790<br>83.4%  | 72.428<br>75.2%  | 35.052<br>11.6%  | 7.731<br>*****   | 1.396<br>*****  | 0.227<br>*****    | -0.000<br>*****   |
| S/DEPTH=0.1 | 0.0<br>*****   | 42.306<br>86.3%  | 69.500<br>83.1%  | 71.839<br>75.1%  | 35.414<br>12.8%  | 7.876<br>*****   | 1.429<br>*****  | 0.219<br>*****    | -0.000<br>*****   |
| S/DEPTH=0.0 | 0.0<br>*****   | 41.928<br>86.2%  | 69.049<br>83.0%  | 71.642<br>75.0%  | 35.533<br>13.1%  | 7.924<br>*****   | 1.441<br>*****  | 0.217<br>*****    | -0.000<br>*****   |



CASE 4-0

TABLE V-DIMENSIONLESS DRAG FORCE COMPONENT FIELD...DEFINED IN EQUATION (25)

| THETA=      | 0.0               | 10.0             | 20.0              | 30.0             | 50.0             | 75.0              | 100.0           | 130.0             | 160.0             |
|-------------|-------------------|------------------|-------------------|------------------|------------------|-------------------|-----------------|-------------------|-------------------|
| ETA/HEIGHT= | 0.689<br>43.7K    | 0.583<br>15.5K   | 0.284<br>-65.4K   | 0.101<br>-326.7K | -0.055<br>661.4K | -0.101<br>2270.7K | -0.110<br>21.4K | -0.112<br>-242.4K | -0.111<br>-348.7K |
| SURFACE     | 242.394<br>55.0K  | 119.799<br>12.1K | 37.004<br>-155.2K | 7.722<br>*****   | -0.254<br>*****  | -2.191<br>*****   | -2.884<br>***** | -2.951<br>*****   | -2.919<br>*****   |
| S/DEPT=1.6  | 209.482<br>100.0K |                  |                   |                  |                  |                   |                 |                   |                   |
| S/DEPT=1.5  | 179.472<br>100.0K |                  |                   |                  |                  |                   |                 |                   |                   |
| S/DEPT=1.4  | 154.379<br>29.4K  | 111.891<br>5.9K  |                   |                  |                  |                   |                 |                   |                   |
| S/DEPT=1.3  | 133.294<br>24.2K  | 98.411<br>0.4K   |                   |                  |                  |                   |                 |                   |                   |
| S/DEPT=1.2  | 115.263<br>26.0K  | 86.495<br>-3.4K  | 34.345<br>-124.1K |                  |                  |                   |                 |                   |                   |
| S/DEPT=1.1  | 99.729<br>16.1K   | 75.867<br>-7.0K  | 33.170<br>-122.8K |                  |                  |                   |                 |                   |                   |
| S/DEPT=1.0  | 86.133<br>12.5K   | 66.306<br>-10.3K | 20.907<br>-121.0K | 7.423<br>*****   |                  |                   |                 |                   |                   |
| S/DEPT=0.9  | 74.105<br>9.2K    | 57.628<br>-13.2K | 26.843<br>-121.3K | 6.957<br>*****   | -0.207<br>*****  | -2.134<br>*****   | -2.799<br>***** | -2.909<br>*****   | -2.877<br>*****   |
| S/DEPT=0.8  | 63.335<br>6.3K    | 49.078<br>-15.0K | 22.721<br>-121.0K | 6.400<br>*****   | -0.143<br>*****  | -1.873<br>*****   | -2.480<br>***** | -2.586<br>*****   | -2.560<br>*****   |
| S/DEPT=0.7  | 53.576<br>3.7K    | 42.326<br>-18.2K | 20.639<br>-120.8K | 5.764<br>*****   | -0.097<br>*****  | -1.620<br>*****   | -2.165<br>***** | -2.263<br>*****   | -2.241<br>*****   |
| S/DEPT=0.6  | 44.624<br>1.5K    | 35.464<br>-20.3K | 17.597<br>-120.7K | 5.060<br>*****   | -0.046<br>*****  | -1.374<br>*****   | -1.851<br>***** | -1.939<br>*****   | -1.922<br>*****   |
| S/DEPT=0.5  | 36.310<br>-0.4K   | 28.997<br>-22.0K | 14.595<br>-120.6K | 4.300<br>*****   | -0.044<br>*****  | -1.135<br>*****   | -1.540<br>***** | -1.616<br>*****   | -1.603<br>*****   |
| S/DEPT=0.4  | 28.495<br>-2.1K   | 22.844<br>-23.4K | 11.629<br>*****   | 3.493<br>*****   | -0.029<br>*****  | -0.901<br>*****   | -1.230<br>***** | -1.293<br>*****   | -1.283<br>*****   |
| S/DEPT=0.3  | 21.028<br>-3.7K   | 16.031<br>-24.5K | 8.693<br>*****    | 2.659<br>*****   | -0.019<br>*****  | -0.672<br>*****   | -0.921<br>***** | -0.969<br>*****   | -0.962<br>*****   |
| S/DEPT=0.2  | 13.893<br>-4.0K   | 11.193<br>*****  | 5.722<br>*****    | 1.781<br>*****   | -0.011<br>*****  | -0.446<br>*****   | -0.614<br>***** | -0.646<br>*****   | -0.642<br>*****   |
| S/DEPT=0.1  | 6.903<br>*****    | 5.568<br>*****   | 2.887<br>*****    | 0.895<br>*****   | -0.005<br>*****  | -0.222<br>*****   | -0.307<br>***** | -0.323<br>*****   | -0.321<br>*****   |
| S/DEPT=0.0  | 0.0<br>*****      | 0.0<br>*****     | 0.0<br>*****      | 0.0<br>*****     | 0.0<br>*****     | 0.0<br>*****      | 0.0<br>*****    | 0.0<br>*****      | 0.0<br>*****      |

CASE 4-D

TABLE VI--DIMENSIONLESS INERTIA FORCE COMPONENT FIELD...DEFINED IN EQUATION (26)

| THEYA=      | 0.0            | 10.0             | 20.0             | 30.0             | 50.0             | 75.0             | 100.0            | 130.0             | 180.0             |
|-------------|----------------|------------------|------------------|------------------|------------------|------------------|------------------|-------------------|-------------------|
| ETA/HEIGHT= | 0.889<br>43.7% | 0.583<br>15.3%   | 0.284<br>-85.6%  | 0.101<br>-326.7% | -0.055<br>681.6% | -0.101<br>227.7% | -0.110<br>214.4% | -0.112<br>-242.4% | -0.111<br>-346.7% |
| SURFACE     | 0.0<br>*****   | 112.130<br>92.4% | 113.485<br>85.0% | 86.554<br>76.0%  | 30.122<br>-34.0% | 6.076<br>-766.7% | 1.025<br>*****   | 0.272<br>*****    | -0.000<br>*****   |
| S/DEPTH=1.6 | 0.0<br>*****   |                  |                  |                  |                  |                  |                  |                   |                   |
| S/DEPTH=1.5 | 0.0<br>*****   |                  |                  |                  |                  |                  |                  |                   |                   |
| S/DEPTH=1.4 | 0.0<br>*****   | 103.558<br>91.7% |                  |                  |                  |                  |                  |                   |                   |
| S/DEPTH=1.3 | 0.0<br>*****   | 89.133<br>91.0%  |                  |                  |                  |                  |                  |                   |                   |
| S/DEPTH=1.2 | 0.0<br>*****   | 76.642<br>96.5%  | 110.460<br>86.6% |                  |                  |                  |                  |                   |                   |
| S/DEPTH=1.1 | 0.0<br>*****   | 65.760<br>89.9%  | 96.880<br>86.1%  |                  |                  |                  |                  |                   |                   |
| S/DEPTH=1.0 | 0.0<br>*****   | 56.297<br>89.3%  | 84.540<br>85.7%  | 77.845<br>78.2%  |                  |                  |                  |                   |                   |
| S/DEPTH=0.9 | 0.0<br>*****   | 47.939<br>86.8%  | 73.286<br>85.2%  | 68.908<br>76.0%  | 28.787<br>1.2%   | 5.989<br>-612.1% | 1.016<br>*****   | 0.266<br>*****    | -0.000<br>*****   |
| S/DEPTH=0.8 | 0.0<br>*****   | 40.546<br>88.3%  | 62.909<br>84.6%  | 60.489<br>78.8%  | 26.227<br>4.0%   | 5.832<br>*****   | 0.958<br>*****   | 0.221<br>*****    | -0.000<br>*****   |
| S/DEPTH=0.7 | 0.0<br>*****   | 33.950<br>87.8%  | 53.456<br>84.4%  | 52.312<br>75.7%  | 23.426<br>6.4%   | 5.003<br>*****   | 0.879<br>*****   | 0.183<br>*****    | -0.000<br>*****   |
| S/DEPTH=0.6 | 0.0<br>*****   | 28.004<br>87.4%  | 44.628<br>84.0%  | 44.364<br>75.5%  | 20.422<br>8.3%   | 4.410<br>*****   | 0.783<br>*****   | 0.149<br>*****    | -0.000<br>*****   |
| S/DEPTH=0.5 | 0.0<br>*****   | 22.588<br>87.1%  | 36.363<br>83.7%  | 36.027<br>78.4%  | 17.254<br>9.9%   | 3.762<br>*****   | 0.673<br>*****   | 0.119<br>*****    | -0.000<br>*****   |
| S/DEPTH=0.4 | 0.0<br>*****   | 17.593<br>86.8%  | 26.587<br>83.5%  | 26.073<br>78.3%  | 13.954<br>11.1%  | 3.087<br>*****   | 0.552<br>*****   | 0.092<br>*****    | -0.000<br>*****   |
| S/DEPTH=0.3 | 0.0<br>*****   | 12.922<br>86.5%  | 21.111<br>83.3%  | 21.669<br>78.2%  | 10.551<br>12.0%  | 2.334<br>*****   | 0.422<br>*****   | 0.067<br>*****    | -0.000<br>*****   |
| S/DEPTH=0.2 | 0.0<br>*****   | 8.487<br>86.3%   | 13.929<br>83.1%  | 14.381<br>78.1%  | 7.075<br>12.6%   | 1.572<br>*****   | 0.285<br>*****   | 0.044<br>*****    | -0.000<br>*****   |
| S/DEPTH=0.1 | 0.0<br>*****   | 4.208<br>*****   | 6.921<br>83.1%   | 7.171<br>75.0%   | 3.849<br>*****   | 0.791<br>*****   | 0.144<br>*****   | 0.022<br>*****    | -0.000<br>*****   |
| S/DEPTH=0.0 | 0.0<br>*****   | 0.0<br>*****     | 0.0<br>*****     | 0.0<br>*****     | 0.0<br>*****     | 0.0<br>*****     | 0.0<br>*****     | 0.0<br>*****      | 0.0<br>*****      |

CASE 4-0

TABLE VII-DIMENSIONLESS DRAG MOMENT COMPONENT FIELD...DEFINED IN EQUATION (27)

| TIME=       | 0.0               | 10.0             | 20.0              | 30.0             | 50.0             | 75.0             | 100.0           | 130.0             | 180.0              |
|-------------|-------------------|------------------|-------------------|------------------|------------------|------------------|-----------------|-------------------|--------------------|
| ETA/HEIGHT= | 0.889<br>43.7%    | 0.583<br>15.5%   | 0.284<br>-65.4%   | 0.101<br>-326.7% | -0.055<br>661.4% | -0.101<br>227.7% | -0.110<br>21.6% | -0.112<br>-282.6% | -0.111<br>-346.67% |
| SURFACE     | 266.018<br>70.6%  | 102.639<br>26.2% | 23.042<br>-190.5% | 3.620            | -0.179           | -1.041           | -1.300          | -1.348            | -1.330             |
| S/DEPTH=1.6 | 213.857<br>100.0% |                  |                   |                  |                  |                  |                 |                   |                    |
| S/DEPTH=1.5 | 167.232<br>100.0% |                  |                   |                  |                  |                  |                 |                   |                    |
| S/DEPTH=1.4 | 130.808<br>39.7%  | 91.355<br>17.1%  |                   |                  |                  |                  |                 |                   |                    |
| S/DEPTH=1.3 | 102.377<br>33.5%  | 73.143<br>9.8%   |                   |                  |                  |                  |                 |                   |                    |
| S/DEPTH=1.2 | 79.641<br>28.5%   | 58.236<br>5.0%   | 22.243<br>-126.5% |                  |                  |                  |                 |                   |                    |
| S/DEPTH=1.1 | 61.935<br>23.7%   | 46.005<br>0.4%   | 18.593<br>-124.3% |                  |                  |                  |                 |                   |                    |
| S/DEPTH=1.0 | 47.645<br>19.2%   | 35.952<br>-3.9%  | 15.261<br>-122.8% | 3.318            |                  |                  |                 |                   |                    |
| S/DEPTH=0.9 | 36.207<br>14.0%   | 27.707<br>-7.6%  | 12.264            | 2.675            | -0.135           | -0.990           | -1.268          | -1.310            | -1.282             |
| S/DEPTH=0.8 | 27.044<br>11.0%   | 20.943<br>-11.5% | 9.611             | 2.403            | -0.080           | -0.768           | -0.998          | -1.035            | -1.021             |
| S/DEPTH=0.7 | 19.716<br>7.4%    | 15.425<br>-14.8% | 7.299             | 1.927            | -0.046           | -0.578           | -0.761          | -0.792            | -0.783             |
| S/DEPTH=0.6 | 13.692<br>4.3%    | 10.961           | 5.121             | 1.470            | -0.026           | -0.418           | -0.557          | -0.582            | -0.576             |
| S/DEPTH=0.5 | 9.315             | 7.402            | 3.070             | 1.052            | -0.014           | -0.287           | -0.386          | -0.404            | -0.400             |
| S/DEPTH=0.4 | 5.794             | 4.630            | 2.335             | 0.690            | -0.007           | -0.181           | -0.246          | -0.259            | -0.256             |
| S/DEPTH=0.3 | 3.199             | 2.559            | 1.307             | 0.395            | -0.003           | -0.101           | -0.138          | -0.145            | -0.144             |
| S/DEPTH=0.2 | 1.395             | 1.123            | 0.579             | 0.178            | -0.001           | -0.045           | -0.061          | -0.065            | -0.064             |
| S/DEPTH=0.1 | 0.346             | 0.279            | 0.144             | 0.045            | -0.002           | -0.011           | -0.015          | -0.016            | -0.016             |
| S/DEPTH=0.0 | 0.0               | 0.0              | 0.0               | 0.0              | 0.0              | 0.0              | 0.0             | 0.0               | 0.0                |

TABLE VIII-DIMENSIONLESS INERTIA MOMENT COMPONENT FIELD...DEFINED IN EQUATION (28)

| THETA       | 0.0            | 10.0             | 20.0            | 30.0             | 50.0             | 75.0             | 100.0           | 130.0             | 180.0             |
|-------------|----------------|------------------|-----------------|------------------|------------------|------------------|-----------------|-------------------|-------------------|
| ETA/HEIGHT  | 0.089<br>43.7% | 0.583<br>15.3%   | 0.284<br>-65.4% | 0.101<br>-328.7% | -0.055<br>681.4% | -0.101<br>227.7% | -0.110<br>21.4% | -0.112<br>-242.4% | -0.111<br>-346.7% |
| SURFACE     | 0.0<br>*****   | 101.722<br>94.7% | 76.463<br>64.7% | 47.467<br>39.3%  | 13.453<br>-91.6% | 2.520<br>*****   | 0.401<br>*****  | 0.142<br>*****    | -0.000<br>*****   |
| S/DEPTH=1.0 | 0.0<br>*****   | 89.401<br>93.2%  | 74.826<br>67.9% | 40.201<br>76.7%  | 15.214<br>-6.0%  | 2.441<br>*****   | 0.395<br>*****  | 0.136<br>*****    | -0.000<br>*****   |
| S/DEPTH=1.5 | 0.0<br>*****   | 89.401<br>93.2%  | 74.826<br>67.9% | 40.201<br>76.7%  | 15.214<br>-6.0%  | 2.441<br>*****   | 0.395<br>*****  | 0.136<br>*****    | -0.000<br>*****   |
| S/DEPTH=1.4 | 0.0<br>*****   | 89.401<br>93.2%  | 74.826<br>67.9% | 40.201<br>76.7%  | 15.214<br>-6.0%  | 2.441<br>*****   | 0.395<br>*****  | 0.136<br>*****    | -0.000<br>*****   |
| S/DEPTH=1.3 | 0.0<br>*****   | 89.401<br>93.2%  | 74.826<br>67.9% | 40.201<br>76.7%  | 15.214<br>-6.0%  | 2.441<br>*****   | 0.395<br>*****  | 0.136<br>*****    | -0.000<br>*****   |
| S/DEPTH=1.2 | 0.0<br>*****   | 89.401<br>93.2%  | 74.826<br>67.9% | 40.201<br>76.7%  | 15.214<br>-6.0%  | 2.441<br>*****   | 0.395<br>*****  | 0.136<br>*****    | -0.000<br>*****   |
| S/DEPTH=1.1 | 0.0<br>*****   | 89.401<br>93.2%  | 74.826<br>67.9% | 40.201<br>76.7%  | 15.214<br>-6.0%  | 2.441<br>*****   | 0.395<br>*****  | 0.136<br>*****    | -0.000<br>*****   |
| S/DEPTH=1.0 | 0.0<br>*****   | 89.401<br>93.2%  | 74.826<br>67.9% | 40.201<br>76.7%  | 15.214<br>-6.0%  | 2.441<br>*****   | 0.395<br>*****  | 0.136<br>*****    | -0.000<br>*****   |
| S/DEPTH=0.9 | 0.0<br>*****   | 89.401<br>93.2%  | 74.826<br>67.9% | 40.201<br>76.7%  | 15.214<br>-6.0%  | 2.441<br>*****   | 0.395<br>*****  | 0.136<br>*****    | -0.000<br>*****   |
| S/DEPTH=0.8 | 0.0<br>*****   | 89.401<br>93.2%  | 74.826<br>67.9% | 40.201<br>76.7%  | 15.214<br>-6.0%  | 2.441<br>*****   | 0.395<br>*****  | 0.136<br>*****    | -0.000<br>*****   |
| S/DEPTH=0.7 | 0.0<br>*****   | 89.401<br>93.2%  | 74.826<br>67.9% | 40.201<br>76.7%  | 15.214<br>-6.0%  | 2.441<br>*****   | 0.395<br>*****  | 0.136<br>*****    | -0.000<br>*****   |
| S/DEPTH=0.6 | 0.0<br>*****   | 89.401<br>93.2%  | 74.826<br>67.9% | 40.201<br>76.7%  | 15.214<br>-6.0%  | 2.441<br>*****   | 0.395<br>*****  | 0.136<br>*****    | -0.000<br>*****   |
| S/DEPTH=0.5 | 0.0<br>*****   | 89.401<br>93.2%  | 74.826<br>67.9% | 40.201<br>76.7%  | 15.214<br>-6.0%  | 2.441<br>*****   | 0.395<br>*****  | 0.136<br>*****    | -0.000<br>*****   |
| S/DEPTH=0.4 | 0.0<br>*****   | 89.401<br>93.2%  | 74.826<br>67.9% | 40.201<br>76.7%  | 15.214<br>-6.0%  | 2.441<br>*****   | 0.395<br>*****  | 0.136<br>*****    | -0.000<br>*****   |
| S/DEPTH=0.3 | 0.0<br>*****   | 89.401<br>93.2%  | 74.826<br>67.9% | 40.201<br>76.7%  | 15.214<br>-6.0%  | 2.441<br>*****   | 0.395<br>*****  | 0.136<br>*****    | -0.000<br>*****   |
| S/DEPTH=0.2 | 0.0<br>*****   | 89.401<br>93.2%  | 74.826<br>67.9% | 40.201<br>76.7%  | 15.214<br>-6.0%  | 2.441<br>*****   | 0.395<br>*****  | 0.136<br>*****    | -0.000<br>*****   |
| S/DEPTH=0.1 | 0.0<br>*****   | 89.401<br>93.2%  | 74.826<br>67.9% | 40.201<br>76.7%  | 15.214<br>-6.0%  | 2.441<br>*****   | 0.395<br>*****  | 0.136<br>*****    | -0.000<br>*****   |
| S/DEPTH=0.0 | 0.0<br>*****   | 89.401<br>93.2%  | 74.826<br>67.9% | 40.201<br>76.7%  | 15.214<br>-6.0%  | 2.441<br>*****   | 0.395<br>*****  | 0.136<br>*****    | -0.000<br>*****   |

CASE 4-0

TABLE IX-DIMENSIONLESS DYNAMIC PRESSURE COMPONENT FIELD...DEFINED IN EQUATION (29)

| THETA=      | 0.0             | 10.0           | 20.0            | 30.0             | 50.0             | 75.0             | 100.0           | 130.0             | 180.0             |
|-------------|-----------------|----------------|-----------------|------------------|------------------|------------------|-----------------|-------------------|-------------------|
| ETA/HEIGHT= | 0.689<br>43.7%  | 0.583<br>15.5% | 0.284<br>-65.4% | 0.101<br>-326.7% | -0.055<br>661.4% | -0.101<br>227.7% | -0.110<br>21.4% | -0.112<br>-242.4% | -0.111<br>-346.7% |
| SURFACE     | 1.719<br>46.3%  | 1.188<br>23.2% | 0.590<br>-48.9% | 0.211<br>-289.9% | -0.112<br>675.8% | -0.203<br>253.5% | -0.225<br>52.3% | -0.226<br>-238.4% | -0.224<br>-372.8% |
| S/DEPTH=1.6 | 1.050<br>100.0% |                |                 |                  |                  |                  |                 |                   |                   |
| S/DEPTH=1.5 | 1.570<br>100.0% |                |                 |                  |                  |                  |                 |                   |                   |
| S/DEPTH=1.4 | 1.492<br>36.1%  | 1.174<br>22.3% |                 |                  |                  |                  |                 |                   |                   |
| S/DEPTH=1.3 | 1.417<br>35.5%  | 1.144<br>21.0% |                 |                  |                  |                  |                 |                   |                   |
| S/DEPTH=1.2 | 1.348<br>32.8%  | 1.112<br>19.6% | 0.596<br>-44.9% |                  |                  |                  |                 |                   |                   |
| S/DEPTH=1.1 | 1.264<br>30.2%  | 1.080<br>17.9% | 0.622<br>-37.6% |                  |                  |                  |                 |                   |                   |
| S/DEPTH=1.0 | 1.227<br>27.5%  | 1.049<br>16.2% | 0.640<br>-32.6% | 0.245<br>-226.2% |                  |                  |                 |                   |                   |
| S/DEPTH=0.9 | 1.175<br>25.0%  | 1.020<br>14.5% | 0.653<br>-29.0% | 0.282<br>-181.9% | -0.100<br>735.0% | -0.202<br>255.9% | -0.225<br>53.2% | -0.226<br>100.0%  | -0.224<br>100.0%  |
| S/DEPTH=0.8 | 1.130<br>22.6%  | 0.993<br>12.8% | 0.662<br>-26.5% | 0.312<br>-153.1% | -0.080<br>*****  | -0.199<br>259.7% | -0.224<br>55.7% | -0.226<br>-238.9% | -0.224<br>100.0%  |
| S/DEPTH=0.7 | 1.091<br>20.3%  | 0.969<br>11.2% | 0.667<br>-24.7% | 0.336<br>-133.4% | -0.063<br>*****  | -0.195<br>263.2% | -0.223<br>57.8% | -0.226<br>-238.9% | -0.224<br>-371.1% |
| S/DEPTH=0.6 | 1.058<br>18.3%  | 0.947<br>9.7%  | 0.671<br>-23.4% | 0.356<br>-119.3% | -0.048<br>*****  | -0.192<br>266.5% | -0.222<br>59.7% | -0.226<br>-234.8% | -0.225<br>-370.0% |
| S/DEPTH=0.5 | 1.030<br>16.5%  | 0.930<br>8.4%  | 0.673<br>-22.4% | 0.372<br>-109.2% | -0.035<br>*****  | -0.189<br>269.4% | -0.221<br>61.3% | -0.226<br>-231.4% | -0.225<br>-365.4% |
| S/DEPTH=0.4 | 1.008<br>15.0%  | 0.915<br>7.3%  | 0.674<br>-21.8% | 0.386<br>-101.6% | -0.025<br>*****  | -0.187<br>271.9% | -0.220<br>62.6% | -0.226<br>-228.6% | -0.225<br>-361.6% |
| S/DEPTH=0.3 | 0.991<br>13.8%  | 0.903<br>6.4%  | 0.674<br>-21.3% | 0.393<br>-96.7%  | -0.017<br>*****  | -0.185<br>273.9% | -0.220<br>63.6% | -0.226<br>-226.4% | -0.225<br>-356.7% |
| S/DEPTH=0.2 | 0.979<br>12.9%  | 0.895<br>5.8%  | 0.675<br>-21.1% | 0.399<br>-93.2%  | -0.011<br>*****  | -0.183<br>275.4% | -0.220<br>64.4% | -0.226<br>-224.9% | -0.225<br>-356.7% |
| S/DEPTH=0.1 | 0.972<br>12.4%  | 0.890<br>5.4%  | 0.675<br>-20.9% | 0.403<br>-91.2%  | -0.008<br>*****  | -0.183<br>276.3% | -0.220<br>64.8% | -0.226<br>-223.9% | -0.225<br>-355.5% |
| S/DEPTH=0.0 | 0.969<br>12.2%  | 0.889<br>5.2%  | 0.675<br>-20.9% | 0.404<br>-90.6%  | -0.007<br>*****  | -0.182<br>276.6% | -0.219<br>64.9% | -0.226<br>-223.6% | -0.225<br>-355.1% |

CASE 4-0

TABLE X-VARIABLES DEPENDING ONLY ON PHASE ANGLE

| THETA=  | 0.0      | 10.0      | 20.0      | 30.0      | 50.0      | 75.0      | 100.0     | 130.0     | 180.0     |
|---|----------|-----------|-----------|-----------|-----------|-----------|-----------|-----------|-----------|
| (1) DIMENSIONLESS KINEMATIC FREE SURFACE BOUNDARY CONDITION ERROR, LINEAR WAVE THEORY REPRESENTATION.... DEFINED IN EQ.(35)     |          |           |           |           |           |           |           |           |           |
| SURFACE   | 0.0      | 0.035157  | 0.063667  | 0.080976  | 0.078797  | 0.032082  | -0.018241 | -0.042202 | -0.000000 |
| (2) DIMENSIONLESS KINEMATIC FREE SURFACE BOUNDARY CONDITION ERROR, STREAM FUNCTION THEORY REPRESENTATION.... DEFINED IN EQ.(35) |          |           |           |           |           |           |           |           |           |
| SURFACE   | 0.0      | -0.000001 | -0.000000 | -0.000000 | -0.000000 | -0.000000 | 0.000000  | 0.000000  | -0.000000 |
| (3) DIMENSIONLESS DYNAMIC FREE SURFACE BOUNDARY CONDITION ERROR, LINEAR WAVE THEORY REPRESENTATION.... DEFINED IN EQ.(36)       |          |           |           |           |           |           |           |           |           |
| SURFACE   | 0.038509 | 0.036560  | 0.030915  | 0.022164  | -0.000722 | -0.026496 | -0.033132 | 0.000406  | 0.028376  |
| (4) DIMENSIONLESS DYNAMIC FREE SURFACE BOUNDARY CONDITION ERROR, STREAM FUNCTION THEORY REPRESENTATION.... DEFINED IN EQ.(37)   |          |           |           |           |           |           |           |           |           |
| SURFACE   | 0.028890 | -0.011249 | -0.010805 | -0.003893 | 0.000668  | 0.000236  | 0.001999  | 0.001258  | 0.000322  |

CASE 4-0

TABLE XI-OVERALL WAVE PARAMETERS... DO NOT DEPEND ON PHASE ANGLE OR ELEVATION

(1) DIMENSIONLESS WAVE LENGTH... DEFINED IN EQUATION (37)  
0.422  
( 17.8X)

(2) DIMENSIONLESS AVERAGE POTENTIAL ENERGY... DEFINED IN EQUATION (38)  
0.213  
(-134.5X)

(3) DIMENSIONLESS AVERAGE KINETIC ENERGY... DEFINED IN EQUATION (39)  
0.254  
(-101.8X)

(4) DIMENSIONLESS TOTAL AVERAGE ENERGY... DEFINED IN EQUATION (40)  
0.467  
(-110.5X)

(5) DIMENSIONLESS TOTAL AVERAGE ENERGY FLUX... DEFINED IN EQUATION (41)  
0.447  
(-116.1X)

(6) DIMENSIONLESS GROUP VELOCITY... DEFINED IN EQUATION (42)  
0.957  
( -0.6X)

(7) DIMENSIONLESS TOTAL AVERAGE MOMENTUM... DEFINED IN EQUATION (43)  
0.505  
( -96.5X)

(8) DIMENSIONLESS TOTAL AVERAGE MOMENTUM FLUX IN WAVE DIRECTION... DEFINED IN EQUATION (44)  
0.603  
(-136.5X)

(9) DIMENSIONLESS TOTAL AVERAGE MOMENTUM FLUX TRANSVERSE TO WAVE DIRECTION... DEFINED IN EQUATION (45)  
0.156  
(-169.5X)

CASE 4-0

TABLE XI (CONTINUED)-OVERALL WAVE PARAMETERS... DO NOT DEPEND ON PHASE ANGLE OR ELEVATION

(10) DIMENSIONLESS ROOT MEAN SQUARE KINEMATIC FREE SURFACE BOUNDARY CONDITION ERROR... DEFINED IN EQUATION (46)  
LINEAR 0.047488  
STREAM FUNCTION 0.000000

(11) DIMENSIONLESS ROOT MEAN SQUARE DYNAMIC FREE SURFACE BOUNDARY CONDITION ERROR... DEFINED IN EQUATION (47)  
LINEAR 0.024081  
STREAM FUNCTION 0.004832

(12) DIMENSIONLESS MAXIMUM KINEMATIC FREE SURFACE BOUNDARY CONDITION ERROR... DEFINED IN EQUATION (46)  
LINEAR 0.085603  
STREAM FUNCTION 0.000001

(13) DIMENSIONLESS MAXIMUM DYNAMIC FREE SURFACE BOUNDARY CONDITION ERROR... DEFINED IN EQUATION (47)  
LINEAR 0.038509  
STREAM FUNCTION 0.028890

(14) DIMENSIONLESS KINEMATIC FREE SURFACE BREAKING PARAMETER... DEFINED IN EQUATION (48)  
LINEAR 0.429147  
STREAM FUNCTION 0.732602

(15) DIMENSIONLESS DYNAMIC FREE SURFACE BREAKING PARAMETER... DEFINED IN EQUATION (49)  
LINEAR 0.040894  
STREAM FUNCTION 0.286145